UNIVERSIDADE REGIONAL DO CARIRI - URCA

CENTRO DE CIÊNCIAS BIOLÓGICAS E DA SAÚDE - CCBS

PROGRAMA DE PÓS-GRADUAÇÃO EM QUÍMICA BIOLÓGICA - PPQB

ALIANE CRISTIANE DE SOUSA FORMIGA

ESTUDO BIOADSORTIVO DE ÍONS Pb (II) E Cu(II), EM EFLUENTES SINTÉTICOS, USANDO COMO ADSORVENTE AS SEMENTES *DE Spondias tuberosa* (UMBU)

Crato

2026

Ficha Catalográfica elaborada pelo autor através do sistema de geração automático da Biblioteca Central da Universidade Regional do Cariri - URCA

Formiga, Aliane Cristiane de Sousa

F725e ESTUDO BIOADSORTIVO DE ÍONS Pb (II) E Cu(II), EM EFLUENTES SINTÉTICOS, USANDO COMO ADSORVENTE AS SEMENTES DE Spondias tuberosa (UMBU) / Aliane Cristiane de Sousa Formiga. Crato-CE, 2026.

84p. il.

Tese. Programa de Pós-Graduação em Química Biológica da Universidade Regional do Cariri - URCA.

Orientador(a): Prof. Dr. Raimundo Nonato Pereira Teixeira

1.Adsorção, 2.Spondias tuberosa, 3.Metais tóxicos; I.Título.

CDD: 577

UNIVERSIDADE REGIONAL DO CARIRI

PROGRAMA DE PÓS-GRADUAÇÃO EM QUÍMICA BIOLÓGICA

ALIANE CRISTIANE DE SOUSA FORMIGA

ESTUDO BIOADSORTIVO DE ÍONS Pb (II) E Cu(II), EM EFLUENTES SINTÉTICOS, USANDO COMO ADSORVENTE AS SEMENTES *DE Spondias tuberosa* (UMBU)

Tese apresentada ao Programa de Pós-Graduação em Química Biológica, da Universidade Regional do Cariri, como requisito parcial à obtenção do título de Doutor em Química Biológica. Área de concentração: Análise Química e Ambiental.

Orientador: Raimundo Nonato Pereira Teixeira

Crato

2026

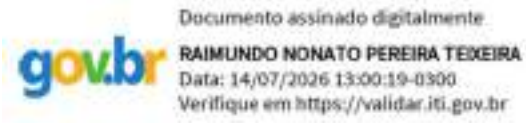
ALIANE CRISTIANE DE SOUSA FORMIGA

ESTUDO BIOADSORTIVO DE ÍONS Pb (II) E Cu(II), EM EFLUENTES SINTÉTICOS, USANDO COMO ADSORVENTE AS SEMENTES *DE Spondias tuberosa* (UMBU)

Tese apresentada ao Programa de Pós-Graduação em Química Biológica, da Universidade Regional do Cariri, como requisito parcial à obtenção do título de Doutor em Química Biológica. Área de concentração: Análise Química e Ambiental.

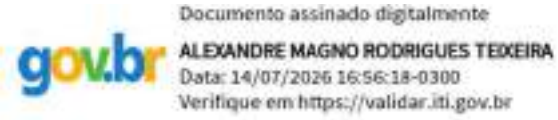
Tese defendida e aprovada em: 14 de julho de 2026

BANCA EXAMINADORA



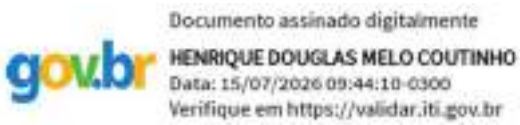
Raimundo Nonato Pereira Teixeira

Orientador – URCA



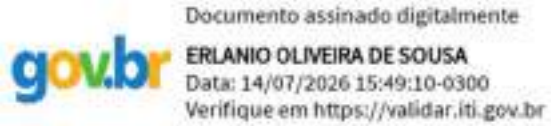
Prof. Dr. Alexandre Magno Rodrigues Teixeira

Membro Titular Interno – URCA



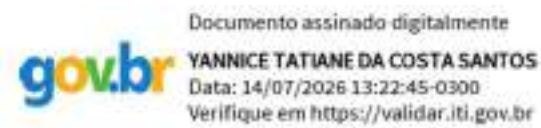
Prof. Dr. Henrique Douglas Melo Coutinho

Membro Titular Interno - URCA



Prof. Dr. Erlânio Oliveira de Sousa

Membro Titular Externo – CENTEC



Prof. Dra. Yannice Tatiane da Costa Santos

Membro Titular Externo - IFCE

Dedico este trabalho, a memória de meus irmãos Aline e Alberto, que durante esta etapa da minha vida, partiram, deixando dor e saudade.

AGRADECIMENTOS

Acima de tudo gratidão a Deus, pois eu não chegaria até aqui se não fosse pela vossa vontade. Obrigada Pai, por sempre me sustentar, ainda mesmo quando quis desistir.

A minha família: minha mãe, pelas suas orações e palavras de incentivo, e por sempre acreditar em min e no meu potencial; ao meu esposo, pela paciência, encorajamento, e por estender-me a mão sempre que precisei; ao meu querido e amado filho, pois foi você que me impulsionou a continuar, hoje és a minha maior razão de viver e lutar a cada dia pela nossa família e o nosso melhor.

Ao meu orientador Dsc. Raimundo Teixeira, o senhor foi essencial nesta caminhada, sua paciência e compreensão foi de extrema importância para que eu chegasse até aqui, obrigada por partilhar seus conhecimentos e aprendizados e por toda força repassada durante este trajeto.

A todos os meus professores, por compartilharem seus saberes na construção dos conhecimentos e aprendizagens ao longo do curso. Em especial a professor Henrique Douglas por toda força e empenho dado na publicação dos artigos científicos.

Aos meus colegas Jorge Marcell e Yannice, por contribuírem com seus conhecimentos, disponibilidades laboratoriais e discursões para melhorias e ampliação na construção da produção científica deste trabalho.

Aos laboratórios LEAS (IFCE), LQAA (URCA), LFQN (URCA) e a Central analítica da UFCA, pela parceria e cedência dos equipamentos para realização de análises e experimentos da pesquisa científica.

À Coordenação de Aperfeiçoamento de Pessoal de Nível Superior (CAPES), pelo apoio financeiro por meio da Bolsa de Produtividade em Pesquisa (BPI).

E, por fim, a todos que contribuíram de maneira direta ou indireta para a execução deste trabalho. Meus sinceros agradecimentos a todos!

Título	Página
Tabela 1. Padrões de lançamento de efluente conforme a legislação (CONAMA)	20
Tabela 2. Vantagens e desvantagens dos principais métodos de remoção de metais de efluentes	21
Tabela 3. Características do processo de adsorção quanto as forças de atração	23
Tabela 4. Adsorventes a base de resíduos agroindustriais presentes na literatura na remoção de íons Pb (II) e Cu (II)	25
Figura 1. Fluxograma de etapas do processo metodológico realizado para o estudo	15
Figura 2: Fluxograma de Estrutura da Tese	16
Figura 3: Ilustração das Interações entre o adsorvente e adsorvato e os principais termos em adsorção	24
Anexo 1 – Tela inicial da publicação do artigo 1 para produção científica	84

Símbolo, sigla ou abreviatura	Significado
As	Arsênio
Cd	Cádmio
Cu	Cobre
$CuFeS_2$	Calcopirita
$Cu(OH)_2$	Hidróxido de Cobre
Pb	Chumbo
AICc	Critério de Informação de Akaike Corrigido
BET	Brunauer-Emmett-Teller (modelo de isoterma)
CAPES	Coordenação de Aperfeiçoamento de Pessoal de Nível Superior
CCBS	Centro de Ciências Biológicas e da Saúde
CONAMA	Conselho Nacional de Meio Ambiente
DOI	Identificador de Objeto Digital
FAAS	Espectroscopia de Absorção Atômica em Chama
FTIR	Espectroscopia no Infravermelho por Transformada de Fourier
FRX / XRF	Fluorescência de Raios X
IF	Fator de Impacto
IFCE	Instituto Federal do Ceará
MEV	Microscopia Eletrônica de Varredura
PFO	Modelo cinético de pseudo-primeira ordem
pH	Potencial Hidrogeniônico
PPQB	Programa de Pós-Graduação em Química Biológica
PSO	Modelo cinético de pseudo-segunda ordem
PSM	Processo de Separação por Membrana
PZC	Potencial de Carga Zero
SEM	Microscopia Eletrônica de Varredura
SST	Semente de *Spondias tuberosa*
SSE	Soma dos erros quadrados
UFCA	Universidade Federal de Cariri
URCA	Universidade Regional de Cariri
°C	Graus Celsius
g	gramas

mg	miligramas
min	minutos

SUMÁRIO

Item	Assunto	Página
1	**INTRODUÇÃO**	13
1.1	ESTRATÉGIAS DE PESQUISA	13
1.2	ESTRUTURA DA TESE	15
2	**OBJETIVOS**	17
2.1	OBJETIVO GERAL	17
2.2	OBJETIVOS ESPECÍFICOS	17
2.3	QUESTIONAMENTOS	17
3	**FUNDAMENTAÇÃO TEÓRICA**	19
3.1	CONTAMINAÇÃO DAS ÁGUAS POR METAIS TÓXICOS	19
3.2	MÉTODOS DE REMOÇÃO DE METAIS TÓXICOS DE EFLUENTES	21
3.3	BIOADSSORÇÃO COM RESÍDUOS AGROINDUSTRIAIS	24
3.4	A SEMENTE DE S*pondias tuberosa* (UMBU) E O SEU USO COMO BIOADSORVENTE	26
4	**PRODUÇÃO CIENTÍFICA**	27
4.1	Artigo 1 – Sementes de *Spondias tuberosa* como bioadsorvente lignocelulósico para remoção eficiente de Pb(II): caracterização, modelagem de adsorção, seletividade e reutilização.	27
4.2	Artigo 2 – Estudo das sementes de *Spondias tuberosa* como bioadsorvente in natura para a remoção de íons Cu(II) de solução aquosa utilizando o método em batelada	50
5	**CONSIDERAÇÕES FINAIS**	76
5.1	ASPECTOS GERAIS DA PRODUÇÃO CIENTÍFICA	76
5.2	CONCLUSÕES GERAIS	77
5.3	PERSPECTIVAS DE INVESTIGAÇÃO FUTURAS	78
6	**REFERÊNCIAS**	79
7	**ANEXOS**	84

Estudo bioadsortivo de íons Pb (II) e Cu(II), em efluentes sintéticos, usando como adsorvente as sementes *de Spondias tuberosa* (umbu)

RESUMO

Introdução: A geração de resíduos agroindustriais em larga escala constitui um dos principais desafios ambientais contemporâneos, especialmente devido ao seu descarte inadequado. Anualmente, volumes expressivos de resíduos agroindustriais são gerados em todo o mundo. Nas últimas décadas, pesquisas tem dado ênfase ao reaproveitamento destes materiais como fonte de biomassa no tratamento, para recuperação e aproveitamento de águas residuais. Dentre os processos de recuperação de efluentes com uso de biomassa agroindustrial, destaca-se a adsorção, uma técnica inovadora, de baixo custo e eficiente na remoção de metais tóxicos. Apesar dos avanços no uso de biomassas agroindustriais como biossorventes, a literatura ainda apresenta limitações importantes, especialmente quanto à compreensão dos mecanismos de adsorção e à integração de parâmetros cinéticos, isotérmicos e termodinâmicos. Além disso, aspectos como regeneração e aplicação prática permanecem pouco explorados. Nesse contexto, o uso de biomassa proveniente de *Spondias tuberosa*, particularmente na forma de sementes, ainda é pouco investigado sob uma abordagem mecanística e aplicada, configurando uma lacuna relevante para o desenvolvimento de materiais sustentáveis no tratamento de efluentes contaminados. **Objetivo**: A pesquisa objetivou investigar a eficiência das Sementes da *Spondias tuberosa* – (SST) como bioadsorvente para remoção de íons Pb (II) e Cu (II) em meio aquoso. **Metodologia:** O resíduo de sementes de *Spondias tuberosa* (SST) foi coletado em indústrias de processamento de polpas na região do Cariri cearense (Juazeiro do Norte–CE, Brasil), submetido à lavagem para remoção de impurezas, seco à temperatura ambiente, triturado e classificado granulometricamente por peneiramento. A caracterização do material foi realizada por meio da determinação do ponto de carga zero (pH_{PZC}), microscopia eletrônica de varredura (MEV), espectroscopia no infravermelho por transformada de Fourier (FTIR) e fluorescência de raios X (FRX), antes e após o processo adsortivo. O desempenho do biossorvente foi avaliado em sistema de batelada, por meio de estudos cinéticos, isotérmicos e termodinâmicos, além de ensaios de dessorção e reutilização, visando analisar a eficiência, os mecanismos de adsorção e o potencial de regeneração do material. **Resultados e discussões:** O pH_{PZC} apresentou um valor médio de 5,3 sendo ajustado para 5,5. Nas imagens emitidas pelo MEV, observou-se a presença de rugosidade e porosidade característica de materiais vegetais fibrosos e a presença de aumento de pontos brilhantes no adsorvente pós contato, com possível indício de adesão do metal. As análises de FTIR e FRX, confirmaram a presença de ambos os íons no adsorvente, indicando provável mecanismo de troca iônica e complexação. Constatou-se uma rápida taxa de adsorção com ambos os íons próximo de 30 min, sendo o modelo de Elovich o que melhor representou a cinética do sistema, evidenciando a heterogeneidade da superfície; a isoterma indicou a presença de monocamadas ajustando-se ao modelo de Sips para o Pb(II) e Temkin para Cu (II) em temperaturas de 25ºC, destacando ainda que alterações de temperaturas, interferem na capacidade de adsorção. Para ambos os íons o sistema é considerado favorável e espontâneo, revelando comportamentos diferentes conforme mudança de temperatura, pois o Pb (II) adsorve melhor em temperaturas mais altas (endotérmico), enquanto o Cu (II) em temperaturas mais baixas (exotérmico), além disso, o baixo valor de entalpia indicou a ocorrência de fisisorção para ambos os íons; no entanto, esse fator, por si só, não confirma o

mecanismo de adsorção. **Conclusão:** Conclui-se que o bioadsorvente SST, possui um desempenho satisfatório em adsorção obtendo uma capacidade máxima de remoção de 46,0 mg. g^{-1} para o Pb (II) e 12,0 mg. g^{-1} para Cu (II), revelando-se com uma alternativa viável e promissora para remoção de metais tóxicos de águas residuais.

Palavras-Chave: Adsorção, S*pondias tuberosa*, metais tóxicos.

Agradecimentos: CAPES, URCA, IFCE e UFCA.

Biosorption of Pb (II) and Cu (II) ions from synthetic effluents using *Spondias tuberosa* seed residues as a sustainable adsorbent

ABSTRACT

Introduction: The large-scale generation of agro-industrial waste represents one of the major contemporary environmental challenges, particularly due to its inadequate disposal. Significant amounts of agro-industrial residues are generated worldwide every year. In recent decades, research efforts have focused on the valorization of these materials as biomass sources for the treatment, recovery, and reuse of wastewater. Among the processes employed for wastewater remediation using agro-industrial biomass, adsorption stands out as an innovative, low-cost, and efficient technique for the removal of toxic metals. Despite the advances in the application of agro-industrial biomasses as biosorbents, important knowledge gaps remain, particularly regarding the understanding of adsorption mechanisms and the integration of kinetic, isotherm, and thermodynamic parameters. Furthermore, aspects related to regeneration and practical applications remain insufficiently explored. In this context, the use of biomass derived from *Spondias tuberosa*, particularly in the form of seeds, remains poorly investigated from a mechanistic and applied perspective, representing a relevant gap for the development of sustainable materials for the treatment of contaminated effluents. **Objective:** This study aimed to investigate the efficiency of *Spondias tuberosa* seeds (SST) as a bioadsorbent for the removal of Pb(II) and Cu(II) ions from aqueous solutions. **Methodology:** *Spondias tuberosa* seed residues (SST) were collected from fruit pulp processing industries located in the Cariri region of Ceará State (Juazeiro do Norte–CE, Brazil). The material was washed to remove impurities, dried at room temperature, ground, and granulometrically classified by sieving. The characterization of the bioadsorbent was performed through the determination of the point of zero charge (pHPZC), scanning electron microscopy (SEM), Fourier-transform infrared spectroscopy (FTIR), and X-ray fluorescence spectroscopy (XRF), before and after the adsorption process. The performance of the biosorbent was evaluated in a batch system through kinetic, equilibrium isotherm, and thermodynamic studies, as well as desorption and reuse experiments, aiming to assess adsorption efficiency, mechanisms involved, and material regeneration potential. **Results and Discussion:** The pHPZC value was determined as 5.3 and adjusted to 5.5. SEM images revealed surface roughness and porosity characteristics of fibrous plant-based materials, as well as an increase in bright spots on the adsorbent surface after metal ion exposure, suggesting metal adsorption. FTIR and XRF analyses confirmed the presence of both ions on the adsorbent surface, indicating a probable ion-exchange and complexation mechanism. The rapid adsorption rate was observed for both ions, close to 30 min. The Elovich model provided the best fit for the kinetic data, indicating surface heterogeneity. The equilibrium studies suggested monolayers adsorption behavior, with the Sips model providing the best fit for Pb (II) and the Temkin model for Cu (II) at 25 °C. Temperature variations significantly influenced adsorption capacity. For both ions, the adsorption process was considered favorable and spontaneous, exhibiting distinct temperature-dependent behaviors: Pb(II) adsorption was enhanced at higher temperatures, indicating an endothermic process, whereas Cu(II) adsorption was favored at lower temperatures, suggesting an exothermic process, Furthermore, the low enthalpy value indicated the occurrence of physisorption for both ions; however, this factor alone does not confirm the adsorption mechanism. **Conclusion:** The SST bioadsorbent exhibited satisfactory adsorption performance, achieving maximum removal capacities of 46.0 mg g^{-1} for Pb (II) and 12.0 mg g^{-1} for Cu (II). These results demonstrate that *Spondias tuberosa* seed residues represent a viable and promising alternative material for the removal of toxic metals from wastewater.

Keywords: Adsorption; *Spondias tuberosa*; toxic metals.

IMPORTÂNCIA/RELEVÂNCIA PARA A SOCIEDADE

O fruto de *Spondias tuberosa* (umbu), espécie nativa da região semiárida brasileira, apresenta como principal resíduo agroindustrial o caroço (semente), gerado em grandes quantidades durante o processamento da polpa para a indústria alimentícia. Esse resíduo, ainda pouco aproveitado, representa uma fonte promissora de biomassa lignocelulósica para a produção de bioadsorventes destinados à remoção de metais tóxicos presentes em efluentes industriais.

Nesse contexto, o presente estudo propõe o desenvolvimento de um bioadsorvente inovador, obtido a partir da semente de *Spondias tuberosa*, material ainda pouco explorado na literatura para processos de adsorção de metais tóxicos. A pesquisa apresenta uma alternativa sustentável, de baixo custo e ambientalmente viável, alinhada aos princípios da economia circular e da valorização de resíduos agroindustriais.

Além disso, a utilização desse resíduo contribui simultaneamente para a mitigação de dois importantes problemas ambientais: a redução do acúmulo de resíduos provenientes da agroindústria e a remoção de contaminantes metálicos tóxicos de efluentes, favorecendo a preservação dos recursos hídricos, a proteção dos ecossistemas e a melhoria da qualidade ambiental e da saúde pública.

1 INTRODUÇÃO GERAL

1.1 ESTRATÉGIAS DE PESQUISA

Sendo o Brasil um dos maiores produtores de alimentos no mundo, devido à atividade agroindustrial desenvolvida, são geradas grandes quantidades de resíduos diversos, seja nas áreas agrícolas, industriais e urbanas. Os mais produzidos no dia a dia pelo homem são o papel, plástico, produtos químicos, lixo eletrônico, e principalmente o lixo orgânico (Pedrassolli, 2017).

Técnicas e tecnologias são empregadas no processo de reciclagem desses resíduos, resultando em outros produtos a serem estudados e lançados no mercado.

Nos últimos anos, especial atenção vem sendo dada para minimização ou reaproveitamento de resíduos sólidos orgânicos gerados nos diferentes processos industriais que envolvem quantidades apreciáveis de casca, caroço e outros (Oliveira *et al*., 2023). Esses materiais, além de fonte de resíduos provenientes da indústria de alimentos, podem ser utilizados como biomassa no tratamento de efluentes, passíveis de recuperação e aproveitamento.

Neste sentido, o crescimento populacional e o aumento do consumismo, contribuem para o elevado acumulo de efluentes, sejam domésticos, ou industriais, este último, muitas vezes contendo altos índices de metais tóxicos que são prejudiciais ao ambiente e a saúde. Barros *et al* (2012) alerta que elementos metálicos tóxicos em excesso, são fonte de poluição ambiental e apresentam diversos efeitos nocivos aos ecossistemas, como alterações físico-químicas na água e solo, provocando queda de sua qualidade e a mortandade de flora e fauna, prejudicando assim a saúde humana.

Além disso, devido à sua toxicidade crônica, não biodegradabilidade e bioacumulação ambiental, os metais tóxicos são poluentes ambientais substancialmente nocivos afetando águas, solos e a vida marinha (Pooja *et al*., 2022).

Neste contexto, com o propósito de minimizar impactos ao ambiente, ocasionados pelo lançamento de metais tóxicos *in natura* sem o devido tratamento e contribuindo com melhorias a saúde da população, técnicas baseadas em processos físicos, químicos e biológicos têm sido aplicadas. Dentre as mais eficazes estão a precipitação, adsorção, troca iônica, biossorção, osmose reversa e filtração por membrana (Ding *et al*., 2014; Cho *et al.*, 2015; Lee *et al*., 2017; Marković *et al*., 2023).

A biossorção, por exemplo, tem se destacado como uma alternativa amplamente utilizada na remoção de metais tóxicos de águas residuais. Por ser um método de baixo custo, alta eficiência, minimização de lodo químico e/ou biológico, ausência de necessidade adicional de nutrientes, regeneração do adsorvente e possibilidade de recuperação de metal (Farhan *et al*., 2013; Syed e Battula, 2023), tem sido consideravelmente abordada e investigada em pesquisas cientificas recentes.

A técnica tem como adsorvente, material composto a base de resíduos da agroindústria, cujas fontes podem ser, microbiana, biomassa, biomassa de algas, ou mesmo biomassa morta, esta última incluindo tecidos específicos de plantas, fibras naturais ou algodão, entre outros (Morin-Crini *et al*., 2018).

Estudos com biomassas a base de vegetais como, Casca de *Caryocar coriaceum* WITTM (Menezes *et al.,* 2020 e 2021), Cascas de *Ziziphus joazeiro* (Santos *et al*., 2022, 2024A e 2024B), Sementes de pimentão (Forgionny *et al*., 2021), semente de *Azadirachta indica* A. Juss. (Costa *et a*l., 2020), sementes de *Paeonia ostii* (Liu *et al*., 2020), casca do caule de *Ximenia americana* L (Cardoso *et al*., 2025), revelaram-se promissoras no tratamento de remoção de metais tóxicos em teste com soluções aquosas destes metais.

Portanto, a fim reduzir estes dois problemas e solucionar questões a eles associadas, buscou-se investigar a eficiência do resíduo da semente *de Spondias tuberosa* – SST, gerado em quantidades pela indústria de fabricação de polpas, como uma alternativa eficaz de remoção de metais tóxicos de águas residuais.

É importante ressaltar, que a biomassa vegetal SST, não fora explorada em estudos para testes de adsorção com metais tóxicos encontrados em pesquisas cientificas, destacando-se como um material inovador e como alternativa eficaz para remoção de íons metálicos de águas residuais.

O estudo desenvolveu-se através de técnicas de caracterização do material utilizando análises físico-químicas, métodos espectroscópicos e microscópico de imagens e para investigar o desempenho e eficiência adsortiva, foram aplicados testes de adsorção em batelada.

Inicialmente foi coletado o material(caroços) em indústrias de fabricação de polpas no Cariri Cearense (município de Juazeiro do Norte), lavado em água corrente para retirada de restos da polpa e secos em temperatura ambiente e ao abrigo do sol. Posteriormente foi triturado em forrageira e peneirado em peneiras com malhas de 32 mesh por partícula, para obtenção de uma granulação mais fina. Em seguida armazenado em sacos plásticos e conduzidos ao laboratório para análises.

Dentre as técnicas utilizadas para caracterizar o material, a pH_{PZC} foi um método usado como fator essencial, contribuindo para indicar a melhor faixa de pH para que ocorra a adsorção do material de interesse. A identificação do material através de espectroscopia e microscopia tratou de averiguar as estruturas morfológicas do material, a fim de investigar as interações adsorvente-adsorvato usando a MEV e analisar as estruturas e compostos presentes na composição do material adsorvente através do infravermelho FTIR e da fluorescência de raios X (FRX).

A aplicação do método específico de adsorção em batelada através de estudos cinéticos, isotermas e termodinâmicos foi proposto para analisar a capacidade máxima de adsorção, eficiência e comportamento do material e a influência de fatores como o tempo, concentração, temperatura e superfície de contato no processo de adsorção. Sendo empregado para isto, modelos matemáticos

contidos na literatura, avaliados através de equações não lineares, bem como representação gráfica destes modelos relacionando aos dados experimentais, a fim de identificar o modelo que melhor se adequou ao experimento. Enquanto o processo de dessorção foi aplicado para determinar a reutilização do material e o provável reaproveitamento do adsorvato.

A Figura 1 traz um resumo dos procedimentos e técnicas realizados no estudo para alcançar o objetivo proposto.

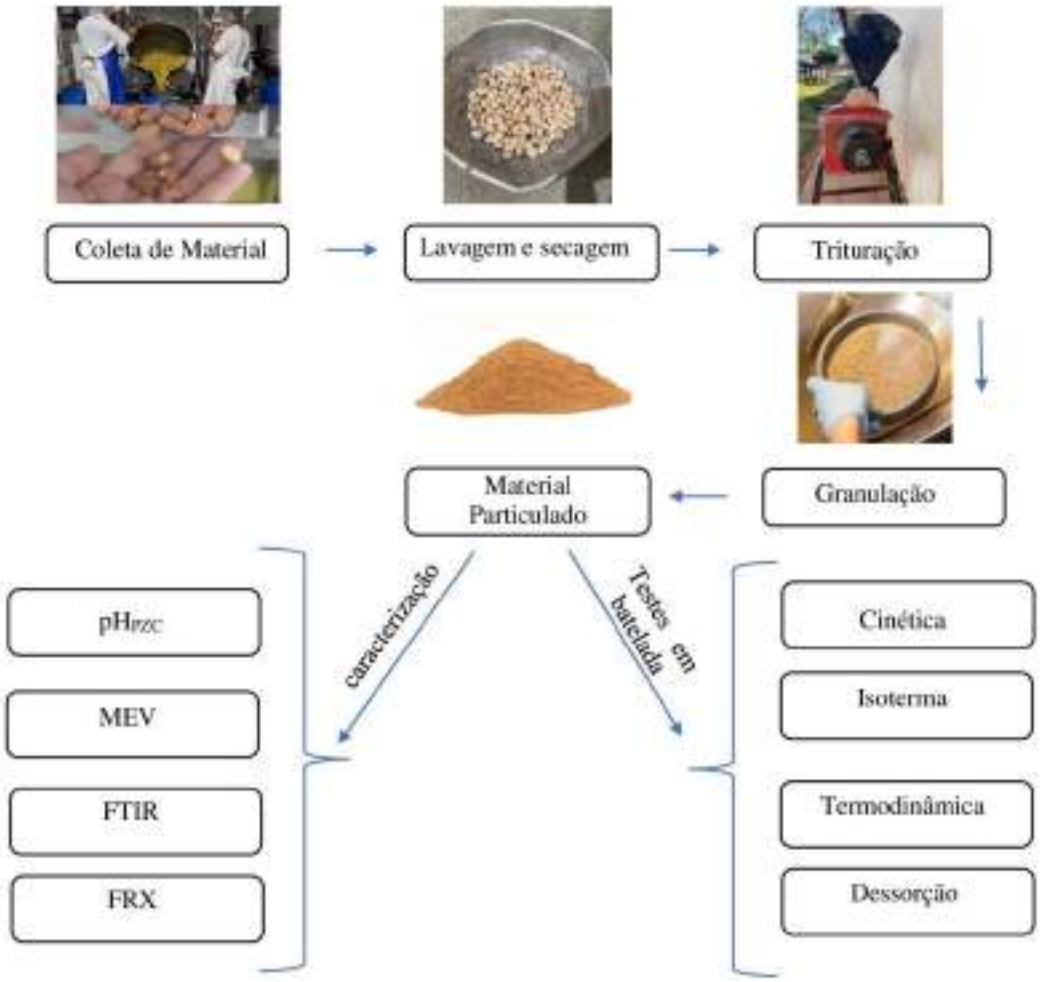


Figura 1 – Fluxograma de etapas do processo metodológico realizado para este estudo.

Em síntese, fundamentado nos dados obtidos, presume-se que o estudo tenha como principal descoberta, a possibilidade de aplicação de um resíduo alimentício na recuperação/remediação de ambientes contaminados por íons metálicos tóxicos como exemplo o chumbo (II) e cobre (II) aplicando a técnica de biossorção.

1.2 ESTRUTURA DA TESE

A tese encontra-se estruturada em 3 Capítulos: Capítulo I que trata da Introdução Geral, dividida em Estratégias de Pesquisa e Estrutura da Tese, em seguida são apresentados os Objetivos

do Estudo e Questionamentos e por último a Fundamentação Teórica, versando sobre: Contaminação das águas por metais tóxicos: Pb(II) e Cu(II); métodos de remoção de metais tóxicos de efluentes; biossorção com resíduos agroindustriais e o umbu – *Spondias tuberosa*. Posteriormente vem o Capítulo II que dispõe sobre a Produção Científica, contendo um artigo científico publicado e outro submetido em revistas seguindo normas do programa. E por fim o Capítulo III contendo as considerações finais, descrevendo os aspectos gerais apresentados no presente estudo, bem como as conclusões gerais e perspectivas futuras, seguida das referências e anexos, conforme detalhada a estrutura geral da tese observada na Figura 2.

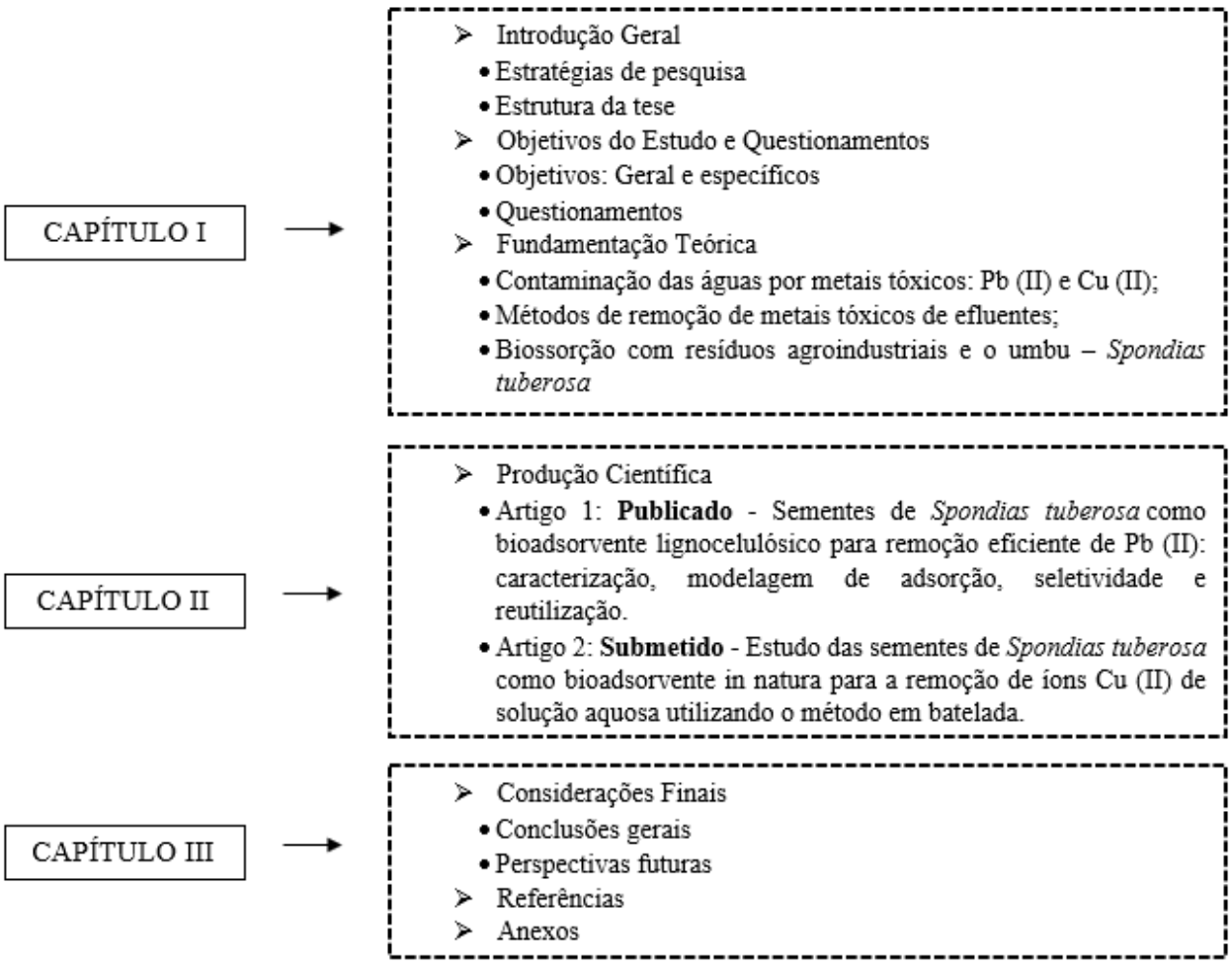


Figura 2 – Fluxograma de Estrutura da Tese

2 OBJETIVOS

2.1. OBJETIVO GERAL

Investigar a eficiência do bioadsorvente derivado da semente de *Spondias tuberosa* (Umbu) através da técnica de biossorção na remoção dos íons metálicos tóxicos Pb (II) e Cu (II) de efluentes.

2.2. OBJETIVOS ESPECÍFICOS

- Preparar um bioadsorvente a partir do resíduo agroindustrial da semente de *Spondias tuberosa* (SST).
- Caracterizar as propriedades físico-químicas, morfológicas e estruturais do bioadsorvente antes e após o processo de adsorção, visando elucidar os mecanismos e as interações adsorvente–adsorbato.
- Determinar as condições operacionais ótimas para o processo de biossorção, avaliando a influência do tempo de contato, velocidade de agitação, pH da solução, concentração inicial do metal e temperatura.
- Avaliar a cinética e o equilíbrio de adsorção do metal por meio de ensaios em sistema batelada, ajustando os dados aos modelos cinéticos e isotérmicos apropriados.
- Investigar a eficiência da dessorção para recuperação dos íons metálicos adsorvidos e avaliar o potencial de regeneração e reutilização do bioadsorvente em ciclos sucessivos de adsorção–dessorção.
- Comparar a capacidade máxima de adsorção do bioadsorvente obtido da semente de *Spondias tuberosa* com a de outros bioadsorventes lignocelulósicos provenientes de resíduos agroindustriais (sementes, cascas e caroços) reportados na literatura.

2.3. QUESTIONAMENTOS

1. A biomassa SST tem potencial para remover íons Pb (II) e Cu (II) de efluentes sintéticos usando a técnica de biossorção? A partir deste questionamento, aplicou-se a técnica de biossorção para investigar o potencial adsortivo do resíduo de SST gerado pela agroindústria da região na remoção de íons metálicos tóxicos Pb (II) e Cu (II) de efluentes sintéticos.

2. Se a biomassa SST tiver potencial para remover íons Pb (II) e Cu (II) de efluentes sintéticos, poderia ser utilizada em ambientes reais? Sim, se os testes com este estudo revelarem um potencial significativo na remoção destes componentes, o adsorvente que é produzido em grande escala pela agroindústria, pode ser aplicado com eficiência no tratamento de efluentes de industrias geradoras de resíduos contendo estes contaminantes.

3. Teria alguma possibilidade de resgatar, ou seja, reaproveitar os íons metálicos adsorvidos e reutilizar a biomassa após o processo de adsorção? Alguns estudos demonstraram que utilizando a

técnica de dessorção, puderam recuperar os íons investigados e reutilizar a biomassa, aplicando testes de dessorção em ciclos. Com esse estudo, também serão realizados estes testes, afim de obter resultados favoráveis a cerca destes dois aspectos que são de suma importância.

4. Qual a vantagem de utilizar esta biomassa em relação a outras já investigadas e presentes na literatura? Dentre as vantagens de utilizar esta biomassa, estão a de ser um resíduo que é gerado em grande escala pela agroindústria local, sendo de fácil aquisição, gerando custos apenas com transporte, e moagem, além disso contribui com a mitigação de acumulo de lixo orgânico pela indústria geradora, beneficiando a economia local e o meio ambiente.

3 FUNDAMENTAÇÃO TEÓRICA

3.1 CONTAMINAÇÃO DAS ÁGUAS POR METAIS TÓXICOS

Toda e qualquer ação ou interferência, seja ela natural ou antrópica, que altere as características física, química ou biológica da água, considera-se poluição hídrica.

Os componentes presentes na água, que podem alterar o seu grau de pureza, são tratados e separados de forma simplificada em características físicas, químicas e biológicas. Essas três características compõem o que se chama de parâmetros de qualidade da água. Dentre os parâmetros químicos de qualidade da água, tem-se os micropoluentes inorgânicos, que em sua parte são tóxicos, e dentre eles pode-se citar os metais tóxicos, que são poluentes inorgânicos prejudiciais a fauna, a flora e a saúde do homem (Von Sperling, 2014).

Metais tóxicos são liberados no ambiente aquático por vários processos domésticos (exaustão de automóveis, processos de fundição, queima de combustíveis fósseis, incineração de resíduos, lixiviação de aterros sanitários, uso de lodo de esgoto, águas residuais municipais e escoamento urbano) e processos industriais (galvanoplastia, refino minério de ferro, mineração, indústrias eletrônicas e de acabamento de metais, indústria de fertilizantes, curtumes, tintas, indústrias de papel e pesticidas) (Gautam, 2015).

Segundo Santana (2018), em ambientes aquáticos, aéreos e no solo, sejam por origens naturais ou antrópicas, os metais tóxicos podem ser adsorvidos pelos vegetais e animais, causando graves intoxicações ao longo da cadeia alimentar, devido às suas elevadas reatividades.

Costa; Mendonça; Wysard Junior (2017), Rodrigues et al. (2007), Acharya; Kumar; Rafi (2018), afirmam que os metais tóxicos, têm recebido atenção especial, pois dentre os poluentes existentes, apresentam-se como extremamente tóxicos, não são degradados quimicamente e nem biologicamente, afetando uma grande variedade de organismos e causando sérias doenças, tais como dor gástrica, náusea, vômitos, diarréia grave, hemorragia e até câncer no trato digestivo e nos pulmões.

Chumbo, mercúrio, cádmio, cromo, cobre, e arsênio são exemplos dos mais tóxicos e cancerígenos que podem existir em efluentes. Os metais não são facilmente eliminados do corpo humano ocasionando doenças ou envenenamento por metais (Reis et al., 2022).

Como forma de controle para o descarte destes metais in natura, as leis de controle ambiental no Brasil preveem através da Resolução Nº 430/2011 em seu Art. 16 que: “Os efluentes de qualquer fonte poluidora somente poderão ser lançados diretamente no corpo receptor desde que obedeçam às

condições e padrões previstos neste artigo" (CONAMA, 2011). A Tabela 1 mostra alguns dos metais tóxicos contaminantes de água e seus padrões exigidos pela legislação para descarte de efluente de qualquer natureza.

Tabela 1 – Padrões de lançamento de efluente

Parâmetros Inorgânicos	Valores Máximos
Arsênio total	0,5 mgL^{-1} As
Cádmio total	0,2 mgL^{-1} Cd
Cobre dissolvido	1,0 mgL^{-1} Cu
Chumbo total	0,5 mgL^{-1} Pb
Manganês total	1,0 mgL^{-1} Mn
Mercúrio total	0,01 mgL^{-1} Hg
Zinco total	5,0 mgL^{-1} Zn

Fonte: Adaptação CONAMA (2011).

3.1.1 Chumbo

O Chumbo está presente na natureza na forma de diversos compostos como carbonato de chumbo, sulfato e sulfeto de chumbo e óxido de chumbo. Pode ser encontrado também, em seu estado livre, nas formas isotrópicas $_{204}Pb$, $_{206}Pb$, $_{207}Pb$ e $_{208}Pb$. Sua grande utilização decorre de seu baixo ponto de fusão (327,46 ºC), grande facilidade de formar ligas e sua ductibilidade (Santos, 2020)

Em nível global, os poluentes que requerem mais cuidados, são os metais potencialmente tóxicos, como arsênio (As), cádmio (Cd), e chumbo (Pb,) que mesmo em baixas concentrações representam uma grave ameaça a plantas, animais e seres humanos, devido a sua toxicidade, além de serem bioacumuláveis e não biodegradáveis (Reis, 2020).

Dentre os metais potencialmente tóxicos, o chumbo é um dos que apresentam riscos mais elevados à saúde humana, já que se acumula no organismo e não possui nenhuma função fisiológica (Moreira, 2004). Ele é utilizado na fabricação de baterias e munições, nas fábricas de impressão de vidro e cerâmica e na linha de produção de indústrias metalúrgicas (Ahmed, 2013).

Sua contaminação depende da intensidade e efeito cumulativo no organismo podendo causar sérios danos ao organismo, como disfunção na formação de hemoglobina, retardo mental, infertilidade, além de comprometer fígado e rins. Nas plantas, a toxidade do chumbo causa redução brusca do crescimento, folhagem comprimida, endurecimento do sistema radicular, diminuição da fotossíntese e adulteração do balanço hídrico (Silva, 2014).

3.1.2 Cobre

O elemento químico Cobre (Cu) de número atômico 29 e massa atômica 63,5 u., é amplamente distribuído na natureza e nutricionalmente essencial. É o vigésimo quinto elemento mais abundante da crosta terrestre e a principal fonte deste metal é o minério calcopirita ($CuFeS_2$), sendo também

encontrado em outros minérios como sulfetos e carbonatos (Lee, 1996; Sousa, 2007). Dentre suas propriedades, destacam-se a elevada condutividade térmica e elétrica, maleabilidade, baixa corrosividade e habilidade de se amalgamar (fundir) (Gama, 2021). Esse metal divalente apresenta tendência à hidrólise e precipitação quando em pH maior que 6,0, tendo esse metal predominante de hidróxido de cobre [Cu $(OH)_2$] em soluções alcalinas (Bakhtiari; Azizian, 2015).

Apesar de ser um nutriente essencial para a saúde humana, o cobre administrado em doses maiores pode causar efeitos adversos ao organismo. O cobre (II), por exemplo, possui propriedades mutagênicas e carcinogênicas e no ser humano, ele pode levar ao câncer de pulmão (Maheshwari *et al.*, 2016; Mota, 2022).

O cobre pode ser encontrado em efluentes, gerado a partir do processo de industrialização, dentre as indústrias de geração de efluentes contendo este metal, encontra-se a galvanoplastia, o refino de petróleo e a catalise química. (Pugazhendhi, *et al*, 2018). A presença simultânea desses íons metálicos em efluentes de revestimento de metais, mineração, galvanoplastia, ligas e aço, e papel e celulose demonstra a importância do estudo da remoção conjunta desses metais antes do descarte dos efluentes em corpos hídricos (Vafajoo *et al*. 2018; Gama, 2021).

3.2 MÉTODOS DE REMOÇÃO DE METAIS TÓXICOS DE EFLUENTES

Os métodos e técnicas utilizados para controlar a poluição das águas residuais causada por metais tóxicos objetivam reduzir a concentração dessas substâncias antes do lançamento dos efluentes industriais em corpos hídricos.

Entre os processos de remoção de metais tóxicos, disponíveis na literatura, destacam-se as seguintes técnicas com suas vantagens e desvantagens: troca iônica, precipitação, adsorção, filtração por membrana, eletrodiálise, fotocatálise, sistema microbiano, processo eletroquímico, tratamento biológico, processo avançado de oxidação e biorreatores de membrana (Carolin *et al*., 2017).

A Tabela 2 apresenta as vantagens e desvantagens de determinados métodos para remoção de íons metálicos em efluentes.

Tabela 2 – Vantagens e desvantagens dos principais métodos de remoção de íons metálicos tóxicos de efluentes

Métodos	**Vantagens**	**Desvantagens**
Adsorção	Alta eficiência, possibilidade de recuperação do adsorvente e adsorvato e possível seletividade dependendo do adsorvente.	Depende do adsorvente. Quando a recuperação do adsorvente não é realizada e o resíduo deve ser destinado.
Electro-diálise	Alta seletividade dos metais	Incrustação de membrana e perdas de carga

Separação por membrana	Pouco espaço e alta remoção de metais pesados	Alto custo de operacional e incrustação da membrana.
Métodos eletroquímicos	Seletividade para íons metálicos, sem produto químico e a maioria dos metais podem ser removidos	Alto custo de operação
Precipitação química	Fácil operação e baixo custo	Geração de lodo e custo extra para a eliminação
Troca iônica	Seletivo para íons metálicos e regeneração de materiais	Alto custo e disponível para pequeno número de íons metálicos

Fonte: Carolin *et al*. (2017).

A técnica de precipitação química consiste na adição de compostos que alteram o pH do meio que contém os metais, causando a precipitação dessas espécies pela transformação dos mesmos em espécies inativas, evitando assim sua solubilização no meio líquido. O precipitado residual pode ser retirado da solução por técnicas de filtração e sedimentação. (Hashim *et al*., 2011).

A troca iônica, trata-se da troca de íons catiônicos e aniônicos entre o metal e a superfície do adsorvente, os íons são trocados devido a fenômenos eletrostáticos (Malik *et al.*, 2018). Na troca iônica os íons de uma dada espécie de um material insolúvel são separados por íons de diferentes espécies de uma solução. Esse processo pode ser realizado por uma coluna de leito empacotado e, devido à diferença de pressão, o efluente passa pelas resinas da coluna (Souza, 2023).

Os processos de separação por membranas (PSM), são operações que utilizam membranas no fracionamento de misturas, soluções e suspensões envolvendo espécies de tamanho e natureza química diferentes, com o objetivo de separar, purificar ou concentrar as substâncias presentes. (Boschi, 2006; Santos et al, 2014). Trata-se de uma tecnologia de separação através da aplicação de um potencial elétrico, causando a migração dos cátions e ânions para os eletrodos contendo cargas opostas enquanto o efluente é bombeado para as membranas separadoras (Souza, 2023).

O método eletroquímico de remoção de metais tóxicos de efluentes, têm como princípio a migração de espécies, sob a ação de um campo elétrico gerado por meio de eletrodos, provocando no sistema uma camada difusa móvel que carrega com ela os compostos polares presentes em solução (Crockford, 1977; Silva e Assis, 2004). Os tratamentos via eletroquímica oferecem diferentes maneiras para a remoção parcial ou completa de vários tipos de poluentes comumente encontrados em meio aquoso. Neste processo o principal reagente e percussor da degradação dos contaminantes é o elétron, fator que favorece a técnica devido à possibilidade de não utilizar produtos químicos. (Rezende *et al.*, 2010).

Dentre as técnicas citadas e respectivas vantagens e desvantagens apresentadas, a técnica de adsorção vem ganhando destaque e tornando-se mais promissora. De acordo com Cooney 1999, a adsorção se tornou um dos métodos mais populares para este fim, ganhando importância como um processo de separação e purificação, nas últimas décadas. A adsorção tem sido objeto de interesse dos cientistas desde o início do século, apresentando importância tecnológica, biológica, além de aplicações práticas na indústria e na proteção ambiental, tornando-se uma ferramenta útil em vários setores.

3.2.1 Adsorção

A técnica de adsorção consiste na transferência de metais pesados para a superfície de um sólido como adsorvente. O material atrai os íons presentes na solução por meio de ligações ou forças de atração eletrostáticas fracas (Cooney, 1999; Souza, 2023). O processo da adsorção é comumente empregado nas indústrias para reduzir os níveis de compostos nocivos ao ambiente dos efluentes, sendo bastante eficaz na eliminação de metais pesados. Esse método também pode ser empregado na purificação de gases e como meios de fracionamento de fluídos (Souza, 2023).

Em função de forças envolvidas, a adsorção pode ser classificada como química ou física. Na adsorção química ocorre o enlace entre o sólido (adsorvente) e as moléculas (adsorvato) e admite-se que há combinação das espécies a serem adsorvidas através de interações fortes (ligações iônicas ou covalente polar). Já na adsorção física, a ligação que ocorre adsorvato na superfície do adsorvente envolve uma interação relativamente fraca que pode ser atribuída às forças de Van der Wall. A entalpia de adsorção física é menor do que da adsorção química (Droguett, 1983).

A Tabela 3 destaca as características da adsorção quanto a forção de atração adsorvente-adsorvato.

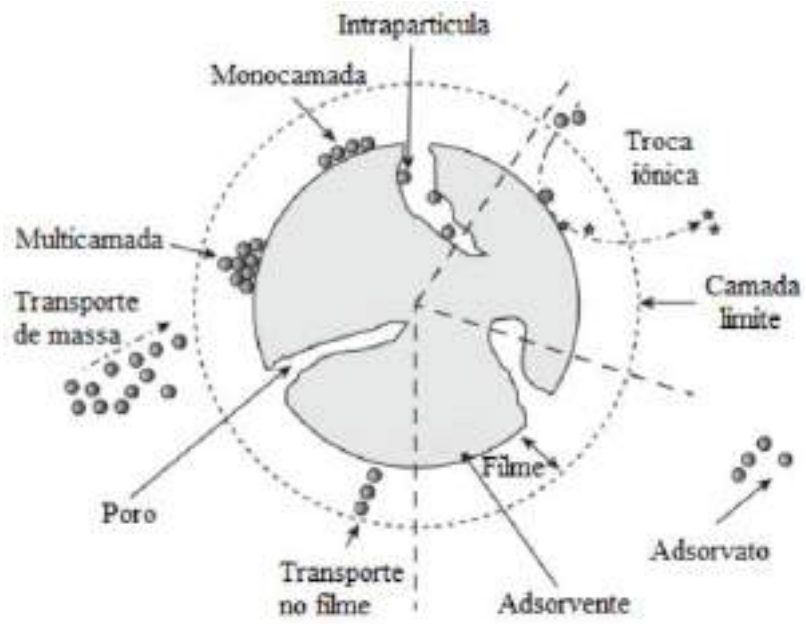
Tabela 3 – Características do processo de adsorção quanto as forças de atração

Adsorção física (fisissorção)	**Adsorção química (quimissorção)**
Baixo calor de adsorção (< 2 a 3 vezes o calor latente de evaporação)	Alto calor de adsorção (> 2 a 3 vezes o calor latente de evaporação)
Não específica	Altamente específica
Mono ou multicamada	Apenas monocamada
Nenhuma dissociação das espécies adsorvidas	Pode envolver dissociação
Apenas significativa em temperaturas relativamente baixas	Possível de ocorrer em uma ampla faixa de Temperaturas
Rápida, não-ativada, reversível	Ativada, podendo ser lenta, irreversível
Nenhuma transferência de elétrons embora possa ocorrer a polarização do adsorvato	Transferência de elétrons levando à formação de uma camada entre a superfície e o adsorvato

Adaptado de Perry; Green; Maloney (1997)

No que diz respeito as diferentes interações entre o adsorvente e o adsorvato, a Figura 3 destaca os principais termos utilizados no processo adsortivo.

Figura 3 – Ilustração das Interações entre o adsorvente e adsorvato e os principais termos em adsorção



Fonte: Adaptada de Gama (2021)

Na Figura 3, características como a área específica, granulometria, porosidade, diâmetro e estrutura dos poros do adsorvente influenciam na eficiência do processo de adsorção, visto que os sólidos adsorventes com maior área específica tendem a ter maior capacidade de sorver solutos (Souza, 2023).

O processo de adsorção, já conhecido há muito tempo, veio a emergir nas últimas décadas como uma tecnologia ecológica e de baixo custo, conhecida por Biossorção – que é a adsorção de espécies químicas de soluções aquosas em materiais biológicos através de mecanismos biológicos, físicos e químicos (Eletta *et al*., 2019; Adeniyi *et al*, 2019).

3.3 BIOADSSORÇÃO COM RESÍDUOS AGROINDUSTRIAIS

A bioadssorção trata da aplicação do processo de adsorção de substâncias presentes em um fluido (adsorvato) à uma matriz sólida (adsorvente), porém essa se restringe a utilizar matrizes biológicas como adsorventes. Com isso, pode ser definida como um processo em que envolve a concentração ou acumulação de íons ou moléculas sobre uma superfície adsorvente biológica, podendo ser composta por microrganismos, vegetais macroscópicos ou mesmo por biomassa morta como partes de tecidos específicos de vegetais, fibras naturais, plantas, algodão, dentre outras (Barros *et al.*, 2006; Morin-Crini *et al*, 2019).

Um dos maiores desafios no campo da biossorção é selecionar a biomassa mais promissora, em um meio de resíduos agroindustriais bastante amplo e de baixo custo. Embora muitos materiais biológicos podem se ligar a metais tóxicos, apenas aqueles com capacidade de ligação a metais suficientemente elevado, e que também possua uma maior seletividade para determinados íons metálicos que são adequados para utilização num processo de biossorção de alta escala (Ziagova *et al.*, 2007; Barros *et al.*, 2017).

Existem dois tipos de biomassa utilizados para adsorver os metais, que são biomassa viva com células ativas e biomassa morta. O primeiro tipo se baseia nas atividades metabólicas, e a adsorção ocorre através da membrana celular, e por ser dependente do metabolismo sofre limitações em relação a toxicidade e manutenção dos nutrientes. No segundo tipo a ligação ocorre na parede da célula, onde as proteínas e os polissacarídeos possuem sítios de ligação, não sofrendo com a toxicidade e nem com a manutenção de nutrientes (El-Sayed e El-Sayed, 2014; Barros, 2017).

A biomassa morta derivada de rejeitos agroindustriais, tem se tornado promissora no tratamento usando a técnica de biossorção. Estes materiais, normalmente oriundos de processos de transformação de matérias-primas agrícolas como beneficiamento de grãos e fabricação de produtos alimentícios, são naturalmente ricos em compostos já conhecidos pela sua capacidade de adsorção, como taninos, lignina e celulose. Essas substâncias possuem em sua estrutura química grupos funcionais como hidroxilas, metilas e carbonilas, responsáveis pela sorção dos íons metálicos (Sulyman *et al.*, 2017). Por isso, sua utilização in-natura, sendo submetidos apenas a processos físicos como retirada de impurezas, moagem e secagem, é interessante na busca por adsorventes promissores.

Desta forma, a biomassa utilizada no processo de adsorção de origem lignocelulosica tem despertado a atenção de pesquisadores, não apenas pelo baixo custo, mas também pela grande disponibilidade (principalmente por se tratar de rejeitos). Conforme Nascimento et al (2014), o uso desses materiais como adsorventes, contribui para redução de resíduos agrícolas relacionado a proteção ambiental e agrega de certa forma, valor econômico ao resíduo.

Na Tabela 4 são destacados materiais de origem lignocelulosicos derivados de rejeitos agroindustriais a base de cascas e sementes utilizados no processo de adsorção para remoção de metais tóxicos presentes na literatura.

Tabela 4 – Adsorventes a base de resíduos agroindustriais presentes na literatura na remoção de íons Pb (II) e Cu (II)

Adsorvente	**Composto Adsorvido**	**Referência**
Casca de Caryocar coriaceum Wittm	Pb (II)	(Menezes et al., 2020)
Neem bruto	Pb (II)	(Costa et al., 2020)
Cascas de *Ziziphus joazeiro*	Pb (II)	(Santos et al., 2022)

Sementes de pimentão.	Pb (II)	(Forgionny et al., 2021)
Semente de Azadirachta indica A. Juss	Cu (II)	(Costa et al., 2020)
Cascas de ovo cru	Cu (II)	(Mohammad; Ahmed; El-sayed, 2020)
Casca de Caryocar coriaceum Wittm	Cu (II)	(Menezes et al., 2021)

3.4. A SEMENTE DE S*pondias tuberosa* (UMBU) E O SEU USO COMO BOADSORVENTE

O umbuzeiro é uma das árvores frutíferas que ocorrem por toda a Caatinga, e pertence à família Anacardiaceae. O umbuzeiro, planta do Nordeste brasileiro, é encontrado nas regiões do Agreste (Piauí), Cariris (Paraíba), Caatinga (Pernambuco e Bahia) e Norte e Nordeste de Minas Gerais. Seu nome em tupi-guarani é "ymbu", que significava "árvore que dá de beber", sendo conhecido, também como umbu, imbu, ambu e ombu. Pela importância de suas raízes foi chamada "árvore sagrada do Sertão" pelo famoso escritor Euclídes da Cunha (Barreto, 2010).

Umbu é constituído por um pericarpo coriáceo (casca) (22 %) polpa suculenta de sabor agridoce (68%) e endocarpo (10%). O endocarpo é muito resistente e nele está contida a semente propriamente dita (LIMA, 2009). Utilizado na comercialização de refrescos, doces, licores, sorvetes e polpas pela indústria. No consumo do fruto para estes fins, há uma considerável quantidade de resíduos gerados. Estes resíduos tem como subproduto, o caroço do fruto que comumente é descartado contribuindo para o acumulo de resíduos oriundos da agroindústria.

De acordo com Silva e colaboradores (2014), os subprodutos de frutos compostos em sua maioria de cascas e sementes, pode levar a indústria para um agronegócio de baixo desperdício, aumentando a lucratividade industrial, uma vez que a massa de subprodutos pode aproximar ou mesmo exceder a da polpa utilizada. O uso de todo o tecido vegetal resultaria em uma economia aos produtores e um impacto benéfico sobre o meio ambiente.

Segundo Ribeiro (2019), o beneficiamento do umbu em polpa, seu principal produto comercial, gera um resíduo composto de casca e semente que, se descartado de maneira inadequada, pode afetar negativamente o meio ambiente.

4 PRODUÇÃO CIENTÍFICA

Artigo 1 – Sementes de *Spondias tuberosa* como bioadsorvente lignocelulósico para remoção eficiente de Pb (II): caracterização, modelagem de adsorção, seletividade e reutilização.

***Spondias tuberosa* Seeds as lignocellulosic bioadsorbent for efficient Pb (II) removal: Characterization, adsorption modeling, selectivity, and reusability**

Autores: Aliane Cristiane de Sousa Formiga, Isaac Moura Araújo, José Augusto Soares de Araújo, Henrique Douglas Melo Coutinho, Francisco José de Paula Filho, Yannice Tatiane da Costa Santos, Jorge Marcell Coelho Menezes, Raimundo Nonato Pereira Teixeira.

Revista: *Chemistry Select* (IF: 2,3) **CitScore**: 3,1

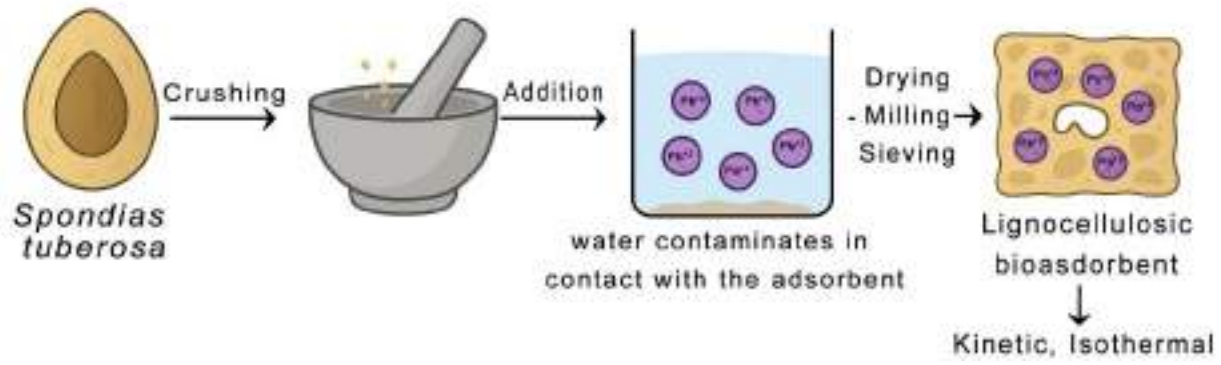
DOI: 10.1002/slct.202502316

Situação: Publicado em 06/10/2025

ABSTRACT

The objective of this research was to investigate the efficiency of *Spondias tuberosa* seeds (SST) as a bioadsorbent for Pb (II) ions in aqueous solutions. Adsorption isotherms and kinetics, as well, thermodynamics were studied in a batch system. The SST residue was collected from pulp manufacturing industries in the Cariri region of Ceará, specifically in the city of Juazeiro do Norte, Ceará, Brazil. For the characterization of the adsorbent material, point of zero charge (PZC), scanning electron microscopy (SEM), and infrared spectroscopy (FTIR) analyses were performed. The pHPZC obtained had an average value of 5.3, which was adjusted to 5.5. SEM images revealed the presence of roughness and porosity typical of fibrous plant materials. With increased magnification, the material showed varying pore shapes and sizes, generally derived from the structure of the plant cell wall of the precursor biomass. It was also observed that the adsorption rate reached equilibrium within 30 minutes. Thus, it was concluded that the SST bioadsorbent demonstrated satisfactory performance in the adsorption of Pb (II) ions, with a maximum adsorption capacity of 46.0 mg. g -1 . These findings support the use of SST as an environmentally friendly low-cost, and efficient biosorbent, contributing to sustainable strategies for toxic metals remediation.

Keywords: batch, biosorption, lead, *Spondias tuberosa*



Infographic- Stages of the Lead (II) ions biosorption process using *Spondias tuberosa* seeds as adsorbent

1. Introduction

Industrial activity generates a significant volume of waste, which, when present in liquid form, is referred to as effluent, resulting from the utilization of water and other materials in the production of specific products. When discharged untreated, these effluents have the potential to cause substantial environmental impacts.

Industrial process residues containing toxic metals, when released into water bodies or onto soil surfaces, contribute to the generation of serious environmental problems due to their persistent nature. Due to their chronic toxicity, non-biodegradability, and environmental bioaccumulation, toxic metals are highly harmful environmental pollutants, affecting water, soil, and marine life (Pooja et al., 2022). The toxic action of these metals can also lead to death or bioaccumulation, which amplifies the harmful effects of these substances through the food chain.

Lead, mercury, cadmium, chromium, copper, and arsenic are examples of toxic and carcinogenic metals that may be present in effluents. These metals are not easily eliminated from the human body, leading to diseases or poisoning (Lesmana, 2009; Reis et al., 2022).

Effluents from industries such as ceramics, paints, plastics, pesticides, automobiles, cement, steel, and batteries (Awual, 2019; Giri et al., 2022) are rich in lead (II) ions, a toxic pollutant. The release of Pb (II) can significantly increase its concentration in the environment and persist for long periods, resulting in severe health effects. Soluble or moderately soluble lead salts readily enter biological systems through polluted water and soil sources, significantly impacting living organisms. Pb (II) severely affects photosynthesis, water management, nitrogen metabolism, and cell division in plants (Giri et al., 2022).

To prevent serious environmental and public health issues, it is necessary to treat generated effluents before discharging them untreated, thereby helping to minimize the concentration of these components in compliance with current legislation.

To protect environmental safety and public health, various treatment methods have been developed and explored across a wide range of environmental and health research areas. Each technology comes with its advantages and disadvantages. Among the most efficient and safe techniques available for the elimination of heavy metals are ion exchange, coagulation, adsorption, membrane filtration, electrodialysis, photocatalysis, microbial systems, electrochemical processes, biological treatment, advanced oxidation processes, and membrane bioreactors (Carolin, 2017). Although effective, some of these methods may have limitations, such as high costs, complexity, time demands, and the generation of residual waste.

One of the effective alternatives for the removal of toxic metals such as Lead (II) from wastewater is the technique of biosorption. This process is a reliable and cost-effective method, characterized by low operational costs, minimal scaling issues, and greater economy in the removal of toxic metals from effluents. Additionally, the adsorption technique is easy to use, flexible, simple in design, and does not produce toxic pollutants (Demirbas, 2008; Carolin et al., 2017).

Therefore, it is important to employ environmentally friendly methods, such as adsorption, to remove Pb (II) from effluents and ensure a healthy environment (El Mouden et al., 2023; Senol et al., 2023). Adsorption is a green process that has been gaining prominence due to its numerous advantages, including versatility, cost-effectiveness (Ghosh et al., 2024), reduced generation of by-products, biodegradability (Benettayeb et al., 2024), and superior efficiency compared to other purification techniques that rely on expensive synthetic and organic compounds (Ghosh et al., 2024; Malbenia et al., 2024; Oussadi et al., 2025).

Agricultural waste biomass, such as cashew nut shell (SenthilKumar, 2011), Caryocar coriaceum Wittm shell (Meneses et al., 2020), raw neem (Costa et al., 2020), Azadirachta indica A.Juss. seeds (Costa et al.,2020), bell pepper seeds (Forgionny et al., 2021), coriander seeds (Shamkhi et al., 2022), among others, have shown effectiveness in the removal of Pb (II) from wastewater.

Although several studies have investigated the adsorption of Pb (II) ions using different bioadsorbents, the novel use of *Spondias tuberosa* (umbu) seeds represents a significant advancement in the search for alternative, sustainable, and low-cost materials for the treatment of water contaminated with heavy metals. This biomass, still scarcely explored scientifically, is abundant in the semi-arid regions of Brazil and is often discarded as agro-industrial waste. By investigating its adsorptive potential, this study not only contributes to the valorization of a regional byproduct but also expands the portfolio of promising materials for environmental remediation. The originality of the raw material used adds innovation to the research and reinforces its importance in the context of the circular economy and the development of environmentally friendly technologies.

This study aimed to evaluate the potential of agro-industrial residues for the removal of toxic metals from effluents by investigating the adsorption performance of raw biomass derived from

Spondias tuberosa seeds (SST). The material was proposed as a novel and sustainable bioadsorbent for the removal or reduction of lead (II) ions present in synthetic effluents, through batch adsorption experiments encompassing kinetic, isothermal, and thermodynamic analyses.

2. Materials and Methods

2.1 Collection and Preparation of Adsorbents

The SST residues were collected from a pulp manufacturing industry located in the Cariri region of Ceará, specifically in the city of Juazeiro do Norte, Ceará, Brazil. After collection, the materials were washed with water 2 to 3 times to remove any remaining pulp, and then exposed to sunlight for natural drying over a period of 3 days.

After the natural drying process, all the material was sent to the Chemistry Laboratory of the Regional University of Cariri, where it initially underwent three cycles of grinding in a forage cutter to achieve a finer appearance. Subsequently, the sieving process was carried out, leaving all the particulate material with a 32-mesh particle fraction.

Once the particulate material was prepared, it was dried in an oven at 60°C to remove all moisture for further use.

2.2 Material Characterization

2.2.1 Point of Zero Charge (pH_{PZC})

The determination of the pH_{PZC} of the adsorbents is an essential factor in characterizing the material, as it helps indicate the optimal pH range for the adsorption of the target material. The pH_{PZC} represents the pH at which the surface of the adsorbent material remains electrically neutral or at zero charge; thus, adsorbents in contact with solutions with a pH above the pH_{PZC} exhibit a negatively charged surface, while below this point, the surface becomes positively charged (Menk et al., 2019).

The point of zero charge (pH_{PZC}) was determined based on the method adapted from Regalbuto and Robles (2004). Thirteen solutions with initial pH values ranging from 1 to 13 were prepared, and 20 mL of each solution was transferred into a 125 mL Erlenmeyer flask containing 0.1 g of the adsorbent, previously weighed using an analytical balance. The flasks were then agitated at 150 rpm using a Nova Ética shaker, model 109-1, for a period of 2 hours. After the contact time, the final pH of each solution was measured.

The pH_{PZC} was determined by plotting ΔpH ($pH_{initial} - pH_{final}$) versus $pH_{initial}$, where the intersection point of the curve with the x-axis corresponds to the pH_{PZC} (Hafshejani, 2015; Santos, 2024; Granado-Castro, 2024).

2.2.2 Scanning Electron Microscopy (SEM)

Electron microscopy is used when information about the morphology of a given material is needed. It is a procedure in which a beam of electrons scans the surface of the material being studied, generating a three-dimensional image (IHA & CRUZ, 2020).

Knowing that the shape, distribution, and size of pores on the surface of bioadsorbents are directly related to adsorption efficiency—since they influence the direct access of solute molecules to adsorption sites—understanding these parameters through three-dimensional imaging indicates the quality of the material for the process (MOREIRA et al., 2019).

The scanning electron microscopy analyses were performed using an SU3500 microscope (Hitachi, Tokyo, Japan) at the Regional University of Cariri (URCA). The SST seed samples were mounted on an aluminum sample holder using carbon tape. The images were acquired under low vacuum (microscope chamber pressure at 100 Pa), with a working distance of 10 mm, using a backscattered electron detector (BSE) in compositional mode and an electron acceleration voltage of 15 kV.

2.2.3 Fourier Transform Infrared Spectroscopy (FTIR)

The FTIR spectra were obtained in transmittance mode using an Agilent Cary 630 FTIR spectrometer. Fourier Transform Infrared Spectroscopy (ATR-FTIR) in the infrared region was performed using the range of 4000-650 cmiha^{-1}. The data were acquired using Microlab and Resolution Pro software, both from Agilent (Santa Clara, USA). The maximum spectral resolution was 2 cm^{-1}, and the presented spectrum corresponds to the average of up to eight readings for each wavenumber.

2.3 Batch Adsorption Experiments

2.3.1 Adsorption Kinetics

The study of adsorption kinetics is important to determine the time at which the samples will reach equilibrium.

The experiment was conducted at the LEAS - Environmental and Sanitary Engineering Laboratory of IFCE, Juazeiro do Norte, at the local temperature of 25°C, in duplicates, using 10 mL aliquots of lead (II) nitrate solution buffered with acetic solution at 102 mg·L^{-1}, obtaining a concentration in the pH range of 5.5. The solution was transferred to a 125 mL Erlenmeyer flask containing 0.05 g of the weighed adsorbent and then placed on a shaker table at 150 rpm for periods of 1, 4, 8, 16, 30, 60, 120, and 240 minutes.

After the established contact times were reached, the samples were filtered through filter paper, stored, and transported to the Analytical Center Laboratory of UFCA, where they were

analyzed by Flame Atomic Absorption Spectroscopy (FAAS) using a Varian SpectrAA 50B spectrometer.

The experimental results were determined by the adsorptive capacity of the material following the study equations below: Lead (II) adsorption efficiency was determined by Equation 1.

$$E(\%) = \frac{(C_0 - C_f)}{C_0} \times 100 \quad (1)$$

Where, C_0 is the initial ion concentration in the solution ($mg \cdot L^{-1}$), and Cf is the ion concentration in the solution at time t ($mg \cdot L^{-1}$).

To fit the data and analyze the metal adsorption rate, linear models of pseudo-first-order kinetics Eq. (2), pseudo-second-order kinetics Eq. (3), and the Elovich kinetic equation Eq. (4) were used.

$$qt = qe \times (1 - e^{-k1 \times t}) \quad (2)$$

$$qt = \frac{qe^2 \times k_2 \times t}{1 + qe \times k_2 \times t} \quad (3)$$

$$qt = \frac{1}{\beta} ln(1 + \alpha\beta t) \quad (4)$$

Where qt and qe represent the adsorption capacity at any time and at equilibrium, respectively, in ($mg \cdot g^{-1}$); k_1 is the pseudo-first-order adsorption rate constant (min^{-1}); k_2 is the pseudo-second-order adsorption rate constant ($g \cdot mg^{-1} \cdot min^{-1}$); α is the initial adsorption rate ($mg \cdot g^{-1} \cdot min^{-1}$), and β is the adsorption constant ($mg \cdot g^{-1}$).

To identify the actual rate-limiting step in the adsorption separations, the intraparticle diffusion kinetic model (5) and the Boyd equation (6) and (7) were applied.

$$qt = K_d * t^{0,5} + C \quad (5)$$

Where qt is the amount of metal adsorbed in the solid phase ($mg \cdot g^{-1}$) at time t (min); Kd is the intraparticle diffusion coefficient ($mg \cdot g^{-1} \cdot min^{0,5}$), obtained from the slope, and C is the intercept of the qt versus $t^{0,5}$ graph, representing the constant related to diffusion resistance ($mg \cdot g^{-1}$).

$$F < 0{,}85: Bt = \left(\sqrt{\pi} - \sqrt{(\pi - (\frac{\pi^2 F}{3})}\right)^2 \quad (6)$$

$$F > 0.85: Bt = -0.49770 - \ln(1 - F)$$

$$B = \frac{\pi^2 D}{r^2} \quad (7)$$

Where F is the ratio qt/qe; Bt is the mathematical function of F; D is the effective diffusion coefficient ($cm^2 \cdot min^{-1}$); r is the particle radius (cm); and B is the Boyd model constant (slope).

2.3.2 Adsorption Isotherm

The adsorption isotherms were determined to evaluate the adsorbent's efficiency. The tests were conducted in duplicates, using 0.05 g of biomass with 10 mL of a lead solution at a buffered pH

of 5.5, with concentrations ranging from 10 mg.L^{-1} to 700 mg.L^{-1}, at the equilibrium time established by the kinetic test, under agitation at 150 rpm.

As in the kinetic method, after reaching the contact time, the samples were filtered, and the concentrations were subsequently determined by FAAS.

Adsorption isotherm models were applied to the experimental data using the nonlinear equations of Langmuir, Freundlich, Temkin, and Sips, respectively, according to the following equations:

$$qe = \frac{qmax \times K_L \times Cf}{1 + K_L \times Cf} \quad (8)$$

$$qe = K_F \times Cf^{\frac{1}{n}} \quad (9)$$

$$qe = \frac{RT}{b} ln(K_T \times Cf) \quad (10)$$

$$qe = \frac{qmax \times Ks \times Cf^{\beta s}}{1 + Ks \times Cf^{\beta s}} \quad (11)$$

Where *qe* is the adsorption capacity at equilibrium (mg·g^{-1}), q_{max} is the theoretical monolayer capacity of the adsorbate on the adsorbent (mg·g^{-1}); Ce is the equilibrium ion concentration in the solution (mg·L^{-1}); K_L is the Langmuir constant directly related to the equilibrium constant (L·mg^{-1}); K_F is the Freundlich constant ((mg·g^{-1})(L·mg^{-1})^{1}/n); 1/n is the Freundlich adsorption intensity constant; K_T is the Temkin constant (L·mg^{-1}); K_S is the Sips constant (L·mg^{-1}); n is the surface heterogeneity factor of the adsorbent; R is the universal gas constant (J·mol^{-1}·K^{-1}); T is the temperature (K); and b is the adsorption heat (J·mol^{-1}).

2.3.3 Adsorption Thermodynamics

The thermodynamic parameters estimated in this study include the standard Gibbs free energy change (ΔG°), which is related to the spontaneity of the adsorption process; the standard entropy change (ΔS°), which is related to the disorder of the system; and the standard enthalpy change (ΔH°), which indicates whether the process absorbs heat (endothermic) or releases heat (exothermic).

To calculate these thermodynamic parameters, three distinct temperatures were used: 25°C (ambient temperature), 15°C, and 35°C.

The calculations for determining the values of ΔG°, ΔH°, and ΔS° were performed using the following linear equations:

$$\Delta G° = \Delta H° - T\Delta S° \quad (12)$$

$$\Delta G° = -RTLn(K) \quad (13)$$

$$Ln(K) = \frac{-\Delta H°}{RT} + \frac{\Delta S°}{R} \quad (14)$$

$$K_g = qe/Ce \quad (15)$$

$$K_e^0 = 1000.Kg.d \quad (16)$$

3. Results and Discussions

3.1 Material Characterization

3.1.1 Point of Zero Charge (pH_{PZC})

Organic functional groups on the surface of the biosorbent can acquire either a negative or positive charge depending on the pH of the solution. At pH values higher than the pH_{PZC}, the sites will primarily be in the dissociated form and will acquire a negative charge. Conversely, at pH values lower than the pHpzc, these groups will be in the protonated form, resulting in a positive charge.

For lead (II) ions (Pb^{2+}), which are cations, it is essential that the adsorbent surface is covered with negatively charged species to promote the electrostatic attraction and removal of this metal.

Figure 1 depicts the graphical representation of the pH_{PZC} of the raw SST bioadsorbent. As shown in the figure, a constant pH range between 5 and 8 is observed, with an average final pH of 5.3, which is considered the pH_{PZC} value. This value was adjusted to a pH of 5.5 to enhance the adsorption of more soluble metal ion compounds.

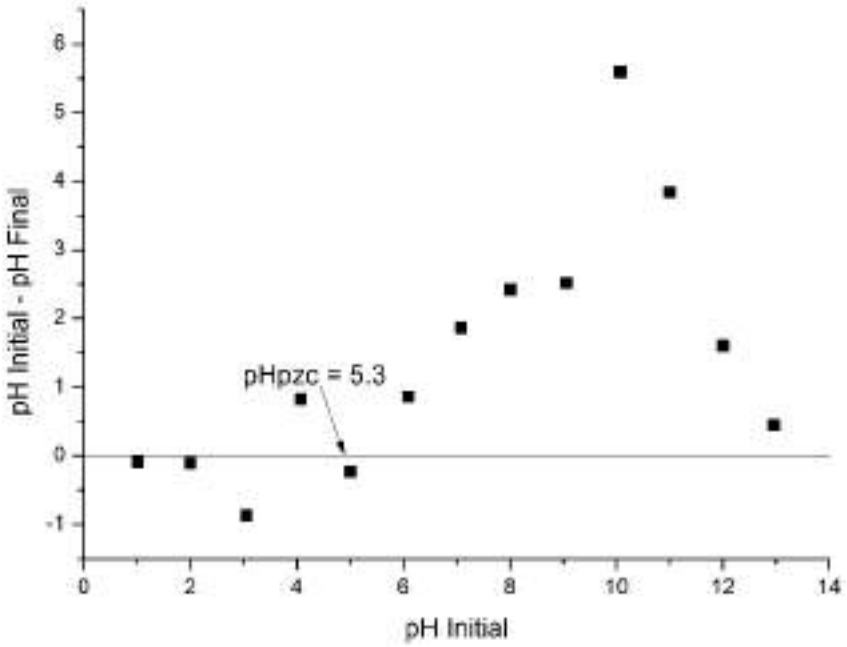


Figure 1 – pHpzc of the SST biosorbent.

3.1.2 Scanning Electron Microscopy (SEM)

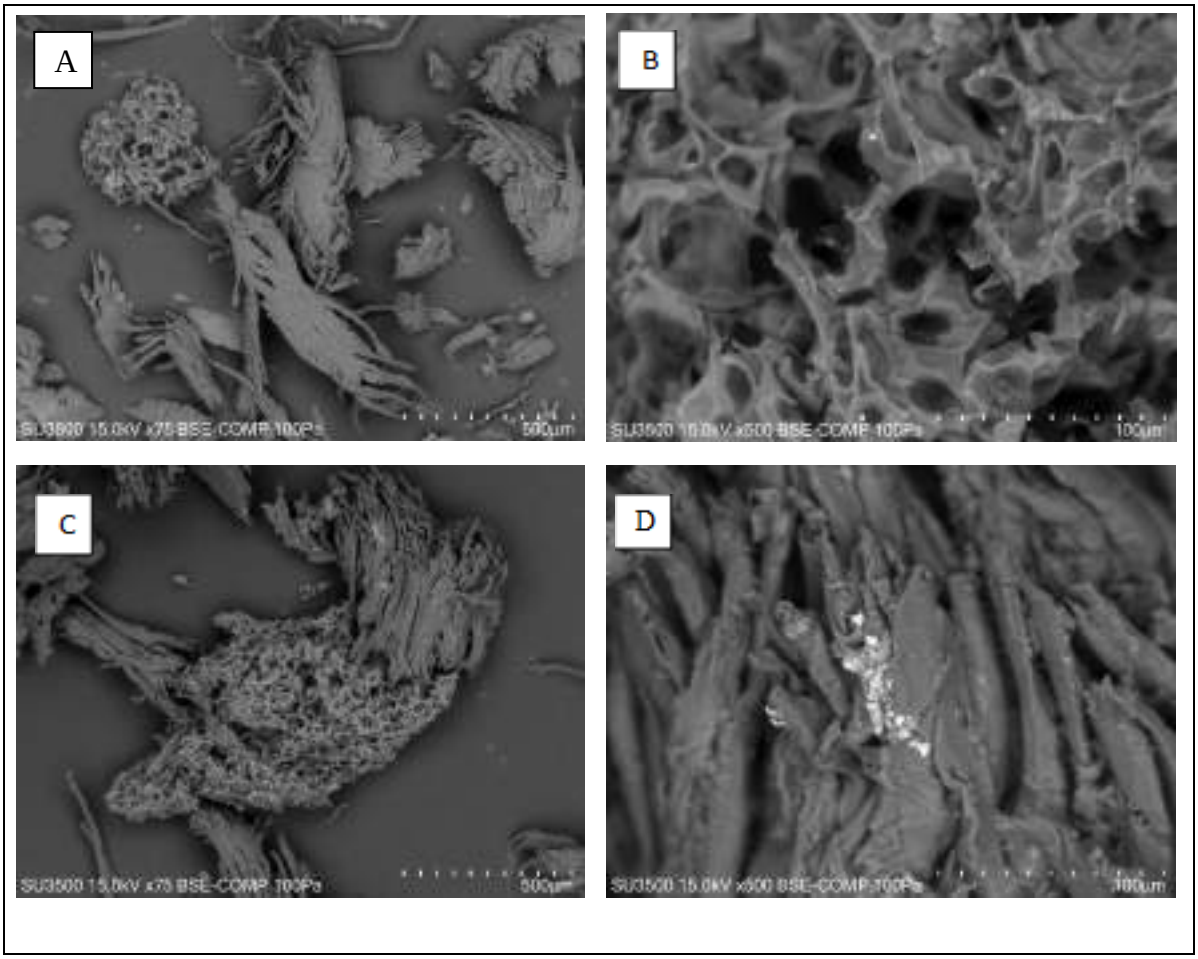


Figure 2 – Scanning Electron Microscopy images of TSM: (A) 75x before the adsorption process, (B) 500x before the adsorption process, (C) 75x after the adsorption process, and (D) 500x after the adsorption process.

The images obtained from the scanning electron microscopy (SEM) allow visualization of the morphology of the raw material before and after contact. The micrographs are presented in Figure 2, with magnifications of 75x (A and C) and 500x (B and D), showing the material before and after the adsorption process, respectively.

In the SEM images, the material exhibits roughness and porosity, characteristics typical of fibrous plant materials. With increased magnification, different shapes and sizes of pores become apparent, generally originating from the cell wall structure of the precursor biomass. At 500x magnification, porous spaces with surface irregularities and varying depths of porous channels are clearly visible.

These characteristics are important for characterizing the adsorbent, as they help identify the adsorption process. As highlighted by Barros (2020), the material's surface is highly porous, irregular, and heterogeneous—features that are advantageous for the adsorption of metals in aqueous solutions. Adsorbed components accumulate on the external surface, and a larger surface area per unit mass enhances adsorption.

In Figures 2C and 2D, a brighter region on parts of the adsorbent's surface is visible, which may indicate the presence of adsorbed Pb (II) ions at those points.

3.1.3 Fourier Transform Infrared Spectroscopy (FTIR)

Through Fourier-transform infrared spectroscopy (FTIR), it was possible to characterize the reactive functional groups present in the material, thereby enabling the investigation of the reaction mechanism involved (Fig. 3) (Salih et al., 2025).

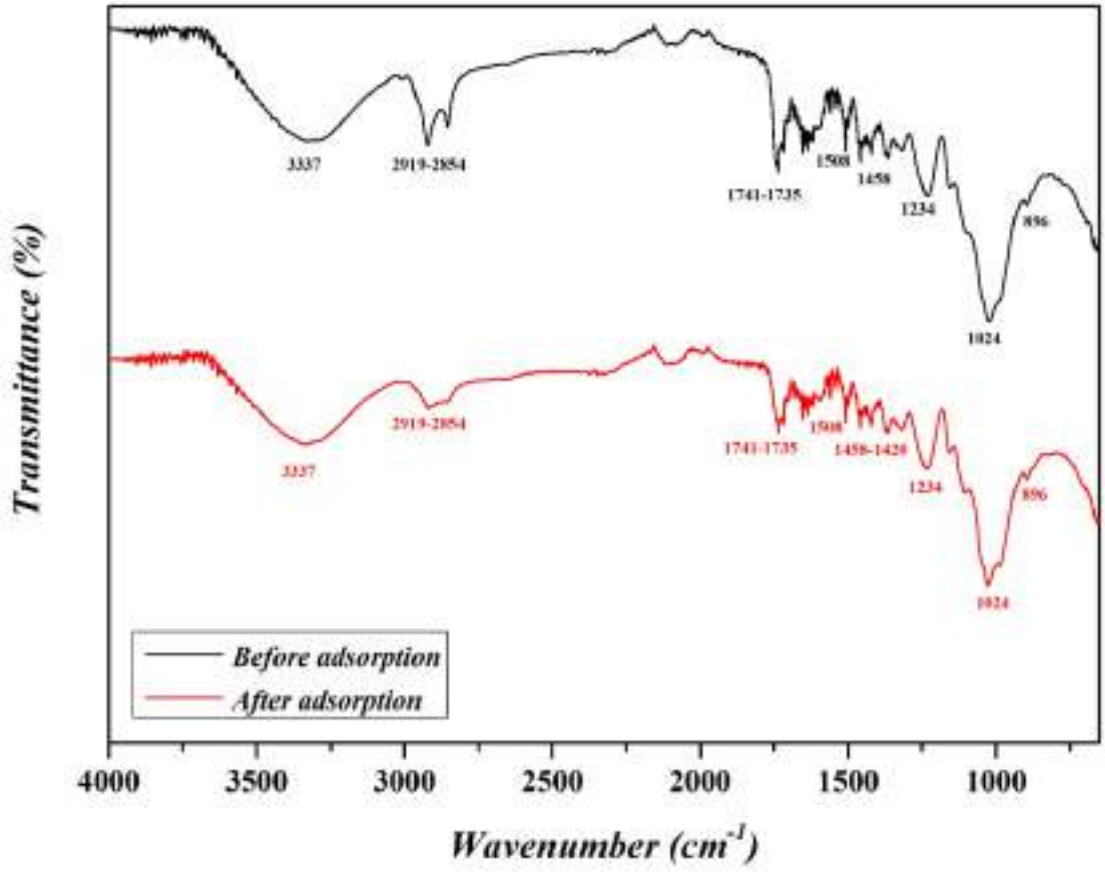


Figure 3 – Characterization of raw SST and post contact with Pb (II) ion

As observed in Figure 3, the peaks in both spectra at the vibration frequency of 3337 cm^{-1} correspond to O-H and N-H stretching, indicating the presence of hydroxyl groups and amino groups from proteins, fatty acids, carbohydrates, and lignin found in plants. The two smaller peaks at 2919 cm^{-1} and 2854 cm^{-1} correspond to asymmetric C-H vibrations of carbonyl groups and the -OH stretch of carboxylic acids, respectively, relating to the methyl groups in lignin and cellulose. The peaks at 1741-1735 cm^{-1} are associated with C=O stretching vibrations, which, along with the O-H observed at 3337 cm^{-1}, justify the presence of carboxylic acids. The peaks at 1458-1420 cm^{-1} correspond to C-H, indicative of alkanes with bending vibrations that may be related to angular vibrations of $-CH_3$ and $-CH_2-$ groups. A peak at 1234 cm^{-1} represents CO and OH stretching in-plane in polysaccharides (Acquah et al., 2016).

Thus, through infrared analysis, it is possible to infer that SST exhibits functional groups characteristic of lignocellulosic materials (Neris et al., 2019). C=O vibrational bonds in hemicelluloses and extractive compounds such as esterified resin acids, waxes, and fats (Javier et al., 2021) are present. The lower peaks at 896 and 1024 cm^{-1}, related to CH deformation in cellulose and CO stretching in polysaccharides, fall within the "fingerprint" region and confirm the presence of polysaccharides (Acquah et al., 2016).

Therefore, the FTIR spectrum characterizes the biomass as lignocellulosic in origin, a component of dried plant material. Lignocellulosic materials composed of cellulose, hemicellulose, and lignin are abundant resources for energy and chemical production (Mohammadabadi et al., 2020).

The presence of hydroxyl (-OH), carboxylic (-COOH), and carbonyl (C=O) groups in the chemical structure of the bioadsorbent significantly contributes to interactions with metal ions. These functional groups contain oxygen atoms with non-bonding electron pairs capable of acting as electron donors, thus facilitating electrostatic attractions, coordination complex formation, or potential ion-exchange mechanisms with Pb (II) ions. The FTIR analysis (Fig. 3) revealed notable shifts in the characteristics bands at 2919–2854, 1741–1735, and 1508 cm^{-1}, corresponding precisely to these functional groups, suggesting potential involvement of these functional groups in the adsorption mechanism. Zolgharnein and Farahani (2023) further explain that a marked decrease in peak intensity confirms the interaction between metal ions and oxygen atoms, reinforcing the potential of the biomass as a promising material for the removal of toxic metals from aqueous solutions.

3.2 Batch Adsorption Tests

3.2.1 Adsorption Kinetics

The adsorption rate, determined through the adsorption kinetics study, was based on the determination of the adsorptive capacity (qt) of SST in the liquid phase relative to the contact time (t) with the Pb II adsorbate, as represented in the graph shown in Figure 4.

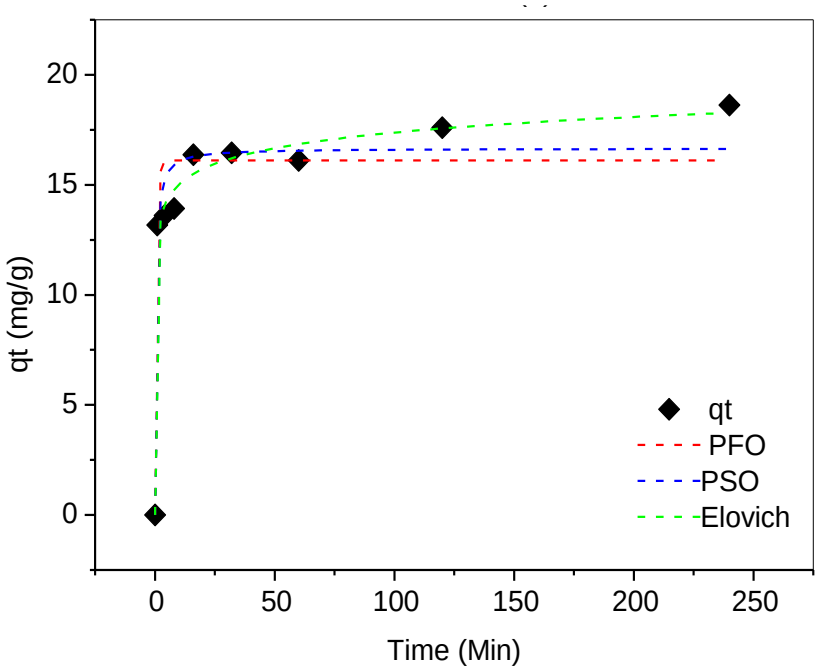


Figure 4 – Adsorption kinetics tested for Pb (II) ion removal under test conditions: 25°C, pH 5.5, 102 mg. L^{-1}, 100 rpm, and 0.05 g of SST adsorbent

Analyzing Figure 4, it is observed that the adsorption rate reaches equilibrium around 30 minutes. Initially, the process occurs quite rapidly, but it slows down over time. The curve of the models indicates that even at the early minutes, the adsorptive capacity (qt) shows a significant reduction in the rate of Pb (II) ions. According to Khan (2020), the higher adsorption rate in the initial stages may be due to the greater number of available sites on the adsorbent surface.

The data in Figure 4 were fitted to the experimental data of pseudo-first-order (PFO) and pseudo-second-order (PSO) adsorption kinetics models, as well as the non-linear Elovich model. The statistical parameters applied to the non-linear regression model fittings are presented in Table 1.

Table 1 – Kinetic parameters of the PFO, PSO and Elovich models using SST as adsorbent.

Models	**Parameters**							
	q_{model} mg.g^{-1}	q_{max} mg.g^{-1}	R^2 Adjusted	χ^2	SSE	k_1 g.mg^{-1}.min^{-1}	α mg.g^{-1}.min^{-1}	β mg.g^{-1}
PFO	16.1097	18.6	0.9091	2.8093	19.6658	1.6831	-	-
PSO	16.6545	18.6	0.9405	1.8390	12.8729	0.16141	-	-
Elovich	18.2698	18.6	0.9873	0.3919	2.7430	-	$2.33069x10^5$	0.97508

According to Figure 4 and the data in Table 1, it is possible to observe a better fit with the Elovich model. Although initially developed for gas adsorption on solid adsorbents, the Elovich model adapts well to studies involving liquid-phase fluids.

The Elovich model demonstrated the best linear regression data and error function, with an R^2 value approaching unity and the lowest SSE and chi² errors compared to other models. Additionally, the maximum experimental capacity (q_{max}) and model capacity (q_{model}) values were very close.

The Elovich equation is generally applicable to chemisorption kinetics, as described by Olivares (2011). The Elovich model is based on a general second-order reaction mechanism for the adsorption process, assuming that the adsorbent's active sites are heterogeneous and exhibit varying activation energies for chemisorption.

Thus, comparing the experimental data to the Elovich model reveals that the adsorption process has predominant characteristics of chemisorption. Furthermore, the high α value indicates a high initial adsorption rate and suggests that the attraction of the material occurs via a chemical pathway. The β value, representing the extent of surface coverage and activation energy involved, is low, indicating a rapid adsorption rate with minimal activation energy required for the process.

To determine the rate-limiting step of the adsorption process in the experiment, the Boyd intraparticle model was applied, resulting in the Bt vs. t (min) graph. The Boyd equations described in section 2.3.1 were used to establish the analytical parameters outlined in Figure 5.

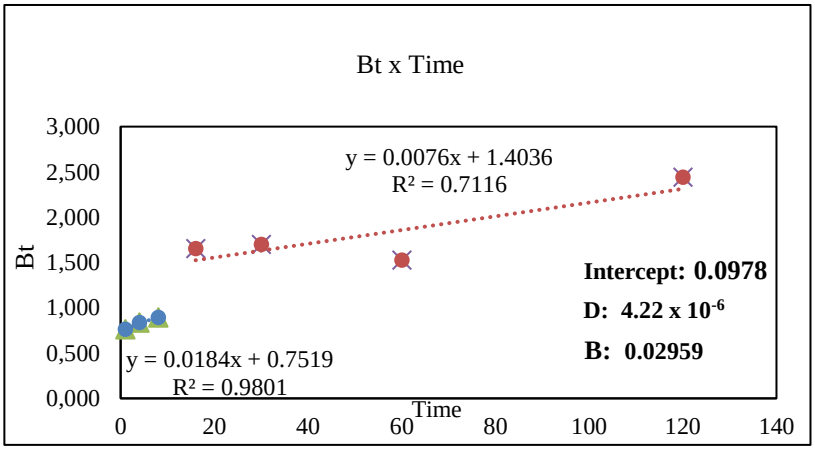


Figure 5 – Boyd's Linear Intraparticle Diffusion Model for SST. Where: BB is the Boyd model constant (determined by the slope of the straight), D is the coefficient for Boyd's Effective Diffusion in $cm^2.min^{-1}$, and b is the linear coefficient of the straight (intercept).

According to the data presented, it is observed that the graph does not pass through the origin. Therefore, the Boyd constant is not zero, suggesting that the rate-limiting step of the process is not intra-film diffusion (Yadav, 2023). Additionally, as noted by El-Khaiary and Malash (2011), whether the graph is non-linear or linear, if it does not intersect the origin, the rate-limiting step may be film diffusion or chemical reaction.

With an R^2 value close to unity, the model shows a favorable fit. Furthermore, since the b value of the linear equation of the first line deviates from zero, it is possible that the rate-limiting step

is governed by external or intraparticle diffusion, where there is a significant mass transfer of Pb (II) in the SST.

3.2.2 Adsorption Isotherm

The adsorption isotherm was evaluated based on the variation in adsorptive capacity (*qe*) as a function of the equilibrium concentration of the adsorbate (*Ce*). Figure 6 shows the experimental results for the adsorption of Pb (II) ions compared with the Langmuir, Freundlich, Temkin, and Sips models. According to Figure 6, it is observed that the adsorptive capacity (*qe*) increases with the concentration of the adsorbate (*Ce*), and equilibrium is reached at a concentration of 100 $mg.L^{-1}$.

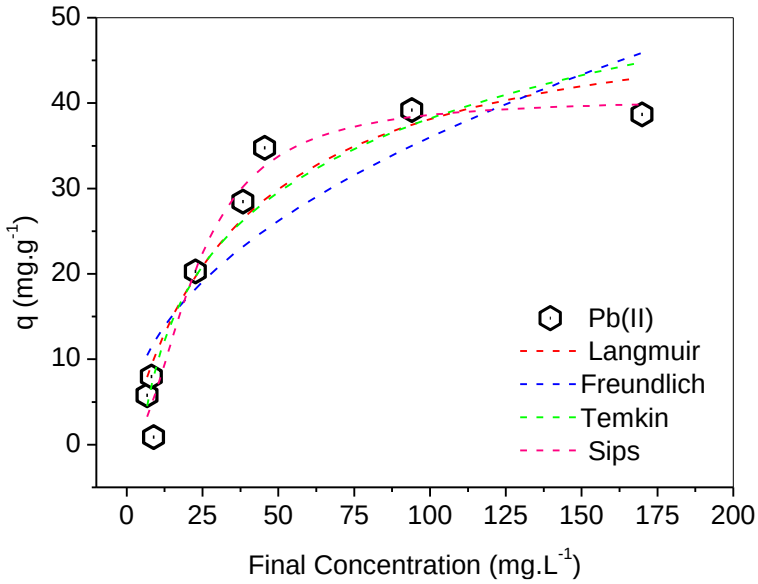


Figure 6 – Equilibrium isotherm models of Pb (II) ions to SST adsorbent, until C_0 = 175 mg. L^{-1}. Test conditions: 25°C, pH 5.5, 60 minutes, 150 rpm e 0.05 g adsorbent.

Table 2 – Statistical parameters calculated for adsorption isotherms applied to the Langmuir, Freundlich, Temkin and Sips models.

Models	**Parameters**				
	$q_{max..experimental}$ ($mg.g^{-1}$)	46.0	**R^2 Adjusted**	**χ^2**	**SSE**
Langmuir	q_{max} ($mg \cdot g^{-1}$) K_L ($L \cdot mg^{-1}$)	52.57 0.02	0.894	25.4060	152.4
Freundlich	K_F ($mg \cdot g^{-1}$) ($L \cdot mg^{-1}$) $^{1/n}$ 1/n N	4.37 0.45 2.18	0.758	58.3360	350.0
Temkin	K_T ($L \cdot mg^{-1}$) b (J/mol)	0.21 12.47	0.903	23.3511	140.1
Sips	q_{max} ($mg \cdot g^{-1}$) K_S ($L \cdot mg^{-1}$) N	40.52 0.04 2.02	0.960	9.4309	47.1

The model that best fit the experimental data was the Sips model, as shown in Figure 6. However, to justify the adsorbent-adsorbate interactions, adsorption mechanisms, and surface-related information, according to Lima (2021), the statistical parameters of the isotherms were determined using the linear equations described in section 2.3.2 and are presented in Table 2.

The maximum adsorptive capacity determined experimentally was 46.0 $mg \cdot g^{-1}$, which is consistent with both the Langmuir and Sips models. However, considering the adjusted R^2 value closest to unity and the lower error functions (χ^2 and SSE), the Sips model demonstrates the best fit for the experiment.

In this regard, Aquareles (2023) notes that the Sips isotherm has the advantage of being more general than the Langmuir and Freundlich isotherms, as it reduces to each of these models under certain limits and can be related to chemical reactions that occur. Thus, the Sips model provides broader insights into the interactions between the adsorbent and adsorbate, elucidating the attractive or repulsive characteristics between them.

Additionally, the Sips model is associated with the energetic heterogeneity of the adsorbent-adsorbate system, which can arise from either the adsorbent, the adsorbate, or their interaction (Sips, 1950). By analyzing the parameter (n) and relating it to heterogeneity, it is observed that when (n) approaches unity (n = 1), it suggests that the system is energetically homogeneous. Conversely, if (n) deviates from 1, the adsorbent-adsorbate system is energetically heterogeneous (Pérez, 2020).

In this case, with (n = 2.02), the system deviated from unity, indicating that it is heterogeneous, which aligns with the infrared data for SST.

According to the experimental data and the Sips mathematical model, it can be inferred that the adsorbent-adsorbate interactions on SST occur heterogeneously and preferentially in a monolayer.

Comparing the adsorption capacity of SST for Pb (II) to other lignocellulosic materials of similar origin, such as biomass from husks and seeds found in the literature, Table 3 highlights SST as an excellent adsorbent for this metal, especially when compared to bioadsorbents derived from seed residuals.

Table 3 – Lignocellulosic bioadsorbents and maximum adsorption capacities with Pb (II)

Adsorbent	**$q_{max,exp}$ ($mg.g^{-1}$)**	**Reference**
Caryocar coriaceum WITTM barks	106.38	(Menezes et al., 2020)
Raw Neem	17.96	(Costa et al., 2020)
Ziziphus joazeiro barks	58.3	(Santos et al., 2022)
Azadirachta indica A.Juss Seeds	17.96	(Costa et al., 2020)
Pepper seeds	48.0	(Forgionny et al., 2021)
Coriander seeds	19.76	(Shamkhi et al., 2022)
Umbu Seed	46.0	This work

3.2.3 Adsorption Thermodynamics

The thermodynamic study provided insight into the effect of temperature on the adsorption of Pb (II) ions by SST. The thermodynamic parameters (ΔG, ΔH, and ΔS) were determined using the equations described in section 2.3.3, utilizing the equilibrium constant (Kg) from equation (15), where *qe* is the equilibrium capacity ($mg.g^{-1}$) and *Ce* is the equilibrium concentration of the metal ions ($mg.L^{-1}$).

Once the values of K are obtained, a correction must be applied to make the constant dimensionless, as it will be used in the natural logarithm function (Ln) within the van't Hoff equation, which requires a dimensionless input. For this purpose, Equation (16) from Section 2.3.3, as described by Lima et al. (2019), should be used. In this equation: Kg is the constant obtained from the isothermal models ($L.mg^{-1}$); 1000 is the conversion factor from $L.mg^{-1}$ to $L.g^{-1}$; and d represents the density of water (1000 $g.L^{-1}$), assuming that the density of the adsorbate solution is approximately equal to that of water.

In Figure 7(A), an increase in adsorption capacity is observed with rising temperature, from 14.1 $mg.g^{-1}$ at 15°C to 16.36 $mg.g^{-1}$ at 35°C, indicating a positive enthalpy change (ΔH > 0), confirming the process is endothermic, as presented in Table 4.

As highlighted by Ozsin (2019), the endothermic nature of adsorption can be attributed to the increased mobility of heavy metal ions and an enhanced diffusion rate of adsorbate molecules through the external boundary layer and into the internal pores of the adsorbent, due to a reduction in solution viscosity.

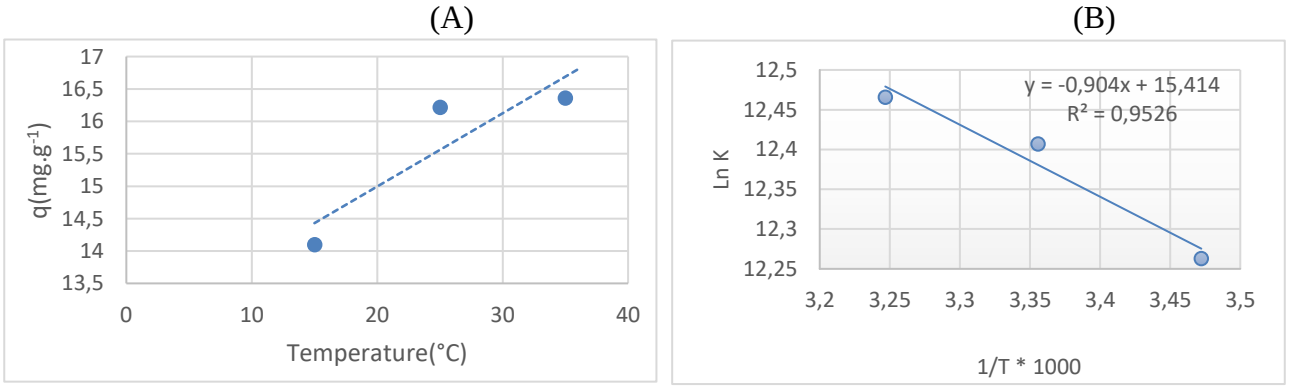


Figure 7 – Linear modeling for the determination of ΔG, ΔH, and ΔS for Pb (II) ions in contact with SST under the conditions of 15 °C, 25 °C, and 35 °C, at 60 minutes, 150 rpm, and pH 5.5.

Table 4 – Thermodynamic Parameters determined from Figure 7 (B).

Temperature (ºC)	**ΔGº (kJ.mol^{-1})**	**ΔHº (kJ.mol^{-1})**	**ΔS (J.mol^{-1}. K^{-1})**
15	-36.90	7.52	128.15
25	-38.18		
35	-39.46		

The data presented in Table 4 were obtained using the slope and intercept values from the linear regression line shown in Figure 7(B). As indicated by the results, Gibbs free energy (ΔG°) decreases with increasing temperature and assumes negative values, indicating the spontaneous nature of the process. Notably, the process becomes more thermodynamically favorable as the standard Gibbs free energy becomes more negative with increasing temperature, regardless of the nature of the adsorbent, suggesting enhanced efficiency in the adsorption of Pb (II) at lower temperatures (Fenti et al., 2019; Erdol-Aydin et al., 2024). Furthermore, the positive value of ΔSads indicates an increase in entropy at the solid–liquid interface, suggesting structural changes in both the adsorbate and the adsorbent (Nascimento, 2014), which is consistent with the findings from the FTIR analysis.

The nature of the adsorption process can be either chemical or physical, depending on the interactions between the binding sites. According to Azadian (2021), negative ΔG° values suggest a physisorption mechanism. Additionally, Hasanzadeh et al. (2024) highlight that enthalpy values below 40 $kJ.mol^{-1}$ indicate that the process does not require activation energy, as physical adsorption involves attractive forces between the adsorbent and the adsorbate. In this context, since the experimental process was spontaneous—with a decrease in the system's free energy—and involved heat absorption (endothermic, $\Delta H° > 0$) with enthalpy values below 40 $kJ.mol^{-1}$, the adsorption mechanism reveals characteristics of physisorption.

4. Conclusion

The present study demonstrated that SST biomass is an effective bioadsorbent for the removal of lead Pb (II) ions from aqueous solutions. Based on batch adsorption experiments, the material reached a maximum adsorption capacity of 46.0 $mg \cdot g^{-1}$. When compared to other bioadsorbents reported in the literature, SST biomass showed competitive efficiency, particularly among seed-derived lignocellulosic materials.

Structural characterization by FTIR and SEM confirmed the lignocellulosic nature of the adsorbent, revealing the presence of cellulose, hemicellulose, and lignin, as well as a porous and irregular surface that enhances its adsorption capacity.

Kinetic studies indicated that the Pb (II) adsorption process is relatively fast, reaching equilibrium within approximately 30 minutes. Among the tested models, the Elovich model showed the best fit, suggesting a possible chemisorption. The Boyd model indicated that the rate-limiting step is governed by external (film) diffusion.

The equilibrium data were best described by the Sips isotherm model, which is consistent with the observed surface heterogeneity. Thermodynamic analysis revealed that the adsorption process is

spontaneous, endothermic, and accompanied by increased system disorder, with characteristics compatible with physisorption.

Overall, SST biomass proved to be a promising, sustainable, and low-cost material for the removal of toxic metals from contaminated water, contributing to the advancement of environmentally friendly technologies and supporting circular economy practices in effluent treatment.

Funding: This research was supported by the Fundação Cearense de Apoio ao Desenvolvimento Científico e Tecnológico Grant Nº BP5--0197-00133.01.00/22 and the Conselho Nacional de Desenvolvimento Científico e Tecnológico – CNPq Grants Nº 409820/2023 – 7 and Nº 316615/2023-4.

References:

ACQUAH, G.E. et al. Rapid Quantitative Analysis of Forest Biomass Using Fourier Transform Infrared Spectroscopy and Partial Least Squares Regression. **Journal of Analytical Methods in Chemistry**, 2016, p.1–10. pmid:28003929

AGUARELES, M. et al. Mathematical analysis of a Sips-based model for column adsorption. **Physica D: Nonlinear Phenomena**. Volume 448, 2023. https://doi.org/10.1016/j.physd.2023.133690.

AWUAL, M.R. Innovative composite material for efficient and highly selective Pb (II) ion capturing from wastewater. **J. Mol. Liq**. 284, 502-510, 2019. https://doi.org/ 10.1016/j.molliq.2019.03.157.

AZADIAN, M. et al. Kinetic, isotherm, thermodynamic, and adsorption capacity studies of magnetic Spirulina microalgae onto zinc (II). **Environ Prog Sustainable Energy**, 2022, 41(2):e13751. doi:10.1002/ep.13751.

BARROS, R. S.; et. al.; Produção de carvão ativado da casca do babaçu e sua eficiência no tratamento de água para o consumo humano. **Engenharia Florestal: Desafios, Limites e Potencialidade, editora cientifica digital,** [S.L.], p. 654-685, 2020.

Benettayeb A, Malbenia J, Chitepo RM, Haddou B (2024) Facile fabrication of new bioadsorbents from Moringa oleifera and alginate for efficient removal of uranium (VI). **J Radioanal Nucl Chem**. https://doi-org.ez152.periodicos.capes.gov.br/10.1007/s10967-024-09470-1

CAROLIN, C. Femina; KUMAR, P. Senthil; SARAVANAN, A.; JOSHIBA, G. Janet; NAUSHAD, Mu. Efficient techniques for the removal of toxic heavy metals from aquatic environment: A review. **Journal of Environmental Chemical Engineering**, [S. l.], v. 5, n. 3, p. 2782–2799, 2017. Disponível em: https://doi.org/10.1016/j.jece.2017.05.029

COSTA, W. D. et al. Removal of copper(II) ions and lead(II) from aqueous solutions using seeds of Azadirachta indica A. Juss as bioadsorvent. **Environ. Res**. V.183, 2020. 109213. dhttps://doi.org/10.1016/j.envres.2020.109213.2020, vol. 183.

DO, Duong D. Adsorption analysis: Equilibria and kinetics. Imperial College Press. Vol. 2. Londres, 1988.

E.C. Lima, A. Hosseini-Bandegharaei, J.C. Moreno-Piraján, I. Anastopoulos A critical review of the estimation of the thermodynamic parameters on adsorption equilibria. Wrong use of equilibrium constant in the Van't Hoof equation for calculation of thermodynamic parameters of adsorption. **J. Mol. Liq**., 273 (2019), pp. 425-434. https://doi.org/10.1016/j.molliq.2018.10.048

E.C Lima, M.H. Dehghani, A. Guleria, F. Sher, R. R. Karri, G.L. Dotto, H.N. Tran. Adsorption: Fundamental aspects and applications of adsorption for effluent treatment. In: Green Technologies for Defluorination of Water (M.H. Dehghani, R.R. Karri, E.C. Lima). **Elsevier**, Amsterdan, Netherlands, 2021. Chapter 3, pp.41-88. DOI: 10.1016/C2020-0-02666-6

EL-KHAIARY, M.I; MALASH, G.F: Common data analysis errors in batch adsorption studies. **Hydrometallurgy**. 2011, V. 105, 314–320.

El Mouden A, El Messaoudi N, El Guerraf A et al (2023) Removal of cadmium and lead ions from aqueous solutions by novel dolomite-quartz@Fe3O4 nanocomposite fabricated as nanoadsorbent. **Environ Res** 225:115606. https://doi-org.ez152.periodicos.capes.gov.br/10.1016/J.ENVRES.2023.115606.

Erdol-Aydin N, Sezer S, Esin B, Nasun-Saygili G. Removal of boron from wastewaters using valonia-tannin-based biosorbent produced via spray drying. **Adsorption Science & Technology.** 2024;42. doi:10.1177/02636174241266707

Fenti A, Iovino P, Salvestrini S (2019) Some remarks on “A critical review of the estimation of the thermodynamic parameters on adsorption equilibria. Wrong use of equilibrium constant in the Van’t Hoof equation for calculation of thermodynamic parameters of adsorption” - **Journal of Molecular Liquids**, 273 (2019) 425–434. https://doi.org/10.1016/j.molliq.2018.12.019

FIDELES, R.A. et al. Trimellitated sugarcane bagasse: A versatile adsorbent for removal of cationic dyes from aqueous solution. Part I: Batch adsorption in a monocomponent system. **Journal of Colloid and Interface Science**, v. 515, p. 172-188, 2018.

FORGIONNY, A. et al. Understanding mechanisms in the adsorption of lead and copper ions on chili seed waste in single and multicomponent systems: a combined experimental and computational study. **Environmental Science and Pollution Research**, 2021, vol. 28, p. 23204–23219.

Ghosh, S., Benettayeb, A., Meskini, M., Lal, B., Al-Sharify, Z. T., Ajala, O. J., Hosseini-Bandegharaei, A. (2024). Advancing wastewater treatment with *Azolla filiculoides* waste: a

comprehensive review of adsorption applications. **Environmental Technology Reviews, 13(1)**, 359–378. https://doi-org.ez152.periodicos.capes.gov.br/10.1080/21622515.2024.2354126.

GIRI, D.D et al. Removal of lead from synthetic wastewater by biosorbents prepared from seeds of Artocarpus heterophyllus and Syzygium cumini. **Chemosphere,** 2022, 287, 132016.

GODIN B.; AGNEESSENS R.; GOFFLOT S. Revue bibliographique sur les méthodes d'analyse des polysaccharides structuraux des biomasses lignocellulosiques. **Biotechnol. Agron. Soc. Environ.** 2011 15(1), (165-182).

Granado-Castro, M.D.; Galindo-Riaño, M.D.; Gestoso-Rojas, J.; Sánchez-Ponce, L.; Casanueva-Marenco, M.J.; Díaz-de-Alba, M. Ecofriendly Application of *Calabrese* Broccoli Stalk Waste as a Biosorbent for the Removal of Pb (II) Ions from Aqueous Media. **Agronomy,** 2024, *14*, 554. https://doi.org/10.3390/agronomy14030554.

IHA, L. C. N.; CRUZ, O. L. M. Use of scanning electron microscopy in the cochlea of guinea pigs. **Brazilian Journal of Otorhinolaryngology**, [S.L.], v. 86, n. 2, p. 222-227, mar. 2020.

JAVIER-ASTETE, R.; JIMENEZ-DAVALOS, J.; ZOLLA, G. Determination of hemicellulose, cellulose, holocellulose and lignin content using FTIR in *Calycophyllum spruceanum* (Benth.) K. Schum. and *Guazuma crinita* Lam. **Plos One** 2021, 16. https://doi.org/10.1371/journal.pone.0256559

K.A.M. Salih, K.G. Zhou, E. Guibal, E.A. Basiony, L.A. Nassar, A.A.H. Abdel-Rahman, M.F. Hamza. Dual strategy for enhanced and selective uranium sorption by ion-imprinting functionalized chitosan - fast and efficient recovery from processed acid ore leachate. **Chemical Engineering Journal,** 505 (2025), Article 159469, https://doi.org/10.1016/j.cej.2025.159469.

KHAN, N. et al. Surface Oxidized and Un-Oxidized Activated Carbon Derived from Ziziphus jujube Stem, and Its Application in Removal of Cd (II) and Pb (II) from Aqueous Media. **SN Applied Sciences**. 2020, 2, 753.

L. Largitte, T. Brudey, T. Tant, P. Couespel Dumesnil, P. Lodewyckx. Comparison of the adsorption of lead by activated carbons from three lignocellulosic precursors. **Microporous and Mesoporous Materials**, 2016, vol. 219, p. 265-275. https://doi.org/10.1016/j.micromeso.2015.07.005.

L.D. Hafshejani, S.B. Nasab, R.M. Gholami, M. Moradzadeh, Z. Izadpanah, S.B. Hafshejani, A. Bhatnagar, Removal of zinc and lead from aqueous solution by nanostructured cedar leaf ash as biosorbent**, J Mol Liq**. 211 (2015) 448–456. https://doi.org/10.1016/j.molliq.2015.07.044.

Malbenia John M, Benettayeb A, Belkacem M et al. (2024) An overview on the key advantages and limitations of batch and dynamic modes of biosorption of metal ions. **Chemosphere,** 357:142051. doi-org.ez152/10.1016/J.CHEMOSPHERE.2024.142051.

MENESES, J. M. C. et al. Equilibrium, kinetics and thermodynamics of lead (II) adsorption in bioadsorvent composed by Caryocar coriaceum Wittm barks. **Chemosphere**, vol. 261, 2020.

MENEZES, J. M. C. et al. Kinetic and thermodynamic study of copper (II) IONS biosorption by Caryocar Coriaceum Wittm bark. **Sustainable Chemistry and Pharmacy**. V. 19, p. 100364, 2021. DOI: https://doi.org/10.1016/j.scp.2020.100364

MOHAMMADABADI S. I.; JAVANBAKHT V. Lignin extraction from barley straw using ultrasound-assisted treatment method for a lignin-based biocomposite preparation with remarkable adsorption capacity for heavy metal. Intern. **Jour. of Biolog. Macromol**., v. 164 p. 1133 – 1148, 2020.

MOREIRA, J. V. I.; et. al. Avaliação da Adsorção de Íons Níquel (II) e Cádmio (II) em Quitosana, Quitosana Reticulada e Carboximetilquitosana Reticulada. **Revista Virtual de Química**, [S.L.], v. 11, n. 1, p. 237-254, 2019.

NASCIMENTO, R. F. do, et al. **Adsorção: aspectos teóricos e aplicações ambientais**. 1. ed. Fortaleza, 2014. p. 256

NERIS, J. B. et al. Evaluation of adsorption processes of metal ions in multi-element aqueous systems by lignocellulosic adsorbents applying different isotherms: A critical review. **Chemical Engineering Journal**, v. 357, p. 404–420, 2019.

OJEDOKUN, A.T; BELLO, O.S. Sequestering heavy metals from wastewater using cow dung. **Water Resour Ind**. 2016, V. 13, Pag. 7–13. https://doi.org/10.1016/j.wri.2016.02.002.

OLIVARES, J. Cruz; et. al. Thermodynamical and analytical evidence of lead ions chemisorption onto *Pimenta dioica*. **Chemical Engineering Journal**. v. 166, p. 814-821, 2011. https://doi.org/10.1016/j.cej.2010.11.041.

Oussadi, K., Al-Farraj, S., Benabdallah, B. *et al.* Wool keratin as a novel, alternative, low-cost adsorbent rich in various –N and –S proteins for eliminating methylene blue from water. **Biomass Conv. Bioref.** 15, 4803–4817 (2025). https://doi-org.ez152/10.1007/s13399-024-05851-4

OZSIN, G. et. al. Chemically activated carbon production from agricultural waste of chickpea and its application for heavy metal adsorption: equilibrium, kinetic, and thermodynamic studies. **Applied Water Science**, v. 9, p. 2-14, 2019. https://doi.org/10.1007/s13201-019-0942-8.

P. SenthilKumar, S. Ramalingam, V. Sathyaselvabala, SD Kirupha, S. Sivanesan. Removal of copper(II) ions from aqueous solution by adsorption using cashew nut shell. **Dessalinização**, v. 266 p. 63–71, 2011.

Pérez Antolinez, L. L., Paz Astudillo, I. C., Sandoval Aldana, A. P., y Peñaloza Atuesta, G. C. (2020). Uso de cáscara de cacao (Theobroma cacao) para la remocion de cromo en solución acuosa. **Revista EIA**, 17(34), 1–13. https://doi.org/10.24050/reia.v17i34.1393

POOJA, S.; DEBLINA, D.; ASWATHY, U.; ASHOK, K.N.; SU, S.L., SUNIL, K. Role of microbes in bioaccumulation of heavy metals in municipal solid waste: Impacts on plant and human being**. Environmental Pollution**. v.305, n.1, p.119248-119279, 2022.

REGALBUTO, J. R.; ROBLES, J. **The engineering of Pt/Carbon Catalyst Preparation**, University of Illinois: Chicago. 2004.

REIS, J. M. et al. Técnicas de remoção de metais de águas residuárias: uma revisão de literatura. **Research, Society and Development**, v. 11, n. 2, e5251126100, 2022. http://dx.doi.org/10.33448/rsd-v11i2.

S. Hasanzadeh, S. Mortazavi-Derazkola and R. Khosravi. Green synthesis of iron nanoparticles using Pistacia-atlantica leaf extract for enhanced removal of Cr (VI) from aqueous solution. **Desalination and Water Treatment**, 318 (2024) 100347. https://doi.org/10.1016/j.dwt.2024.100347.

SANTOS, et al. Pb (II) Ion Removal Potential in Chemically Modified *Ziziphus joazeiro Barks***. Int. J. Environ. Res. Public Health,** v. 19, p. 16283, 2022. https:// doi.org/10.3390/ijerph192316283

SANTOS, Y. T. da C. et al. Adsorption of Zn (II) íons by Ziziphus joazeiro barks in aqueous solutions. **Results in Chemistry**, v. 7, p. 101339, 2024. https://doi.org/10.1016/j.rechem.2024.101339

Şenol ZM, Elma E, El Messaoudi N, Mehmeti V (2023) Performance of cross-linked chitosan-zeolite composite adsorbent for removal of Pb2+ ions from aqueous solutions: experimental and Monte Carlo simulations studies. **J Mol Liq** 391:123310. https://doi-org.ez152.periodicos.capes.gov.br/10.1016/J.MOLLIQ.2023.123310.

SHAMKHI, H. J., HUSSEIN, T. K. Adsorption of Lead, Zinc, and Nickel Ions from Wastewater Using Coriander Seeds as an Adsorbent. **Journal of Ecological Engineering**, vol. 23, p. 158–168, 2022.

Sips, R. (1948) The Structure of a Catalyst Surface. **The Journal of Chemical Physics**, 16, 490-495. http://dx.doi.org/10.1063/1.1746922

W. L. L. da Silva et al. Estudo termodinâmico da adsorção de cobre (II) em montmorilonita organicamente modificada. **Cerâmica,** v. 64, p. 403-412, 2018. https://doi.org/10.1590/0366-69132018643712395

Zolgharnein J. e Farahani S. D. Experimental design optimization and isotherm modeling for removal of copper (II) by calcium-terephthalate MOF synthesized from recycled PET waste. **Journal of Chemometrics**, 2023, 37, 1, e3396. https://doi.org/10.1002/cem.3396.

Artigo 2 – Estudo das sementes de *Spondias tuberosa* como bioadsorvente in natura para a remoção de íons Cu (II) de solução aquosa utilizando o método em batelada.

Study of *Spondias tuberosa* seeds as an in natura bioadsorbent for the removal of Cu (II) ions from aqueous solution using the batch method.

Autores: Aliane Cristiane de Sousa Formiga, Yannice Tatiane da Costa Santos, Jorge Marcell Coelho Menezes, José Augusto Soares de Araújo, Henrique Douglas Melo Coutinho, Roseni da Silva Cardoso, Francisco José de Paula Filho, Raimundo Nonato Pereira Teixeira, Thâmara Martins Ismael de Sousa.

Revista: CLEAN-Soil Air Water (IF: 2,0) **CitScore**: 3,6

Situação: Submetido em 18/05/2026

ABSTRACT

Toxic metals, such as copper, widely used in industry, have been contaminating water resources, leading to severe environmental and health consequences. Therefore, it is crucial to implement techniques capable of removing or minimizing their accumulation in aquatic systems. In this context, this study aimed to investigate the efficiency of *Spondias tuberosa* seed residues (SST) in the removal of Cu (II) from aqueous solutions through the biosorption technique. The material was characterized by X-ray Fluorescence (XRF), Fourier Transform Infrared Spectroscopy (FTIR), and Scanning Electron Microscopy (SEM) before and after contact with the adsorbate. Batch adsorption experiments were then conducted using aqueous solutions containing the metal. The bioadsorbent exhibited porosity and surface roughness characteristics, as revealed by SEM. XRF analysis indicated a significant increase in copper concentration after contact, accompanied by a considerable decrease in the concentrations of K and Ca, suggesting a probable ion-exchange mechanism. FTIR analysis showed significant reductions in characteristic absorption bands, indicating the coordination of Cu(II) ions with surface chemical groups of the bioadsorbent, consistent with a complexation mechanism. Kinetic studies demonstrated rapid adsorption within the first 30 minutes, followed by a slower process reaching equilibrium at 240 minutes, best fitting the Elovich model, with the rate-limiting step occurring through film diffusion. The adsorption mechanism suggested that the process is favored at lower temperatures, with a maximum adsorption capacity of 12.0 $mg \cdot g^{-1}$. Different adsorption behaviors were observed at varying temperatures, described by the BET, Temkin, and Langmuir isotherm models at 288.15 K, 298.15 K, and 308.15 K, respectively. Thermodynamic parameters indicated a favorable, spontaneous, and exothermic adsorption process, with evidence supporting a predominantly physical adsorption mechanism. Reuse tests showed that SST has

potential for reuse, desorbing a considerable fraction of the adsorbed metal without structural damage. Thus, this study confirms that SST biomass can be effectively reused as a promising adsorbent for Cu (II) ion removal from aqueous solutions, contributing to both wastewater treatment and the mitigation of biomass accumulation in agro-industrial sectors, Presenting high efficiency, low cost, selectivity, and reusability.

Keywords: Biosorption; Copper (II) Ions; *Spondias tuberosa*, characterization, batch experiment

1. INTRODUTION

Copper is an essential trace element for living organisms, serving as a crucial nutrient for their normal development and physiological functions. However, both its deficiency and excess can be harmful[1-4]. Cu (II), for instance, interacts with lipid hydroperoxides to form malondialdehyde and 4-hydroxynonenal, which are considered carcinogenic and can cause DNA and tissue damage[5-6].

As one of the most commonly used metals in industry and agriculture, copper (II) ions can enter the environment through various sources, including industrial effluents from copper wire production for electrical applications, electroplating, battery manufacturing, paints and pigments and catalyst production, as well as agricultural activities such as the use of fertilizers and pesticides[7-8].

The contamination of wastewater with Cu (II) is a severe environmental and public health concern. Copper ion concentrations exceeding 1 mg/dm³ in wastewater can lead to significant environmental consequences, such as poisoning aquatic life and contaminating drinking water. Additionally, copper ions can accumulate in animal and plant tissues, causing adverse health effects and food contamination[9].

To mitigate environmental and health risks associated with the discharge of untreated toxic metals, various physical, chemical and biological techniques have been applied. Among the most effective technologies are precipitation, adsorption, ion exchange, biosorption, reverse osmosis and membrane filtration[10-13].

Among these techniques, adsorption stands out due to its flexibility in design and operational conditions and, in many cases, its ability to produce high-quality treated effluents.[14] Furthermore, owing to the reversible nature of most adsorption processes, adsorbents can be regenerated through appropriate desorption procedures, enabling their reuse over multiple cycles.[14–15] In this context, the use of biosorbents has emerged as an innovative and sustainable technological approach. Agroindustrial biomaterials constitute a class of biosorbent materials distinguished by their low cost, wide availability, and high removal efficiency[16].

Several studies have demonstrated the potential of lignocellulosic materials, such as bean husk[13] *Azadirachta indica* seed[17], rice husk[18], *Caryocar coriaceum* WITTM barks[19], orange peel and *Thamara* seeds[20], sunflower seed husk[21] and *Paeonia ostii* seeds[22] for Cu (II) removal in aqueous solutions.

Studies employing *Spondias tuberosa* seeds (SST) as biosorbents show a lack of investigations, which makes their application for the removal of toxic Cu(II) ions from aquatic environments scientifically relevant. It is highlighted that this residue is commonly discarded in sanitary landfills; therefore, its reuse contributes to reducing environmental impacts associated with agroindustrial waste accumulation. Moreover, the cost of reuse is low, requiring only transportation, drying, and grinding processes.

Thus, this study aimed to investigate the synthesis and application of a natural, low-cost biosorbent for the removal of Cu(II) ions from synthetic effluents through batch adsorption experiments, considering the physicochemical characteristics of the material and its adsorption performance.

This research contributes to the sustainable management of agroindustrial residues by promoting their reuse for the reduction of toxic metals in wastewater and provides a basis for future studies focused on material modification to improve the removal efficiency of potentially hazardous elements.

2. METHODOLOGY

2.1 Adsorbent collection and preparation

The *Spondias tuberosa* seed residue was collected from a pulp manufacturing industry located in the Cariri region of Ceará, specifically in the city of Juazeiro do Norte, Ceará, Brazil. After collection, the material was washed with water to remove any remaining pulp and then sun-dried naturally. The dried material was milled using a forage grinder to obtain a finer granulate and subsequently sieved through a 25-mesh sieve to achieve a powdered form. Finally, the material was oven-dried at 60°C to ensure complete moisture removal before further use.

2.2 Adsorbent characterization

The characterization of the point of zero charge (pHpzc), was performed following the methodology of Regalbuto and Robles[23]. In this procedure, 0.1 g of each adsorbent was placed in contact with 20 mL of solutions with different pH values, ranging from 1 to 13, for 2 hours under agitation at 100 rpm on a shaking table. The pH of the solutions was adjusted by adding HCl and

NaOH solutions to set the pH from 1.0 to 13.0. The pHpzc was determined by plotting a graph of ΔpH (pHinitial – pHfinal) versus pHinitial, where the intersection of the resulting curve with the x-axis (where ΔpH = 0) indicated the point of zero charge.

To observe the surface characteristics of the adsorbent material, samples before and after contact with the effluent were examined using scanning electron microscopy (SEM) on a SU3500 microscope. Images were acquired under low vacuum (chamber pressure of 100 Pa) and a working distance of 10 mm, employing a backscattered electron (BSE) detector in compositional mode with an electron acceleration voltage of 15 kV. For the identification and quantification of elemental compositions in the powder, X-ray fluorescence (XRF) analysis was performed using a Panalytical XRF spectrometer, model Epsilon 1, in semi-quantitative mode. Additionally, to investigate the functional and structural groups present, infrared spectra were recorded using an FTIR spectrometer (FT-IR Cary 630 Agilent, ATR) in the infrared range of 4000–650 cm^{-1} with a resolution of 2 cm^{-1}.

2.3 Batch adsorption experiments

2.3.1 Equilibrium kinetics

Batch kinetic tests were conducted at a temperature of 25°C and in duplicate, using aliquots of 25 mL of Cu (II) sulfate pentahydrate ($CuSO_4 \cdot 5H_2O$) solution buffered with acetic acid at pH = 5.5, transferred to a 125 mL Erlenmeyer flask containing 0.1 g of the adsorbent. The mixtures were placed on a shaker table at 100 rpm with contact times of 1, 4, 8, 16, 30, 60, 120, and 240 minutes. Afterward, the solutions were filtered, conditioned, and transferred to the Central Analytical Laboratory of Federal University of Cariri (UFCA), where they were analyzed by Flame Atomic Absorption Spectroscopy (FAAS).

The adsorption capacity (q) of the material and efficiency (E%) were determined using **Equations 1 and 2**, respectively, where C_0, Cf, W, and V represent initial concentration, final concentration ($mg.L^{-1}$), adsorbent weight (g) and volume (L).

$$q\ (mg.g^{-1}) = \frac{(C_0 - C_f)V}{W} \quad (1)$$

$$E(\%) = \frac{(C_0 - C_f)}{C_0} \times 100 \quad (2)$$

The adsorption dynamics of the metal were verified using non-linear kinetic models of Pseudo-first order (PFO), Pseudo-second order (PSO), and Elovich. The intraparticle diffusion mechanism was investigated by applying the Boyd model (**Table 1**).

Table 1 – Equations Kinetic and parameters used in the study

Kinetic Models	Nonlinear equations	Parameters
Pseudo-first order equation (PFO)	$qt = qe \times (1 - e^{-k1 \times t})$	qt: Adsorption capacity in any time ($mg.g^{-1}$) qe: Adsorption capacity at equilibrium ($mg.g^{-1}$) k_1: Pseudo-first order adsorption rate constant (min^{-1}) t: Time (min)
Pseudo-second order equation (PSO)	$qt = \frac{qe^2 \times k_2 \times t}{1 + qe \times k_2 \times t}$	k_2: Pseudo-second order adsorption rate constant ($g.mg^{-1}.min^{-1}$)
Elovich's kinetic model	$qt = \frac{1}{\beta}\ln(1 + \alpha\beta t)$	α: Initial adsorption rate ($mg.g^{-1}.min^{-1}$) β_E: Desorption constant ($mg.g^{-1}$)
Boyd (Diffusion model)	$If\ F < 0.85: Bt = \pi\left(1 - \sqrt{(1 - \frac{\pi F}{3}}\right)^2$ $If\ F > 0.85: Bt = -0.49770 - \ln(1 - F)$ $F = \frac{qt}{qe}$ $D = \frac{r^2 B}{\pi^2}$	F: Ratio qt/qe Bt: Parameter calculated as a function of F D: Coefficient for effective diffusion ($cm^2.min^{-1}$) r: Radius particle (cm) B: Boyd model constant (slope) -0.49770 corresponds to the term: $-\ln \pi^2/6$

2.3.2 Equilibrium Isotherm

The equilibrium isotherm experiments, conducted in duplicates, were performed using synthetic copper ion solutions prepared with $CuSO_4 \cdot 5H_2O$ (PA purity). The solutions were prepared by mixing different amounts of copper sulfate with an acetic buffer solution (pH 5.5) to obtain eight different concentrations ranging from 20 to 350 $mg \cdot L^{-1}$. Then, 10 mL of each solution was brought into contact with 0.05 g of the adsorbent for 60 minutes (equilibrium time determined from the best kinetic tests), under agitation at 150 rpm and temperatures of 288.15 K, 298.15 K, and 308.15 K. After the tests, they were filtered using filter paper, and the concentrations of the respective metal ions were determined by Flame Atomic Absorption Spectroscopy (FAAS) using a Varian SpectrAA 50B spectrometer at the Analytical Center Laboratory of the Federal University of Cariri (UFCA). The adsorption equilibrium was studied using the Langmuir, BET, Temkin and Sips models through non-linear fitting, applying the equations and parameters described in **Table 2**.

Table 2 – Equations and equilibrium isotherm parameters applied to the experimental data with SST.

Isotherm Models/ Functions	Nonlinear equations	Parameters
Langmuir	$qe = \frac{qmax \times K_L \times Cf}{1 + K_L \times Cf}$	qe: Adsorption capacity at equilibrium ($mg.g^{-1}$) qmax: Maximum biosorption capacity teorical for monolayer ($mg.g^{-1}$) K_L: Langmuir constant ($L.mg^{-1}$) Cf: Ion final concentration in solution ($mg.L^{-1}$)

BET	$q = \left[\frac{q_{max} b_1 C_f}{1 + (b_1 - b_2) C_f}\right]\left[\frac{1}{1 - b_2 C_f}\right]$	q_{max}: Maximum adsorption capacity (mg·g^{-1}) Cf: Ion final concentration in solutions (mg·L^{-1}) b_1: Equilibrium constants (L·mg^{-1}) b_2 Equilibrium constants (L·mg^{-1})
Temkin	$qe = \frac{RT}{b} ln(K_T \times Cf)$	qe: Adsorption capacity at equilibrium (mg.g^{-1}) K_T: Constant Temkin (L.mg^{-1}) R: Universal gas constant (J.mol^{-1}.K^{-1}) T: Temperature (K) Cf: Ion final concentration in solution (mg.L^{-1}) b: Heat of adsorption (J.mol^{-1})
Sips	$qe = \frac{qmax \times Ks \times Cf^{\beta s}}{1 + Ks \times Cf^{\beta s}}$	qe: Adsorption capacity at equilibrium (mg.g^{-1}) qmax: Maximum adsorption capacity (mg.g^{-1}) Ks: Sips equilibrium constant (L.mg^{-1}) Cf: Ion final concentration in solution (mg.L^{-1}) βs: Heterogeneity factor
R^2 Adjusted	$R^2 adj. = 1 - \frac{(1 - R^2)(N - 1)}{N - P - 1}$	P: Number of model parameters N: Sample size (number of experimental data) R^2: Coefficient of determination q_{exp}: Experimental sorption capacity (mg.g^{-1}) q_{model}: Adsorption capacity calculated by model ν: degree of freedom
Sum of square error	$SSE = \sum_{i=1}^{N} (qexp - qmodel)^2$	
Chi-square	$\chi^2 = \sum_{i=1}^{N} \frac{(qexp - qmodel)^2}{qexp}$	
Akaike Information Criterion (AIC)	$AIC = 2P + N \times ln\left(\frac{SSE}{\upsilon}\right)$	
Corrected Akaike Information Criterion (AICc)	$AICc = AIC + \frac{2P^2 + 2P}{N - P - 1}$	

2.3.3 Adsorption Thermodynamics

The adsorption thermodynamics experiments were conducted based on adsorption isotherms until equilibrium (Ce = 150 mg·L^{-1}) at the same temperatures, aiming to understand the nature and mechanisms of the adsorption process by analyzing thermodynamic parameters, such as the thermodynamic equilibrium constant (Ke°, **Equation 3**); enthalpy change (ΔH°) and entropy change (ΔS°) using the nonlinear Van't Hoff equation (**Equation 4**); and Gibbs free energy (ΔG°) calculated through **Equation 5**.

$$Ke° = \frac{(1000 \cdot K_{model} \cdot M_{adsorbate}) \cdot \lfloor Adsorbate \rfloor°}{\gamma} \quad (3)$$

$$Ke° = exp\left[\frac{\Delta S°}{R} - \left(\frac{\Delta H°}{R}\right) \cdot \frac{1}{T}\right] \quad (4)$$

$$\Delta G^0 = \Delta H° - T\Delta S° \quad (5)$$

Where:

Ke°: Thermodynamic Equilibrium Constant (dimensionless)

K_{model}: Isotherm model equilibrium constant (L mg^{-1})

$M_{sorbate}$: Molecular weight of sorbate (in this study: Cu = 63.55 g.mol^{-1})

[*Sorbate*]°: Standard concentration of the sorbate (1 mol L^{-1})

γ: Coefficient of activity (unitary for dilute solutions and dimensionless)

$\Delta H°$: Standard sorption enthalpy (kJ mol^{-1})

$\Delta S°$: Standard sorption entropy (J.mol^{-1} K^{-1})

$\Delta G°$: Standard sorption Gibbs free energy (J mol^{-1})

T: Absolute temperature (K)

R: Universal gas constant (8.3145 J K^{-1} mol^{-1})

2.3.4 Desorption and reuse tests

The desorption experiments were conducted following the method described in Gunawardene et al.[24]. After the isotherm experiments, the SST sample with Cu(II) adsorbed was dried in an oven at 323 K for 22 min and subsequently contacted with 100 mL of a 0.1 M HCl solution (in triplicate) under agitation at 150 rpm and 298 K. The liquid phase was collected by filtration at three different contact times (10, 20, and 30 min), and the concentration of Cu(II) ions was determined by flame atomic absorption spectroscopy (FAAS). The desorption efficiency (DE) was calculated according to Eq. (6)[24].

$$DE(\%) = \frac{Ct \cdot v}{m_0} \cdot 100 \quad (6)$$

where Ct (mg·L^{-1}) is the concentration of Cu(II) ions in the desorption solution at time t (min), V is the volume of the desorption solution, and m0 (g) is the mass of Cu(II) adsorbed during the sorption experiment.

Reusability tests were performed using the same sorbent sample, which was subjected to three successive sorption–desorption cycles under the conditions previously described.

3. RESULTS AND DISCUSSIONS

3.1 Material characterization

3.1.1 Zero charge point (pH_{PZC})

Figure 1 presents the graph of initial pH versus initial pH - final pH. pH values above the PZC indicate that the surface of the adsorbent presents a negative charge, whereas pH values below the PZC is positive[25-26]. The *Spondias tuberosa* seed waste (SST) exhibited a PZC value of 5.3, which was adjusted to 5.5, as pH values above the PZC enhance the adsorption of metal ions in an aquatic environment. This parameter is important since an effective electrostatic interaction between the adsorbate and adsorbent requires opposite charges.

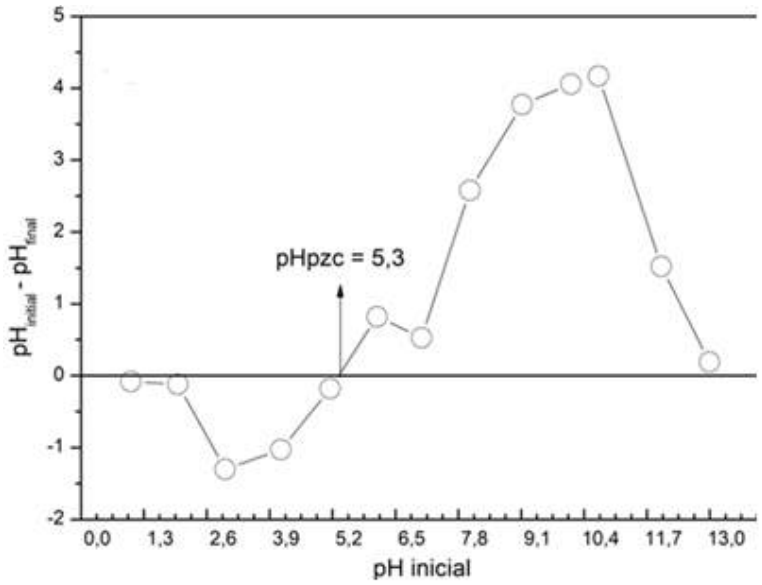


Figure 1 - pH_{PZC} SST biosorbent

3.1.2 SEM/XRF/FT-IR

Through the micrographs presented in **Figure 2**, it is possible to observe the morphological surface of the adsorbent with porous, irregular, and rough structures, typical of lignocellulosic plant materials. These raw lignocellulosic biomasses have demonstrated competitive adsorption properties for the removal of a wide variety of metal species from aqueous solutions[27-29]

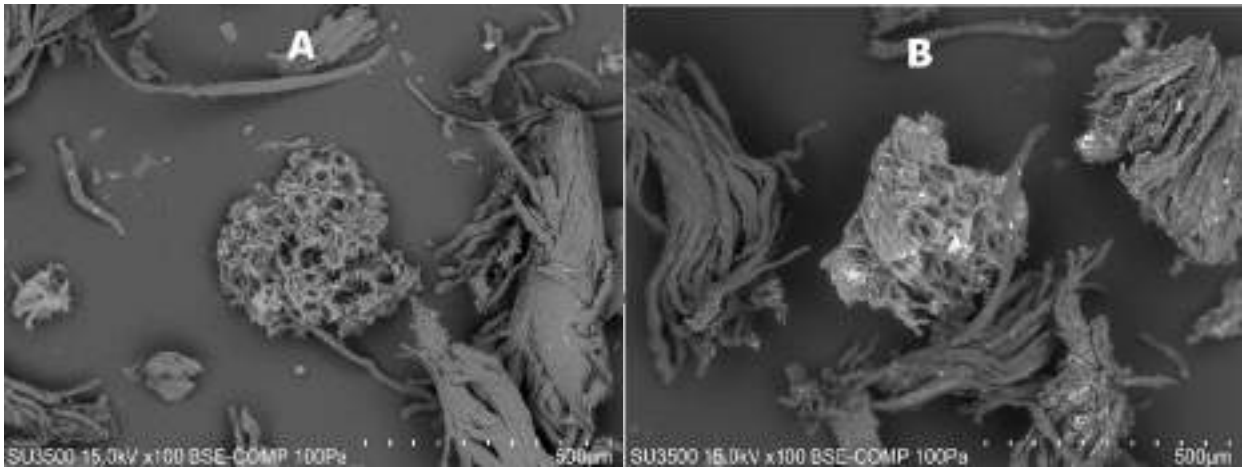


Figure 2 - Scanning Electron Microscopy Images of the SST adsorbent before (A) and after contact with the adsorbate (B).

Comparing **Figures 2A and 2B**, the presence of brighter spots is observed in the micrograph of the adsorbent surface post-contact **(Figure 2B)**, which possibly indicates the adhesion of the adsorbed metal to the surface of the SST adsorbent. This finding was confirmed by XRF spectroscopy

analysis, as shown in **Table 3**, which reveals an increase in the Cu(II) ion percentage, ranging from 0.70% to 7.10%, representing more than a 10-fold increase in the amount present in the material.

According to the data presented in Table 3, a considerable reduction in the concentrations of elements such as Ca and K was observed, suggesting that the adsorption mechanism may involve ion-exchange processes. These findings are consistent with previous reports[30–31], which indicate that the reaction occurs due to the neutralization of surface charges by cations after the biosorption of Cu(II) retained within the pores of the adsorbent.

Table 3 - Elemental composition of the SST bioadsorbent by XRF spectrometry

SST bioadsorbent	**Composition (%)**							
	S	P	Si	Cl	Ca	K	Fe	**Cu**
Before biosorption	0.21	0.47	0.53	0.38	2.26	1.00	0.60	**0.70**
After biosorption	0.14	0.25	0.58	0.37	1.60	0.40	0.27	**7.10**

Through the FTIR spectrum (**Figure 3**), it is possible to observe the adsorption in the 3322–3341 cm^{-1} range, which corresponds to the presence of hydroxyl (OH) groups found in cellulose and lignin compounds. The hydroxyl group acts as a proton donor, which can be one of the main contributors to the adsorption of toxic metal ions[32], integrating Cu (II)[33].

The presence of methyl ($–CH_3$) and methylene ($–CH_2–$) groups, through the vibration of C–H bonds in these groups, is evidenced by the peaks identified at 2928 and 2926 cm^{-1}. Peaks between 2890–2950 $cm^{-1}$are associated with cellulose, hemicellulose and lignin in lignocellulosic plants[34-35]. Furthermore, the peaks at 1740 and 1022 cm^{-1} correspond, respectively, to C=O stretching found in ketones and esters of hemicellulose and to C–O stretching in holocellulose and lignin[36-37].

A reduction in the peaks is also observed in the spectrum of the adsorbent post-contact with Cu (II). The most pronounced peaks observed are around 3400–3300, 2900–2800, 1600, and 900–800 cm^{-1}, corresponding respectively to O–H groups, C–H stretching, C═O stretching in carboxylates, and C–H deformation in cellulose[38]. Zolgharnein and Farahani[39] further explain that the significant decrease in peak intensity confirms the interaction between Cu (II) ions and oxygen atoms in water molecules. Thus, the observed changes indicate that structures such as C=O and functional groups like CH and OH contribute to Cu (II) adsorption.

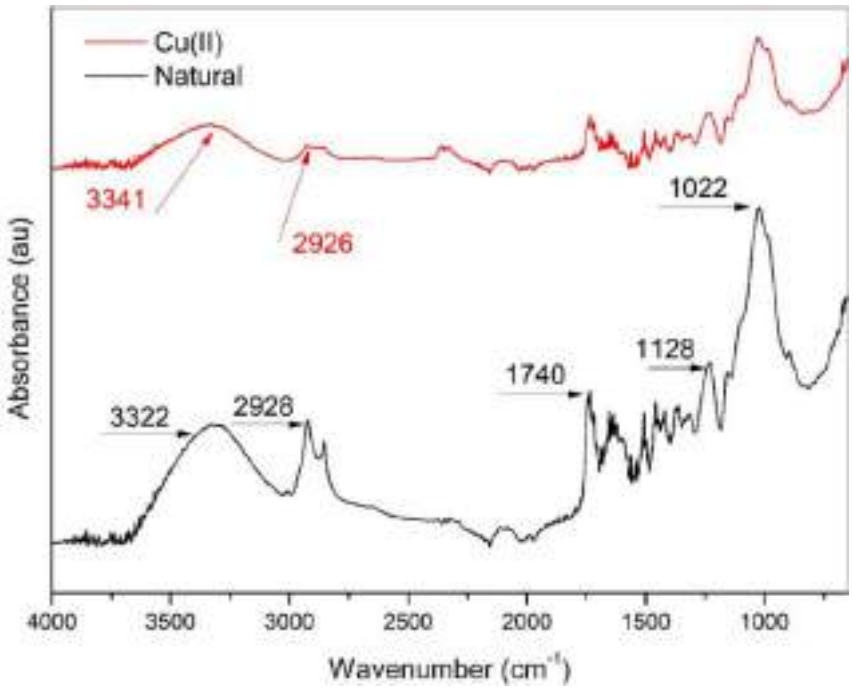


Figure 3 - FT-IR spectrum of the SST adsorbent, before and after contact with Cu (II) ions.

In summary, in addition to the adsorption mechanism possibly involving ion exchange, the uptake of Cu(II) by SST is also associated with surface functional groups, suggesting a probable complexation mechanism at the adsorbent surface.

3.2 Batch adsorption

3.2.1 Adsorption kinetics

The experimental adsorption data and kinetic curves for the models are shown in **Figure 4**, with the corresponding results of the fit presented in Table 4. The maximum adsorption capacity was 6.4 $mg.g^{-1}$. The adsorption by SST was relatively rapid in the first 30 minutes, gradually reaching equilibrium after 240 minutes. According to Zhang et al.[40], this behavior is attributed to the abundance of active sites on the adsorbent at the beginning. As the adsorption reaction progresses, the available active sites gradually decrease, thus limiting the adsorption rate.

The kinetic model that best fitted the experimental data was the Elovich model, as shown in **Figure 4** and **Table 4**, with an R^2 of 0.97, compared to the PFO and PSO models, which had R^2 values of 0.22 and 0.49, respectively. The error functions also supported a better fit for the Elovich model. The basic assumptions of the Elovich model are: (1) the activation energy for chemisorption increases with adsorption time, meaning the adsorption rate decreases exponentially as the amount adsorbed increases, due to the coverage of active sites, and (2) the adsorbent surface is heterogeneous[41-42].

Although the Elovich[43] model suggests a tendency toward chemisorption, these mathematical kinetic models are descriptive (empirical) and are useful for predicting the temporal evolution of the adsorbate. However, they do not provide information about the actual adsorption mechanism

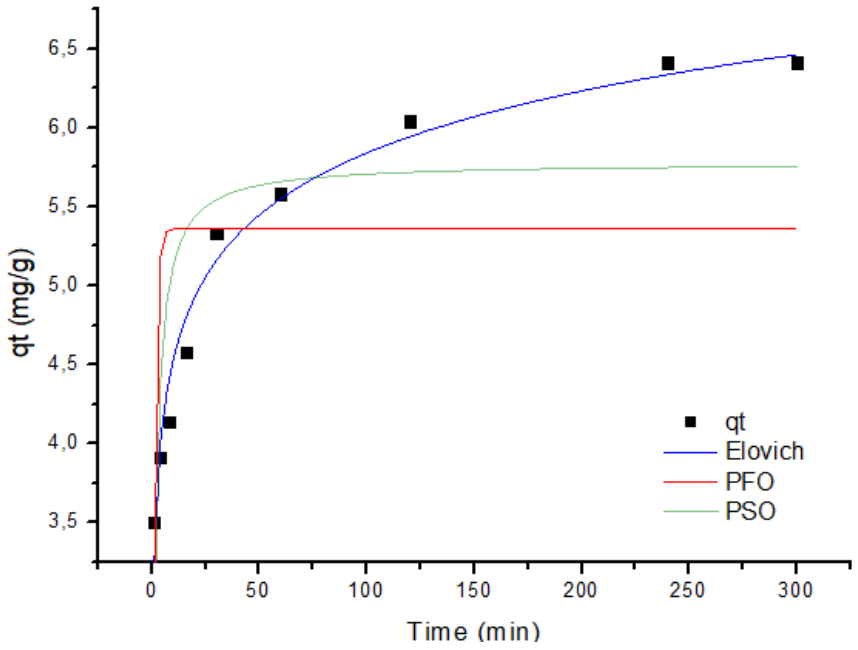


Figure 4 - Pseudo-first order, Pseudo-second order and Elovich kinetic models applied to Cu (II) adsorption with SST

Table 4 - Statistical kinetic parameters PFO, PSO and Elovich model of Cu(II) adsorption with SST

Pseudo-first order - PFO Model nonlinear					
q_{exp} ($mg.g^{-1}$)	q_{model} ($mg.g^{-1}$)	R^2 adjusted	SSE	χ^2	k1 (min^{-1})
6.41	5.36	0.227	6.60	0.94	0.86
Pseudo-second order - PSO Model nonlinear					
q_{exp} ($mg.g^{-1}$)	q_{model} ($mg.g^{-1}$)	R^2 adjusted	SSE	χ^2	k2 ($g.mg^{-1}.min^{-1}$)
6.41	5.78	0.496	3.47	0.49	0.13
Elovich Model nonlinear					
q_{exp} ($mg.g^{-1}$)	q_{model} ($mg.g^{-1}$)	R^2 adjusted	SSE	χ^2	β ($g.mg^{-1}$)	α ($mg.g^{-1}.min^{-1}$)
6.41	_	0.970	0.25	0.03	1.76	169.8

To understand the adsorption mechanism, the Boyd model was used[44-45], which is based on the assumption that the rate of adsorption is controlled by diffusion phenomena.

The Boyd intraparticle diffusion model was applied to determine the rate-limiting step of the adsorption process in the experiment, resulting in the Bt versus time (min) plot. Using the Boyd equations described in Table 1, the analytical parameters were established, as shown in **Figure 5**.

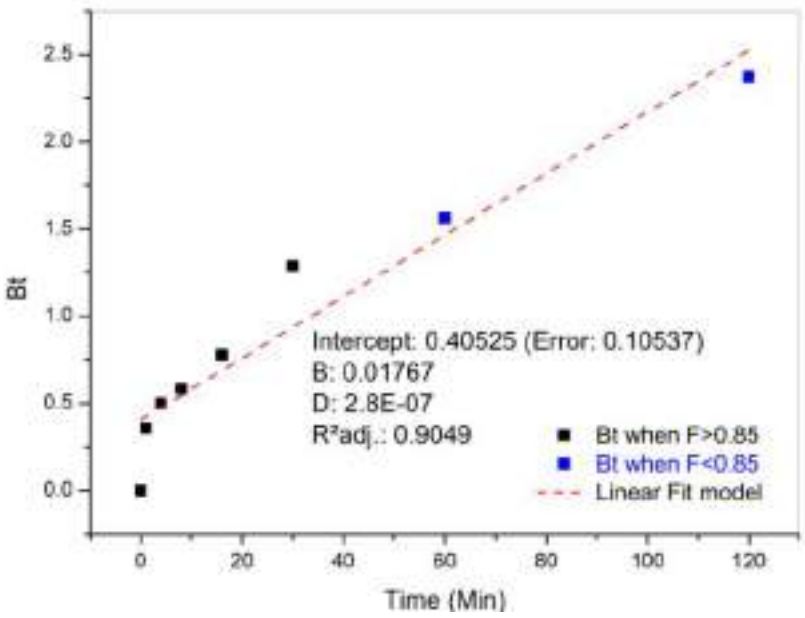


Figure 5 – Boyd's linear Intraparticle Diffusion Model for the SST (Bt x t)

Intraparticle diffusion will be the rate-limiting step of the adsorption process if the plot generates a straight line passing through the origin, for the specified time range[36]. As shown in **Figure 5**, the experimental data fit to the Boyd model did not produce a straight line passing through the origin, indicating that intraparticle diffusion is not the rate-limiting step in the adsorption process of Cu (II) onto *Spondias tuberosa* seeds (SST). Therefore, the process is governed by film diffusion (external diffusion) or both film and intraparticle diffusion, as described in[46-47.]

Other studies have applied the Boyd model to experimental data and suggested that the adsorption processes were not solely limited by intraparticle diffusion. For example, Santos et al[36] investigated the adsorption of Cu(II) on "Juá" (*Ziziphus joazeiro)* stem bark, and Mohammadabadi and Javanbakht[48] assessed the adsorption of lead on biodegradable biopolymers derived from cellulose.

3.2.2 Adsorption isotherm

The adsorption isotherm models applied at three temperatures are shown in **Figure 6** and the curve fitting results are reported in **Table 5**.

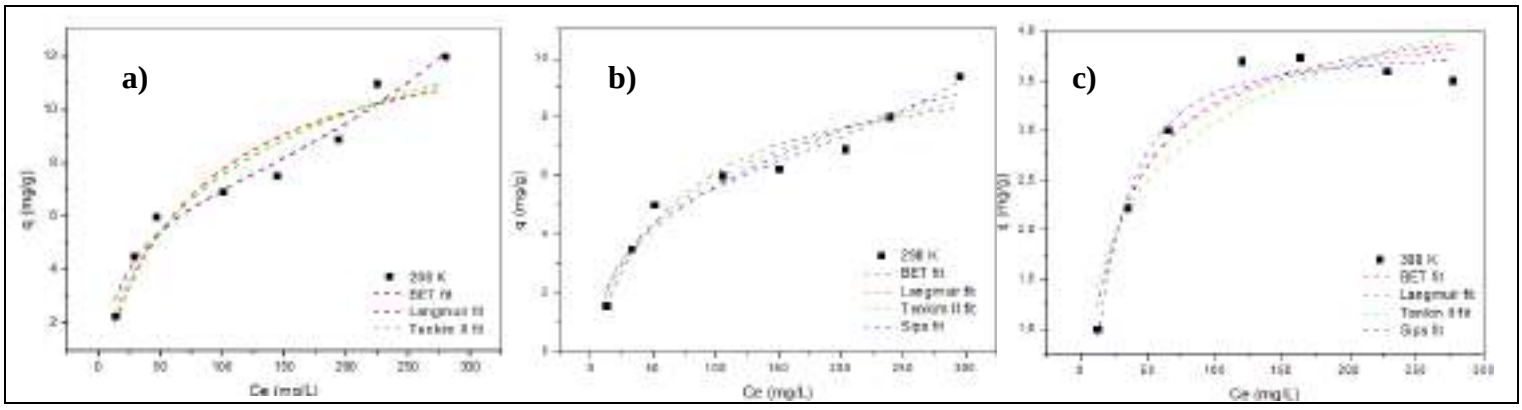


Figure 6 – Adsorption isotherms applied to nonlinear models for Cu (II) ions with SST at 288.15K(a); 298.15K(b) and 318.15K (c) at 60 min, 150 rpm and pH of 5.5

Table 5 – Statistical parameters of the nonlinear isotherm models applied to experimental data on Cu (II) adsorption with SST at the three respective temperatures.

Isotherms nonlinear models			
Parameters / Temper. (K)	**288.15**	**298.15**	**318.15**
q_{max}. *experimental* (mg·g^{-1})	12.0	9.4	3.7
Langmuir			
q_{max} (mg·g^{-1})	13.70	10.15	4.2265
k_L (L·mg^{-1})	0.0131	0.015	0.033
R^2 adjusted	0.887	0.921	0.938
SSE	7.068	2.95	0.320
χ^2	1.178	0.49	0.64
Aicc (%)	9.8	16.2	58.5
BET			
q_{max} (mg.g^{-1})	6.78996	5.822	4.301
b1	0.0509	0.0427	0.032
b2	0.0016	0.0013	0.00
R^2 adjusted	0.962	0.962	0.920
SSE	1.971	1.088	0.331
χ^2	0.394	0.217	0.082
Aicc (%)	47.3	25.6	1.3
Temkin			
q_{max} (mg. g^{-1})	3.6787	2.649	0.886
K_T (L·mg^{-1})	0.0680	0.082	0.3129
R^2 adjusted	0.920	0.942	0.850
SSE	4.99	2.156	0.777
χ^2	0.832	0.359	0.155
Aicc (%)	39.1	56.6	1.7

	Sips		
q_{max} **(mg·g^{-1})**	N.C.*	45.90	3.799
K_S **(L·mg^{-1})**	N.C.*	0.0146	0.0065
β	N.C.*	0.49	1.544
R^2 adjusted	N.C.*	0.929	0.966
SSE	N.C.*	2.174	0.1415
χ^2	N.C.*	0.435	0.035
Aicc (%)	3.8	1.6	38.5

N.C.* = Not Converged

According to **Figure 6**, q_{max} decreases with increasing temperature, presenting the following adsorption capacities in mg·g^{-1}: 12.0, 9.4, and 3.7 at 288.15, 298.15, and 318.15 K, respectively. This phenomenon indicates that adsorption is favored at lower temperatures, a behavior that will be further analyzed in the thermodynamic study of adsorption.

It is also observed that, for all three temperatures studied, an increase in adsorbate concentration enhances adsorption capacity until the equilibrium is reached at Ce = 150 mg·L^{-1} (**Figure 6**). However, beyond this initial equilibrium stage, with a continuous increase in concentration at 288.15 and 298.15 K (**Figures 6a and 6b**, respectively), the material continues adsorbing, though the adsorption rate gradually decreases as temperature increases in this second stage. A different behavior is observed at 308.15 K (**Figure 6c**), where, after reaching the first equilibrium, the adsorption capacity progressively decreases with increasing concentration. This confirms a promising adsorption tendency at lower temperatures.

As shown in **Table 5**, the Langmuir model predicted adsorption capacities higher than the maximum experimental capacity at all studied temperatures, whereas the other models estimated lower values. Additionally, the Sips model did not converge to the experimental data at 288.15 K.

The AICc criterion was used to predict the adsorption mechanism between Cu(II) and SST at different temperatures through equilibrium isotherm modeling. This approach ensures a more reliable assessment by integrating all regression parameters, increasing the accuracy of model selection.

According to the AICc results (**Table 5**), each temperature favored a different model: BET at 288.15 K, Temkin at 298.15 K, and Langmuir at 308.15 K.

The BET Type II isotherm has a sigmoidal, concave-upward shape[48-50]and describes multilayer adsorption[51-52]. As the Langmuir model, it assumes adsorption occurs at specific sites but extends this to multiple layers with varying adsorption energies[52-53]. Its behavior suggests that adsorption occurs through physisorption[54].

The Temkin model considers adsorbent saturation and adsorbate-adsorbate interactions, treating adsorption as a multilayer process[55-56]. It also assumes that adsorption heat decreases linearly with increasing surface coverage[57-58].

In contrast, the Langmuir isotherm describes monolayer adsorption on a homogeneous surface, without interactions between adsorbed molecules[55,59-61].

3.2.3 Adsorption Thermodynamics

The thermodynamic behavior of adsorption was evaluated until equilibrium was reached in the adsorption isotherm at the studied temperatures (Figure 7 - Supplementary Material). The Langmuir constant - K_L (Table 6 - Supplementary Material) was employed in the Van't Hoff equation to estimate the thermodynamic parameters of adsorption, which are presented in **Figure 8** and **Table 7**.

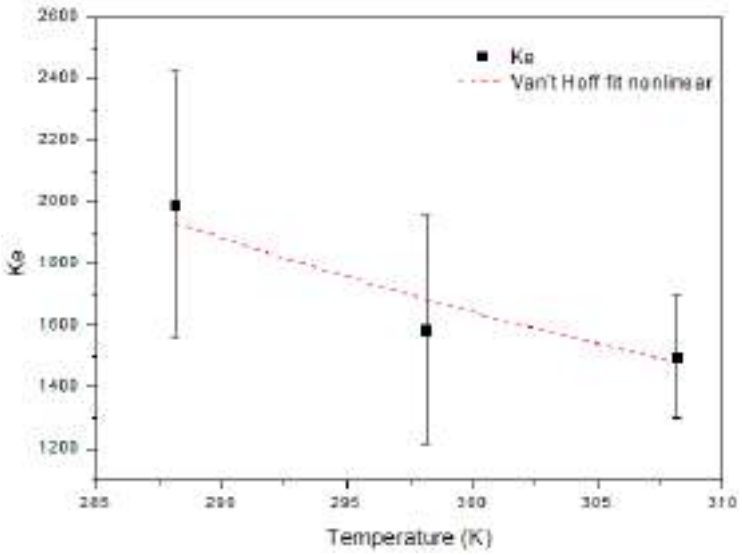


Figure 8 - Van't Hoff nonlinear model at 288.15, 298.15 and 308.15K and representation of the standard error.

Table 7 - Estimated thermodynamic parameters for Cu (II) sorption on SST.

T (K)	ΔG° (kJ mol^{-1})	ΔH° (kJ mol^{-1})	ΔS° (kJ mol^{-1} K^{-1})
288.15	-18.70 ± 0.01		
298.15	-18.42± 0.09	-9.87 ± 2.95	0.0287 ± 0.009
308.15	-18.13± 0.18		

After analyzing the data presented in **Table 6**, it is evident that the adsorption process exhibits a spontaneous, feasible, and exothermic nature, as evidenced by the negative values of ΔG˚ and ΔH°,

both of which are below zero[41]. Notably, this pattern indicates enhanced efficiency in Cu (II) adsorption at lower temperatures, as the standard Gibbs free energy decreases with a reduction in temperature, regardless of the adsorbent's nature[62-65] corroborating the behavior observed in the equilibrium isotherm.

Since the enthalpy values remain below 40 kJ/mol, the adsorption mechanism is classified as physical (physisorption), suggesting that the process does not require activation energy, as physical adsorption is driven by attractive forces between the adsorbent and adsorbate[61]. On the other hand, the positive value of ΔS° indicates a strong affinity of the biosorbent for Cu(II) ions and reflects an increase in disorder at the solid/solution interface. This entropy change is likely associated with structural modifications in both the adsorbate and the biosorbent during adsorption, supporting findings from FTIR analysis[66].

3.2.4 Desorption and reuse

Adsorbent reuse aims to reduce costs associated with contaminant removal. In this context, the efficiency calculated over three successive cycles indicates that SST is capable of desorbing Cu(II) with an efficiency close to 25%, allowing its reuse in each tested cycle, as shown in Figure 9. However, a gradual decrease in removal efficiency was observed with each reuse cycle, resulting in an overall reduction of approximately 50% from the first to the third cycle, with the optimal elution time being 30 min. In summary, SST demonstrated good recyclability and remained preserved during repeated use, indicating its potential for practical applications.

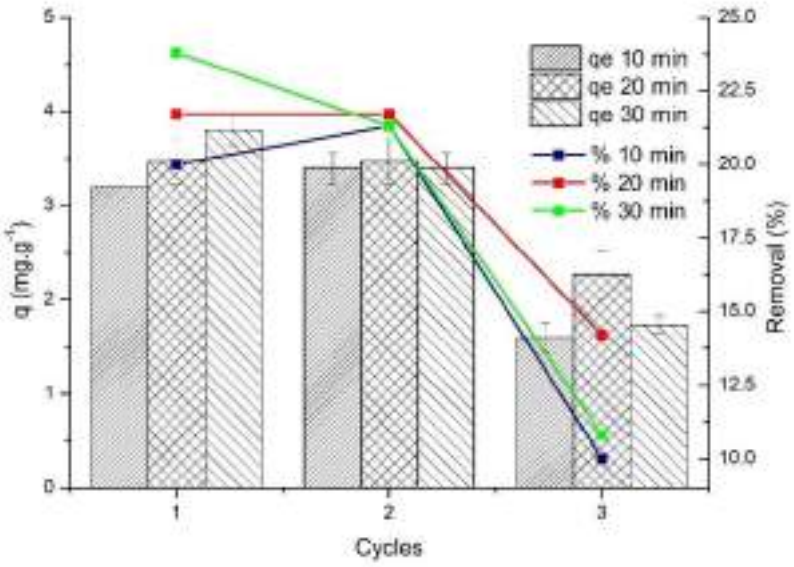


Figure 9 – Desorption performance and reusability efficiency of SST for Cu(II). Test conditions: Cu(II) concentration: 0.1 mol L^{-1}; rotation rate: 150 rpm; solution volume: 10 mL; sorbent mass: 0.05 g; temperature: 298.15 K; pH: 5.5; contact time: 60 min.

3.3 Comparative study of the adsorbent

Table 9 presents a comparative analysis of the adsorption capacity of SST for Cu(II) ions in relation to other lignocellulosic biomasses of similar origin, mainly derived from seeds and peels reported in the literature. Among the reported findings, some biomasses exhibited lower adsorption performance than SST, whereas others showed superior performance.

Table 9 – Comparison of lignocellulosic biosorbents and their maximum Cu(II) adsorption capacities (qmax)

Biosorbent materials	**q_{max} (mg.g $^{-1}$)**	**Reference**
bean shells	18.0	(13)
Caryocar coriaceum WITTM barks	26.9	(19)
Stem bark of *Ziziphus joazeiro*	8.4	(64)
Olive pit	0.56	(67)
Almond shell	2.39	(68)
Moringa stenopetala seeds	10.2	(69)
pomegranate seed waste	14.9	(70)
Nigella sativa seed	2.83	(71)
Spondias tuberosa seed	12,0	This work

It is noteworthy that, beyond the adsorption efficiency of biosorbents, aspects related to operational requirements and associated costs should also be considered in order to ensure the selection of materials with the best cost–benefit ratio.

Therefore, future studies should focus on improving biosorption strategies to enhance wastewater treatment processes, considering evaluations at both laboratory and larger scales, including synthetic systems as well as real effluents, to enable the efficient and economically viable application of this technique.

4. CONCLUSIONS

In this study, the adsorptive performance of an innovative, residual, low-cost biomass derived from *Spondias tuberosa* seeds (SST) was evaluated for the removal of toxic Cu(II) ions from contaminated effluents. The SST powder showed promising biosorption capacity, reaching a maximum adsorption of 12.0 mg·g^{-1} within 60 min at 288.15 K and pH 5.5.

Material characterization confirmed the occurrence of adsorption through adsorbent–adsorbate interactions, as evidenced by spectral band shifts and intensity reductions, along with changes in

elemental composition. These results suggest that Cu(II) removal occurs mainly through ion-exchange and surface complexation mechanisms. Furthermore, the rough and porous surface morphology favored the diffusion and retention of copper ions within the SST structure during the biosorption process.

Batch adsorption experiments revealed a rapid uptake during the first 30 min, followed by a slower stage until equilibrium was reached at 240 min, with film diffusion identified as the rate-limiting step. Isotherm analysis indicated higher adsorption efficiency at lower temperatures and concentrations, while different adsorption models better described the system depending on the temperature. Thermodynamic parameters demonstrated that the process is favorable, spontaneous, and exothermic, with decreasing adsorption capacity at higher temperatures. The low enthalpy values indicated weak interactions, suggesting that physisorption predominates, while entropy changes pointed to structural modifications in both the adsorbent and adsorbate, in agreement with FTIR results.

Although desorption efficiency was moderate, SST maintained its structural integrity and adsorption performance over reuse cycles. Overall, this study demonstrates that SST is a low-cost, abundant, reusable, and environmentally sustainable biosorbent, offering a viable solution for both agroindustrial waste valorization and the removal of Cu(II) ions from contaminated aqueous systems.

Conflict of interest

Not applicable.

5. REFERENCES

1. Linder, M.C. *Biochemistry of Copper*. Plenum Press: New York, **1991**.
2. Uriu-Adams, J.Y.; Scherr, R.E.; Lanoue, L.; Keen, C.L. Influence of copper on early development: prenatal and postnatal considerations. *Biofactors* **2010**, 36, 136–152.
3. Peng, F. Positron emission tomography for measurement of copper fluxes in live organisms. *Ann. N. Y. Acad. Sci.* **2014**, 1314, 24–31.
4. Priessner, M.; Suntsova, M.; Alekseeva, A.; Stepanova, S. Selective detection of Cu^{+} ions in live cells via fluorescence lifetime imaging microscopy. *Angew. Chem. Int. Ed.* **2021**, 60(43), 23148–23153.
5. Deswati, H.; Suyani, I.; Rahmi, R.; Suyani, E. Application of central composite design optimization technique for determination of copper in fruit and vegetable samples. *Rasayan J. Chem.* **2017**, 10, 1359–1367.

6. Costa, F.S.; Leal, R.V.P.; Pacheco, C.S.V.; Silva, J.F.; Oliveira, J.F. Multivariate optimization of ultrasound-assisted extraction for Cu, Fe, Mn, Zn in plants. *Anal. Methods* **2020**, 12, 2509–2516.
7. Jakku, R.S.; Fernandez-Andrade, K.J.; Ntamu, T.E.; Adesina, O.A. Efficient removal of congo red dye using activated lychee peel biochar. *Results Eng.* **2022**, 14, 100449.
8. Baharim, N.; Mokif, L.A.; Abdulhusain, N.A. Removal performance of bio-sorption on sunflower seed husk for copper and lead ions. *J. Ecol. Eng.* **2024**, 24, 110–117.
9. Stepanova, S.; Alekseeva, A.; Suntsova, M. Studies of removing copper ions from water with seed coats of grain crops. *E3S Web Conf.* **2023**, 389, 03025.
10. Ding, Z.; Hu, X.; Morales, V.L.; Gao, B. Filtration and transport of heavy metals in graphene oxide enabled sand columns. *Chem. Eng. J.* **2024**, 257, 248–252.
11. Cho, D.W.; Song, H.; Kim, B.; Schwartz, F.W.; Jeon, B.H. Reduction of nitrate in groundwater by Fe(0)/Magnetite nanoparticles entrapped in Ca-alginate beads. *Water Air Soil Pollut.* **2015**, 226, 206.
12. Lee, C.G.; Kim, S.B.; Park, J.H.; Jeon, B.H. Removal of copper, nickel and chromium mixtures from wastewater using modified carbon foam. *Chemosphere* **2017**, 166, 203–211.
13. Marković, M.; Petrović, M.; Jovanović, M.; Stojanović, M. Copper ions biosorption onto bean shells: kinetics, equilibrium and optimization. *J. Serb. Chem. Soc.* **2023**, 88, 921–935.
14. S. Sobhanardakani ; M. Ahmadi ; R. Zandipak. Efficient removal of Cu(II) and Pb(II) heavy metal ions from water samples using 2,4-dinitrophenylhydrazine loaded sodium dodecyl sulfate-coated magnetite nanoparticles. *Journal of Water Supply: Research and Technology-Aqua*, **2016,** 65 (4), 361–372.
15. Ahmadi, M., Madrakian, T. & Afkhami, A. Enantioselective solid phase extraction prior to spectrofluorometric determination: a procedure for the determination of naproxen enantiomers in the presence of each other. *RSC Adv*, **2015a**, 5, 5450–5457
16. Sharifpour, M., Cheraghi, M., Sobhanardakani, S., & Lorestani, B. Biosorption of Pb(II) and Cd(II) ions from aqueous solution using chia (*Salvia hispanica*) seed. *Journal of Dispersion Science and Technology*, **2025**, 1–10. https://doi.org/10.1080/01932691.2025.2469740.
17. Costa, W.D.; Leal, R.V.P.; Pacheco, C.S.V.; Silva, J.F. Removal of copper(II) ions and lead(II) using Azadirachta indica seeds. *Environ. Res.* **2020**, 183, 109213.
18. Sobhanardakani, S., Parvizimosaed, H. & Olyaie, E. Heavy metals removal from wastewaters using organic solid waste—rice husk. *Environ Sci Pollut Res*, **2013**, 20, 5265–5271.

19. MENEZES, J. M. C. et al. Kinetic and thermodynamic study of copper (II) IONS biosorption by Caryocar Coriaceum Wittm bark. *Sustainable Chemistry and Pharmacy*, **2021,** 19, 100364. doi.org/10.1016/j.scp.2020.100364
20. Neisan, R.S.; Mokif, L.A.; Abdulhusain, N.A. Adsorption of copper using TiO_2-modified activated carbon from orange peels and date seeds. *Heliyon* **2023**, 9, e21420.
21. Abdulhusain, N.A.; Mokif, L.A. Removal of copper and lead ions using sunflower seed husk. *J. Ecol. Eng.* **2023**, 24, 110–117.
22. Liu, Q.; Zhang, R.; Wang, H.; Chen, Y. Enhanced adsorption of copper ions by phosphoric acid-modified Paeonia ostii seed coats. *Environ. Sci. Pollut. Res.* **2020**, 27, 43906–43916.
23. Regalbuto, J. R.; Robles, J. *The engineering of Pt/Carbon Catalyst Preparation,* University of Illinois: Chicago. 2004.
24. Gunawardene, OHP; Gunathilake, CA; Amaraweera, APSM; Fernando, NML; Manipura, A; Manamperi, WA; Kulatunga, KMAK; Rajapaksha, SM; Gamagem, A; Dassanayake, RS; Weerasekara, BGND; Fernando, PNK; Fernanda, CAN; Jayasinghe, JASC. Remoção de íons Pb(II) de solução aquosa usando amido modificado. *J. Compos. Ciência.* **2021**, *5*, 46, DOI: 10.3390/jcs5020046
25. Amaringo, F.A.; Hormaza, A.A. Determination of zero charge point of agricultural residues and their application in dye removal. *J. Agric. Environ. Res.* **2023**, 4, 27–36.
26. **Valerio-Cárdenas, C.; Martínez-Herrera, J.; Velázquez-Vargas, D. L.; De la Cruz-Burelo, P.** *Determination of the point of zero charge of pineapple (Ananas comosus L.) peel and its application as copper adsorbent. Agro Prooductividad*, **2021.** https://doi.org/10.32854/agrop.v14i11.2009
27. **Ho, Y.S.; Chiu, W.T.; Hsu, C.S.; Huang, C.T.** Sorption of lead ions from aqueous solution using tree fern as a sorbent. *Hydrometallurgy* **2004**, *73*, 55–61.
28. Miretzky, P., Cirelli, A. F. *Cr(VI) and Cr(III) removal from aqueous solution by raw and modified lignocellulosic materials: A review.* J. of Hazardous Materials, **2010,** 180(1–3), 1–19.
29. Castillo, J. M.; Rivas, B. L.; Pereira, E. D. *Removal of metal ions using lignocellulosic materials: A review. J. Applied Polymer Sci.,* **2014,** 131(18), 40745.
30. Aninda T. Puari, Arti Azora, Rusnam Rusnam, Nika R. Yanti, Feri Arlius, M.Y. Shukor. Carbonization parameters optimization for the biosorption capacity of Cu^{2+} by a novel biosorbent from agroindustrial solid waste using response surface methodology. *Case Studies in Chemical and Environmental Engineering,*Volume, **2024**, 9, 100645

31. Zhou, R., Zhang, M., Zhou, J. et al. Optimization of biochar preparation from the stem of *Eichhornia crassipes* using response surface methodology on adsorption of Cd^{2+}. *Sci Rep*, **2019**, 9, 17538. https://doi.org/10.1038/s41598-019-54105-1
32. **Yahya, M. D.; Ihejirika, C. V.; Iyaka, Y. A., Garba, U.; Olugbenga, A. G.** Continuous sorption of chromium ions from simulated effluents using citric acid modified sweet potato peels. *Nigerian Journal of Technological Development*, **2020**,
33. Saleh, M. E.; El-Damarawy, Y. A.; Assad, F. F.; Abdesalam, A. A.; Yousef, R. A. Removal of copper metal ions by sugarcane bagasse and rice husk biochars from contaminated aqueous solutions. *Med. J. Soil Sci*, **2020**, 1, 1–17.
34. Fernández-Andrade, K. J.; González-Vargas, M. C.; Rodríguez-Rico, I. L.; Ruiz-Reyes, E.; Quiroz-Fernández, L. S.; Baquerizo-Crespo, R. J.; Rodríguez-Díaz, J. M. Evaluation of mass transfer in packed column for competitive adsorption of Tartrazine and brilliant blue FCF: A statistical analysis. *Results in Engineering*, **2022**, 14, 100449.
35. Sousa, T. M. I.; Sá, G. B.; Coura, M. A.; Oliveira, A. M. B. M.; Coelho, L. F. O.; Gomes, N. A.; Menezes, J. M. C.; Oliveira, J. T.; Paula Filho, F. J. Cu (II) adsorption in rice husk for water treatment: Batch and fixed column experiments. *Desalination and Water Treatment*, **2024**, 320, 100762
36. Santos, Y.T.C.; Costa, F.S.; Menezes, J.M.C.; Coutinho, H.D.M. Adsorption of Zn(II) ions by Ziziphus joazeiro barks in aqueous solutions. *Results Chem.* **2024(a)**, *7*, 101339.
37. Javier-Astete, R.; Jimenez-Davalos, J.; Zolla, G. Determination of hemicellulose, cellulose, holocellulose and lignin content using FTIR in Calycophyllum spruceanum (Benth.) K. Schum. and Guazuma crinita Lam. *PLoS One* **2021**, *16*(10), e0256559.
38. Mébarki, M.; Boudjema, K.; Bensmail, A.; Drouiche, N.; Lounici, H. Lignocellulosic fraction of the pericarps of the acorns of Quercus suber and Quercus ilex: isolation, characterization, and biosorption studies in the removal of copper from aqueous solutions. *Pol. J. Chem. Technol.* **2019**, *21*(3), 40–47.
39. Zolgharnein, J.; Farahani, S.D. Experimental design optimization and isotherm modeling for removal of copper(II) by calcium-terephthalate MOF synthesized from recycled PET waste. *J. Chemom.* **2023**, *37*, e3396.
40. Zhang, L.; Wang, Y.; Li, Y.; Liu, Y.; Zhang, Y.; Wang, Z. H_2O_2 modified peanut shell-derived biochar/alginate composite beads as a green adsorbent for removal of Cu(II) from aqueous solution. *Int. J. Biol. Macromol.* **2023**, *240*, 124466.
41. **Elovich, S. Y.; Larionov, O. G.** Theory of adsorption from solutions of non-electrolytes on solid: (I) Equation adsorption from solutions and the analysis of its simplest form. (II)

Verification of the equation of adsorption isotherm from solutions. *Izvestiya Akademii Nauk SSSR, Otdelenie Khimicheskikh Nauk*, **1962**, 2, 209–216.

42. **Wang, J.; Guo, X.; Guo, Y.; Zhang, Y.; Liu, Y.; Li, Y.** Adsorption kinetics and isotherm models of heavy metals by various adsorbents: An overview. *Environmental Technology Reviews*, **2024**, 53(21), 1–25.
43. Boyd, G. E.; Schubert, J.; Adamson, A. W. The exchange adsorption of ions from aqueous solutions by organic zeolites. I. Ion-exchange equilibria. *Journal of the American Chemical Society*, **1947**, 69, 2818–2829.
44. Reichenberg, D. Properties of ion exchange resins in relation to their structure. III. Kinetics of exchange. *Journal of the American Chemical Society*, **1953**, 75(3), 589–597.
45. Benjelloun, M.; Miyah, Y.; Evrendilek, G. A.; Zerrouq, F.; Lairini, S. Recent advances in adsorption kinetic models: their application to dye types. *Arabian Journal of Chemistry*, **2021**, 14(4), 103031
46. Okewale, A. O.; Babayemi, K. A.; Olalekan, A. P. Adsorption isotherms and kinetics models of starchy adsorbents on uptake of water from ethanol–water systems. *International Journal of Applied Science and Technology*, **2013**, 3(1), 35–42.
47. Mohammadabadi, S.I.; Javanbakht, V. Fabrication of dual cross-linked spherical treated waste biomass/alginate adsorbent and its potential for efficient removal of lead ions from aqueous solutions. *Ind. Crops Prod.* **2021**, *168*, 113575.
48. Brunauer, S.; Emmett, P.H.; Teller, E. Adsorption of gases in multimolecular layers. *J. Am. Chem. Soc.* **1938**, *60*, 309–319.
49. Andrade, R.D.P.; Lemus-Mondaca, R.; Vega-Gálvez, A.; Miranda, M.; Pérez-Won, M. Models of sorption isotherms for food: uses and limitations. *Vitae* **2011**, *18*(3), 325–334. https://doi.org/10.17533/udea.vitae.10682
50. Adebowale, A.A.; Akinola, O.O.; Adebayo, A.O.; Olayemi, F.F. Adsorption isotherms and thermodynamic properties of dried tomato slices. *Adv. Nutr. Food Sci.* **2022**, *7*, 249–262.
51. Saadi, R.; Saadi, Z.; Fazaeli, R.; Fard, N.E. Modelos de isotermas de adsorção monocamada e multicamada para sorção de meios aquosos. *Korean J. Chem. Eng.* **2015**, *32*, 787–799.
52. Al-Ghouti, M.A.; Da'ana, D.A. Guidelines for the use and interpretation of adsorption isotherm models: a review. *J. Hazard. Mater.* **2020**, *393*, 122383.
53. Thongsamer, T.; Chunkao, K.; Chunkao, K.; Srisatit, T.; Srisatit, T. Chitosan impregnation of coconut husk biochar pellets improves their nutrient removal from eutrophic surface water. *Sustain. Environ. Res.* **2022**, *32*(39), 1–19.

54. Adelaja, O.A.A.; Babaniyi, B.R. Evaluating the potential of modified mango leaves as a biosorbent for the removal of mercury(II) ion and congo red from wastewater. *SCE* **2024**, *5*, 411–425.
55. Chen, Y.; Zhang, R.; Wang, H.; Li, Y. Alkali activated winter melon peel as absorbent: Characterization and its adsorption performance for heavy metal ions in aqueous solutions. *Desalination and Water Treatment*, **2024**, 317, 100055.
56. Bagherzadeh, M.; Salehi, G.; Rabiee, N. Rapid and efficient removal of methylene blue dye from aqueous solutions using extract-modified Zn–Al LDH. *Chemosphere*, **2024**, 350, 141011.
57. Sampranpiboon and Charnkeitkong, P. Sampranpiboon, P. Charnkeitkong Equilibrium isotherm, thermodynamic and kinetics studies of lead adsorption onto pineapple and paper waste sludges J. Energy Environ. Eng, **2010,** 4 (3), 89-93.
58. Sharifi, M. J.; Nouralishahi, A.; Hallajisani, A.; Askari, M. Magnetic chitosan nanocomposites as adsorbents in industrial wastewater treatment: a brief review. *Cellulose Chem. Technol.*, **2021**, 55, 185–205.
59. Nasseh, N.; Barikbin, B.; Taghavi, L.; Nasseri, M. A. Adsorption of metronidazole antibiotic using a new magnetic nanocomposite from simulated wastewater (isotherm, kinetic and thermodynamic studies). *Composites Part B: Engineering*, **2019**, 159, 146–156.
60. Kalam, S.; Abu-Khamsin, S. A.; Kamal, M. S.; Patil, S. Surfactant adsorption isotherms: a review. *ACS Omega*, **2021**, 6(48), 32342–32348.
61. Hasanzadeh, S.; Mortazavi-Derazkola, S.; Khosravi, R. Green synthesis of iron nanoparticles using Pistacia-atlantica leaf extract for enhanced removal of Cr (VI) from aqueous solution. *Desalination and Water Treatment*, **2024**, 318, 100347.
62. Fenti A, Iovino P, Salvestrini S. Some remarks on "A critical review of the estimation of the thermodynamic parameters on adsorption equilibria. Wrong use of equilibrium constant in the Van't Hoof equation for calculation of thermodynamic parameters of adsorption *J. Mol. Liq.* **2019**, *273*, 425–434.
63. Salvestrini, S.; Ambrosone, L.; Kopinke, F.-D. Some mistakes and misinterpretations in the analysis of thermodynamic adsorption data. *Journal of Molecular Liquids*, **2022**, 352, 118762.
64. Santos, Y.T.C.; Costa, F.S.; Menezes, J.M.C.; Coutinho, H.D.M. Sorption thermodynamic and kinetic study of Cu(II) onto modified plant stem bark. *Environ. Sci. Pollut. Res.* **2024(b)**, 1–23.
65. Erdol-Aydin, N.; Sezer, S.; Esin, B.; Nasun-Saygili, G. Removal of boron from wastewaters using valonia-tannin-based biosorbent produced via spray drying. *Adsorpt. Sci. Technol.* **2024**, *42*, 1–25.

66. Alqarni, L. S.; Algethami, J. S.; Billah, R. E. K.; Alorabi, A. Q.; Alnaam, Y. A.; Algethami, F. K.; Bahsis, L.; Jawad, A. H.; Wasilewska, M.; Lopez-Maldona, E. A. A novel chitosan-alginate@Fe/Mn mixed oxide nanocomposite for highly efficient removal of Cr (VI) from wastewater: Experiment and adsorption mechanism. *International Journal of Biological Macromolecules*, **2024**, 263, 129989.
67. Amar, M.B.; Walha, K.; Salvadó, V. Evaluation of Olive Stones for Cd(II), Cu(II), Pb(II) and Cr(VI) Biosorption from Aqueous Solution: Equilibrium and Kinetics. *Int. J. Environ. Res.* **2020**, *14*, 193–204.
68. Yahya, M.D.; Abubakar, H.; Obayomi, K.S.; Iyaka, Y.A.; Suleiman, B. Simultaneous and Continuous Biosorption of Cr and Cu (II) Ions from Industrial Tannery Effluent Using Almond Shell in a Fixed Bed Column. *Results Eng.* **2020**, *6*, 100113.
69. Kebede, T.G.; Mengistie, A.A.; Dube, S.; Nkambule, T.T.I.; Nindi, M.M. Study on Adsorption of Some Common Metal Ions Present in Industrial Effluents by Moringa Stenopetala Seed Powder. *J. Environ. Chem. Eng.* **2018**, *6*, 1378–1389.
70. Hoda Ganji, Mohsen Taghavijeloudar. Efficient adsorption of lead and copper from water by modification of sand filter with a green plant-based adsorbent: Adsorption kinetics and regeneration. *Environmental Research*, **2024**, 259, 119529.
71. Addala, A., Boudiaf, M., Zizi, Z. et al. Utilization of *Nigella sativa* seed biomass for copper (II) adsorption from aqueous solutions and wastewater: performance evaluation, kinetics, thermodynamics, and theoretical insights. *Biomass Conv. Bioref.*, **2025,** 15, 25205–25222. https://doi-org.ez152.periodicos.capes.gov.br/10.1007/s13399-025-06822.

SUPPLEMENTARY MATERIAL

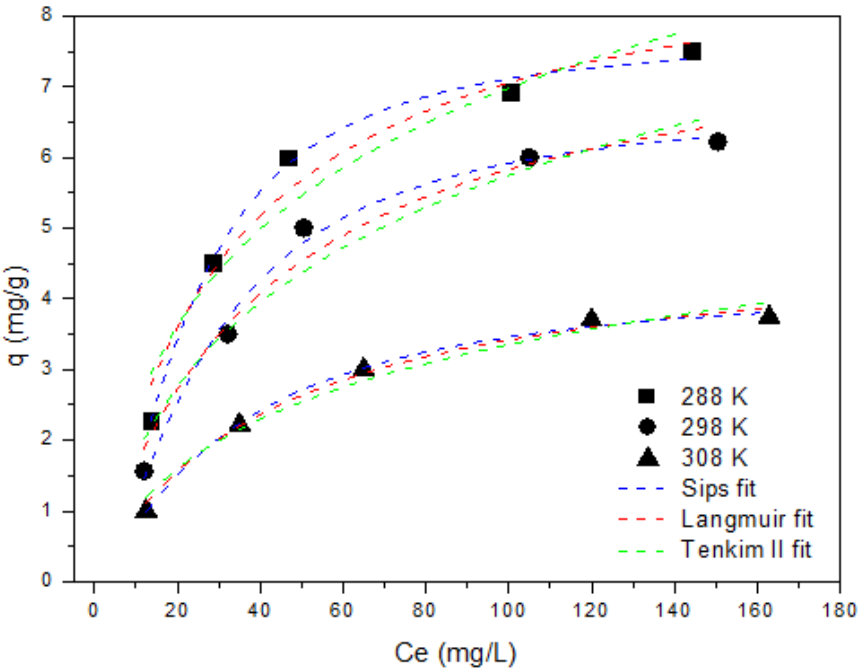


Figure 7 – Isothermal equilibrium models of Cu (II) ions for SST adsorbent, up to Ce = 160.0 mg· L−1. Under conditions 288.15K; 298.15K and 318.15K in 60 min at 150 rpm and pH of 5.5.

Table 6 – Statistical parameters of the nonlinear isotherm models applied to the experimental equilibrium of Cu (II) adsorption with SST at the three respective temperatures.

Isotherms nonlinear models			
Parameters / Temper. (K)	**288**	**298**	**318**
Langmuir			
q_{max} (mg·g^{-1})	9.3087	8.1668	4.8676
k_L (L·mg^{-1})	0.0313	0.0249	0.0235
R^2 adjusted	0.962	0.966	0.989
SSE	0.4490	0.3828	0.0406
χ^2	0.1663	0.1276	0.0135
Aicc %	85.2	84.3	94.7
Temkin			
qt (mg. g^{-1})	2.3706	2.2206	1.3067
K_T (L·mg^{-1})	0.1799	0.1229	0.1198
R^2 adjusted	0.923	0.933	0.967
SSE	1.0100	0.7501	0.1284
χ^2	0.3367	0.250	0.0428
Aicc %	14.6	15.7	5.3

	Sips		
q_{max} **(mg·g^{-1})**	7.7552	6.8012	4.3296
K_S **(L·mg^{-1})**	0.0059	0.0065	0.0126
β	1.6367	1.503	1.2488
R^2 **adjusted**	0.992	0.985	0.994
SSE	0.0664	0.1095	0.1415
χ^2	0.0332	0.0547	0.035
Aicc %	0.2	0.0	0.0

5 CONSIDERAÇÕES FINAIS

5.1 ASPECTOS GERAIS DA PRODUÇÃO CIENTÍFICA

Os metais tóxicos são potenciais poluentes da água devido à sua natureza tóxica e não biodegradável que representam uma grave ameaça à saúde pública e ao meio ambiente (Khan et al, 2020; Rahim et al, 2016). Neste contexto, destaca-se a necessidade de pesquisas voltadas ao desenvolvimento de ferramentas capazes de combater o acúmulo destes poluentes no ambiente, contribuindo para redução de impactos negativos aos ecossistemas e consequentemente favorecendo melhorias a saúde de toda população.

Estudos mostram que a remoção de metais tóxicos do meio ambiente, através do processo de biosorção com bioadsorventes, mostraram-se eficientes no tratamento de efluentes sintéticos contendo estes contaminantes. Como exemplo, as biomassas de composição lignocelulósico, que atualmente veem sendo investigadas em estudos recentes, revelando-se favoráveis à adsorção de diversos compostos.

A semente de *Spondias tuberosa* (SST) investigada neste estudo, como bioadsorvente in natura e ainda não explorada em testes de adsorção, revelou-se como um excelente material com capacidades de remover metais tóxicos Pb (II) e Cu(II) de efluentes sintéticos. Utilizando testes experimentais em batelada, a SST conseguiu remover os referidos metais com capacidades máximas de adsorção de 46,0 $mg.g^{-1}$ a 25°C e 12,0 $mg.g^{-1}$ a 15°C respectivamente.

A caracterização estrutural teve papel central ao revelar através das análises de infravermelho (FTIR) e MEV, que o material era composto a base de celulose, hemicelulose e lignina, apresentando superfície porosa e irregular, características bastante presentes em vegetais de estruturas fibrosas. Neste contexto a análise do FTIR sugeriu uma possível adsorção por complexação dos grupos carboxila (–COOH/–COO^{-}) e hidroxila (–OH) presentes na superfície do adsorvente. Além disso, a análise de FRX, constatou a remoção de íons Cu (II) indicando provável a ocorrência de troca iônica, característica comum presente na remoção de metais com materiais de mesma origem.

Estudos em batelada, revelaram que a cinética do processo de adsorção para ambos os íons ocorreu de maneira relativamente rápida, atingindo o equilíbrio em cerca de 30 min. para o Pb (II) e 240 min. para o Cu (II). A partir da utilização dos modelos teóricos, verifica-se que o modelo de Elovich foi o que melhor se ajustou aos dados experimentais revelando a heterogeneidade do sistema, com a etapa limitante do processo sendo controlado por difusão externa, conforme modelo de Boyd. Os testes de isoterma corroboraram com as características do MEV e do modelo Elovich apontando para heterogeneidade da superfície e a ocorrência preferencialmente de monocamada com Pb(II)

ajustando-se ao modelo de Sips testado a temperatura de 25°C, enquanto o Cu(II) entre as 3 diferentes temperaturas investigadas apresentou modelos diferentes, com comportamentos que apontaram para heterogeneidade, multicamadas e fisissorção revelados pelo modelo de BET à temperatura de 15°, onde obteve a melhor capacidade de adsorção. Portanto, ambos os íons indicaram cooperatividade e alta afinidade do adsorvente-adsorbato em que o Pb (II) sucedeu melhor em temperaturas mais altas e Cu(II) em temperaturas mais baixas. O estudo termodinâmico confirmou a interferência da temperatura na capacidade de adsorção, sendo considerado o processo endotérmico para Pb(II) e exotérmico para Cu(II), com ambos os processos apresentando desordem, baixa quantidade de energia envolvida e alta afinidade do adsorvente pelo adsorbato (processo favorável), o que corroborou com os achados no FTIR, apontando para ocorrência de grande probabilidade de fisissorção conforme baixos valores determinados de entalpia, embora esta isoladamente, não comprova o mecanismo global de adsorção. Além disso os testes de dessorção aplicados com o Cu(II), apontaram que o material tem capacidade de dessorver e pode ser reaproveitado após ciclos de dessorção.

Os resultados obtidos nos testes foram ainda confrontados com trabalhos descritos na literatura, referentes a outros adsorvente de mesma origem, compostos de casca e/ou sementes usados no processo de adsorção, apresentando excelentes capacidades de adsorção.

A pesquisa teve fundamental importância, no sentido de revelar um novo adsorvente, de baixo custo, eficiente, abundante e reutilizável, que gerado a partir de resíduos da agroindústria, revelou considerável capacidade de adsorção para o íons Pb (II) e Cu(II), contribuindo com a redução de impactos ocasionados ao meio ambiente, tanto pelo acúmulo de resíduos agroindustriais, como pelo elevado índice de metais tóxicos, que além de ocasionar diversos problemas de ordem ambiental, interferem negativamente na saúde da população

5.2 CONCLUSÕES GERAIS

O bioadsorvente de SST foi eficiente no processo de adsorção com Pb (II) e Cu(II) a partir de soluções aquosas contendo o metal. O estudo revelou que o resíduo quando aplicado como adsorvente de metais tóxicos, pôde ser útil na remoção de Pb(II) e Cu(II) (potenciais contaminantes de águas residuais). Os resultados ainda revelaram excelentes capacidade de adsorção dos referidos metais em um curto período de tempo (30 min) e baixas concentrações, sendo a temperatura um interferente de ambas as capacidades adsortivas dos diferentes íons metálicos avaliados. O processo foi conduzido por um provável mecanismo simultâneo de quissorção/fisiosorção por provável complexação e troca iônica, supostamente o que permitiu a reversibilidade do processo e recuperação do material. Em comparação com outros estudos envolvendo os materiais de mesma origem recém apresentados na

literatura, o SST demonstrou excelente desempenho na capacidade de remoção com os referidos metais tóxicos.

5.3 PERSPECTIVAS DE INVESTIGAÇÕES FUTURAS

A partir dos resultados presentes neste estudo, novos testes poderão ser realizados para avaliar o efeito de adsorção do material adsorvente. Como testes com outros metais tóxicos presentes em efluentes; avaliação da competitividade iônica (sistema multielementar); estudos em sistemas contínuos como coluna de leito fixo; modificação química da biomassa (pré-tratamento, alcalino ou ácido); confecção de biocarvão afim verificar melhor eficiência deste material.

Para aprofundar os conhecimentos ainda mais sobre as diversas características do material para efeitos de adsorção, é importante ainda a inclusão de técnicas como o BET (Brunauer-Emmett-Teller) e EDX/EDS (Espetroscopia de Energia Dispersiva de Raios X) a fim de ampliar compreensões acerca das interações adsorvente-adsorbato.

6 REFERÊCIAS

ADENIYI A. G., IGHALO J. O. Biosorption of pollutants by plant leaves: An empirical review. **Journal of Environmental Chemical Engineering**, v. 7, p. 103100, 2019.

AHMED, M. A. et al. Magnetite-hematite nanoparticles prepered by green methods for heavy metal ions removal from water. **Materials Science & Engineering**, v. 178, p. 744-751, 2013.

BAKHTIARI, N.; AZIZIAN, S. Adsorption of copper ion from aqueous solution by nanoporous MOF-5: a kinetic and equilibrium study. **Journal of Molecular Liquids**, v. 206, p.114- 118, 2015.

BARROS, A. J. M. et al. Estudo termogravimétrico do processo de sorção de metais pesados por resíduos sólidos orgânicos. **Engenharia Sanitaria e Ambiental**, v. 11, p. 184–190, 2006.

BARROS, D. C. et al. Processo de biossorção para remoção de metais pesados por meio de resíduos agroindustriais: uma revisão. **Revista Biotecnologia & Ciência,** v.6, n.1, p.01-15, 2017.

BARROS, M. J. S. et al. Influência da agitação para remoção dos íons tóxicos manganês, ferro e zinco com polissacarídeos de *Hymeneae courbaril* em amostras sintéticas. *In:* Congresso Norte e Nordeste de Pesquisa e Inovação, 7., 2012, Palmas. **ENGENHARIAS – ENGENHARIA SANITÁRIA – Ciência, tecnologia e inovação: ações sustentáveis para o desenvolvimento regional**, 2012, p. 23 Disponível em:< http://propi.ifto.edu.br/ocs/index.php/connepi/vii/paper/viewFile/238/2223>. Acesso em: 10 dez. 2023.

BOSCHI J. R. **Concentração e Purificação das Proteínas do Soro de Queijo por Ultrafiltração**. 2006. Dissertação (Mestrado em Engenharia Química), Universidade Federal do Rio Grande do Sul. Porto Alegre, 2006.

CAROLIN, C. Femina; KUMAR, P. Senthil; SARAVANAN, A.; JOSHIBA, G. Janet; NAUSHAD, Mu. Efficient techniques for the removal of toxic heavy metals from aquatic environment: **A review. Journal of Environmental Chemical Engineering**, v. 5, n. 3, p. 2782–2799, 2017. Disponível em: https://doi.org/10.1016/j.jece.2017.05.029.

CHO, D.W., Song, H., Kim, B., Schwartz, F.W., Jeon, B.H. Reduction of nitrate in groundwater by Fe (0) Magnetite nanoparticles entrapped in Ca-alginate beads. **Water Air Soil Pollut**, V. 226, p. 206, 2015.CONAMA. Resolução CONAMA 430/2011. Diário Oficial da União, p. 9, 2011.

COSTA, T. B. DA; SILVA, M. G. C. DA; VIEIRA, M. G. A. Recovery of rare-earth metals from aqueous solutions by bio/adsorption using non-conventional materials: a review with recent studies

and promising approaches in column applications. **Journal of Rare Earths**, v. 38, n. 4, p. 339–355, 2020.

COSTA, W. D. et al. Removal of copper (II) ions and lead (II) from aqueous solutions using seeds of Azadirachta indica A. Juss as bioadsorvent. **Environmental Research**, v. 183, p. 109213, 2020.

CROCKFORD, H. D. **Fundamentos de físico-química**. 1. ed. Rio de Janeiro: LTC, 1977. 383 p.

DING, Z., Hu, X., Morales, V.L., Gao, B. Filtration and transport of heavy metals in graphene oxide enabled sand columns. **Chem. Eng. J**., v. 257, p. 248-252, 2014.

ELETTA, A.A.O., IGHALO J.O., A Review of fish scales as a source of biosorbent for the removal of pollutants from industrial effluents, **J. Res. Inform. Civ. Eng**. v. 16, p. 2479–2510, 2019.

EL-SAYED, H. E. M.; EL-SAYED, M. M. H. Assessment of Food Processing and Pharmaceutical Industrial Wastes as Potential Biosorbents: A Review**. BioMed Research International**, v. 2014, 24 p., 2014. Disponível em: http://dx.doi.org/10.1155/2014/146769

FARHAN AM, Al-Dujaili AH, Awwad AM. Equilibrium and kinetic studies of the biosorption of cadmium (II) and lead (II) ions in *Ficus carcia* leaves. **Revista Internacional de Indústria Química**, v. 24, p. 1-8, 2013.

FORGIONNY, A. et al. Understanding mechanisms in the adsorption of lead and copper ions on chili seed waste in single and multicomponent systems: a combined experimental and computational study. **Environmental Science and Pollution Research**, vol. 28, p. 23204–23219, 2021.

GAMA, B. M. V. **Adsorção dos íons cádmio e cobre em adsorventes preparados a partir de casca de amendoim.** 2021, 158 p. Tese (Doutorado em Engenharia Química). Faculdade de Engenharia Química, Universidade Federal do Pernambuco, Recife, 2021.

GAUTAM, R. K.et al. Heavy Metals In Water: Presence, Removal and Safety. **The Royal Society of Chemistry**, 2014.

HASHIM, M. A. et al. Remediation technologies for heavy metal contaminated groundwater. **Journal of Environmental Management**, v. 92, 2011. Disponível em: < http://www.sciencedirect.com/science/article/pii/S0301479n. 10, p. 2355-2388711002064 >

KHAN, N. et. al. Surface oxidized and un-oxidized activated carbon derived from Ziziphus jujube Stem, and its application in removal of Cd (II) and Pb (II) from aqueous media. **SN Applied Sciences.** v. 2, p. 753, 2020.

KYZAS, GEORGE Z.; FU, JIE; MATIS, KOSTAS A. The change from past to future for adsorbent materials in treatment of dyeing wastewaters. **Materials**, v.6, n.11, p.5131-5158, 2013

LEE, C.G.et al. Removal of copper, nickel and chromium mixtures from metal plating wastewater by adsorption with modified carbon foam. **Chemosphere**, v. 166, p. 203-211, 2017.

LEE. J. D. **Química inorgânica não tão concisa**. 4 ed., São Paulo: Edgard Blucher, São Paulo, 1996.

LIMA, S. C. **Germinação de sementes e otimização de técnicas de micropropagação de umbuzeiro (*Spondias tuberosa*, Arr.) – Anacardiaceae**, 2009, 95 p. Dissertação em Ciências Biológicas. Universidade Federal do Rio Grande do Norte, Natal, 2009.

LIU, Q. et al. Enhanced adsorption of copper ions by phosphoric acid-modified *Paeonia ostii* seed coats. **Environ Sci Pollut Res.**, v. 27, p. 43906–43916, 2020. https://doi.org/10.1007/s11356-020-10296-z.

MAHESHWARI, U.; SURESHGUPTA, S. Performance evaluation of activated neem bark for the removal of Zn (II) and Cu (II) along with other metal ions from aqueous 42 solution and synthetic pulp & paper industry effluent using fixed-bed reactor. **Process Safety and Environmental Protection**, p. 547-557, 2016.

MALIK, D. S.; JAIN, C. K.; YADAV, A. K. Heavy Metal Removal by Fixed-Bed Column – A Review. **Chem. Bio. Eng. Rev**., v. 5, n. 3, p. 173–179, 2018.

MARKOVIĆ, M. et al. Copper ions biosorption onto bean shells: Kinetics, equilibrium and process optimization studies. **J. Serb. Chem. Soc.** v. 88, p. 921-935, 2023. https://doi.org/10.2298/JSC221018014M

MENESES, J. M. C. et al. Equilibrium, kinetics and thermodynamics of lead (II) adsorption in bioadsorvent composed by Caryocar coriaceum Wittm barks. **Chemosphere**, v. 261, p. 128-144, 2020.

MENEZES, J. M. C. et al. Kinetic and thermodynamic study of copper (II) IONS biosorption by Caryocar Coriaceum Wittm bark. **Sustainable Chemistry and Pharmacy**. v. 19, p. 100364, 2021. DOI: https://doi.org/10.1016/j.scp.2020.100364.

MOHAMMAD, S. G.; AHMED, S. M.; EL-SAYED, M. M. H. Removal of copper (II) ions by eco-friendly raw eggshells and nano-sized eggshells: a comparative study. **Chemical Engineering Communications**, v. 209, p. 83-95, 2020.

MOREIRA, F. R.; MOREIRA, J. C. A Importância da análise de especiação do chumbo em plasma para a avaliação dos riscos à saúde. **Quim. Nova,** v. 27, p. 251-260, 2004.

MORIN-CRINI, N. et al. Hemp-based adsorbents for sequestration of metals: a review. **Environmental Chemistry Letters**, v. 17, p. 393–408, 2019.

MOTA, J. M. N. **Estudo do potencial de remoção do cobre pela *Pistia stratiotes* L. Em efluente sintético da indústria de papel e celulose**, 2022, 46 p. TCC (Bacharelado em Engenharia Florestal), Universidade Federal de Uberlândia, Monte Carmelo, 2022.

NASCIMENTO, R. F. et al. Uso de bioadsorventes lignocelulósicos na remoção de poluentes de efluentes aquosos. **Fortaleza: Imprensa Universitária**, 2014.

OLIVEIRA, E. A. et al. Avaliação da toxicidade dos resíduos do abacaxi utilizando o bioensaio de Artemia salina. **Research, Society and Development**, v. 12, n. 10, e20121043275, 2023. https://rsdjournal.org/index.php/rsd/article/view/43275.

PEDRASSOLLI, I.M.; HOMEM-JUNIOR, A.C.; PANDOLFI, M.A.C. Aproveitamento dos resíduos de manga das agroindústrias. In: III SIMTEC –Simpósio de Tecnologia da FATEC Taquaritinga. Disponível em: <www.fatectq.edu.br/simtec> 7 p. Outubro de 2015.

PERRY, Robert H.; GREEN, Don W.; MALONEY, James O. **Chemical Engineers Handbook**. 7 ed. [S. l.]: McGraw-Hill, 1997. v. 27E-book. DOI: https://doi.org/10.1021/ed027p533.1.

PUGAZHENDHI, A. et al Biosorptive removal of copper (II) by Bacillus cereus isolated from contaminated soil of electroplating industry in India. **Water Air Soil Pollut**, v. 229, p. 76, 2018.

RAHIM M, Ullah I, Khan A, Haris MRHM. Health risk of heavy metals through consumption of food crops in the vicinity of the district of Shangla**. J Chem Soc Pak** v. 38(1), p. 165–169, 2016.

REIS, João Marcos Dos. **Técnicas de remoção de metais de águas residuárias: uma revisão de literatura.** Portal tratamento de água. Disponível em: https://tratamentodeagua.com.br/artigo/tecnicas-remocao-metais-aguas-residuarias/. Acesso em: 24/01/2023.

REIS, P. F. **Investigação da capacidade adsortiva de nanopartículas magnéticas híbridas modificadas com l-cisteína na remoção de chumbo de soluções aquosas**, 2020, 61 p. Dissertação (Mestrado em Ciências de materiais). Universidade de Brasília, Brasília, 2020.

REZENDE, L. G. P.; PRADO, V. M. Degradação eletroquímica do cloranfenicol em reator de fluxo, **Quim. Nova**, Vol. 33, No. 5, 1088-1092, 2010.

SANTOS, J. S. et al. Processo de Separação por Membrana (PSM): aplicação da tecnologia na indústria láctica. **Revista Interdisciplinar da Universidade Federal do Tocantins** – V. 1, n. 01, p. 210 - 226, 2014. DOI: http://dx.doi.org/10.20873/uft.2359-3652+2014v1n1p210.

SANTOS, M. R. **Avaliação da eficiência dos carvões ativados produzidos a partir da casca da banana nanica (*Musa paradisíaca*) na biossorção de íons chumbo em água**, 2020, 62 p. Dissertação (Mestrado em Agroquímica). Instituto Federal de Goiânia, Rio Verde, 2020.

SILVA, E. R.; ASSIS, O. B. G. Avaliação de técnica eletroquímica na remoção de resíduos orgânicos em água com emprego de unidade em escala de laboratório. **Eng. San. Ambient**. V. 9, N° 3 p. 193-196, 2004.

SILVA, L. M. R.; FIGUEIREDO, E. A. T.; RICARDO, N. M. P. S.; VIEIRA, I. G. P.; FIGUEIREDO, R. W.; BRASIL, I. M.; GOMES, C. L. Quantification of bioactive compounds in pulps and by-products of tropical fruits from Brazil. Food. **Chemistry,** v. 143, p. 398-404, 2014.

SILVA, N. C. R. **Utilização da casca de banana como biossorvente para a adsorção de chumbo (II) em solução aquosa**, 2014, 45 p. Trabalho de Conclusão de Curso (Bacharel em Engenharia Ambiental) – Universidade Tecnológica Federal do Paraná. Campo Mourão, 2014.

SOUSA, F. W. de. **Adsorção de metais tóxicos em efluente aquoso usando pó da casca de coco verde tratado**, 2007. 105 p. Dissertação (Mestrado em Engenharia Civil. Saneamento Ambiental). Universidade Federal do Ceará, Fortaleza, 2007.

SOUZA, A. F. B**. Isotermas de langmuir e freundlich da adsorção de zinco por resíduos da construção civil cerâmicos**, 2023, 53 p. Trabalho de Conclusão de Curso (Graduação em Engenharia Ambiental e Sanitária). Universidade federal de Uberlândia, Uberlândia, 2023.

SULYMAN, M. et al. Low-cost Adsorbents Derived from Agricultural By-products/Wastes for Enhancing Contaminant Uptakes from Wastewater: A Review. **Polish Journal of Environmental Studies**, v. 26, n. 2, p. 479–510, 2017. Disponível em: https://doi.org/10.15244/pjoes/66769

SYED, F. A.; Battula, V. Evaluation of adsorptive performance of Adhatoda vasica on lead by batch process. **Environmental Progress & Sustainable Energy**, v. 42, 2023. https://doi-org.ez1.periodicos.capes.gov.br/10.1002/ep.14218.

VAFAJOO, L.; CHERAGHI, R.; DABBAGH, R.; MCKAY, G. Removal of cobalt (II) ions from aqueous solutions utilizing the pre-treated 2-Hypnea Valentiae algae: Equilibrium, thermodynamic, and dynamic studies. **Chemical Engineering Journal**, v. 331, p. 39-47, 2018.

VON SPERLING, M.; **Princípios do tratamento biológico de águas residuárias**. Vol. 1. Introdução à qualidade das águas e ao tratamento de esgotos. Departamento de Engenharia Sanitária e Ambiental – UFMG. 4a ed. Belo Horizonte, 2014.

ANEXO

Anexo 1 – Tela inicial da publicação do artigo 1 para produção científica

ChemistrySelect | Research Article
doi.org/10.1002/slct.202502316 | Chemistry Europe
www.chemistryselect.org

Spondias Tuberosa Seeds as Lignocellulosic Bioadsorbent for Efficient PB (II) Removal: Characterization, Adsorption Modeling, Selectivity, and Reusability

Aliane Cristiane de Sousa Formiga,[a] Isaac Moura Araújo,[a] José Augusto Soares de Araujo,[a] Henrique Douglas Melo Coutinho,*[a] Francisco José de Paula Filho,[b] Yannice Tatiane da Costa Santos,[c] Jorge Marcell Coelho Menezes,[b] and Raimundo Nonato Pereira Teixeira[a]

The objective of this research was to investigate the efficiency of *Spondias tuberosa* seeds (SST) as a bioadsorbent for Pb (II) ions in aqueous solutions. Adsorption isotherms and kinetics as well thermodynamics were studied in a batch system. The SST residue was collected from pulp manufacturing industries in the Cariri region of Ceará, specifically in the city of Juazeiro do Norte, Ceará, Brazil. For the characterization of the adsorbent material, point of zero charge (PZC), scanning electron microscopy (SEM), and infrared spectroscopy (FTIR) analyses were performed. The pHPZC obtained had an average value of 5.3, which was adjusted to 5.5. SEM images revealed the presence of roughness and porosity typical of fibrous plant materials. With increased magnification, the material showed varying pore shapes and sizes, generally derived from the structure of the plant cell wall of the precursor biomass. It was also observed that the adsorption rate reached equilibrium within 30 min. Thus, it was concluded that the SST bioadsorbent demonstrated satisfactory performance in the adsorption of Pb (II) ions with a maximum adsorption capacity of 46.0 mg. g^{-1}. These findings support the use of SST as an environmentally friendly low-cost and efficient biosorbent contributing to sustainable strategies for toxic metals remediation.

1. Introduction

Industrial activity generates a significant volume of waste which, when present in liquid form is referred to as effluent, resulting from the utilization of water and other materials in the production processes. Many of these effluents contain highly harmful environmental pollutants, affecting water, soil, and marine life.[1] The toxic action of these metals can also lead to death or bioaccumulation, which amplifies the harmful effects of these substances through the food chain.

Lead, mercury, cadmium, chromium, copper, and arsenic